NASA Tech Briefs

Official Publication of
National Aeronautics and
Space Administration
Volume 14 Number 5

Transferring Technology to
American Industry
and Government
May 1990

Ames Research Center: Fifty Years On The Cutting Edge

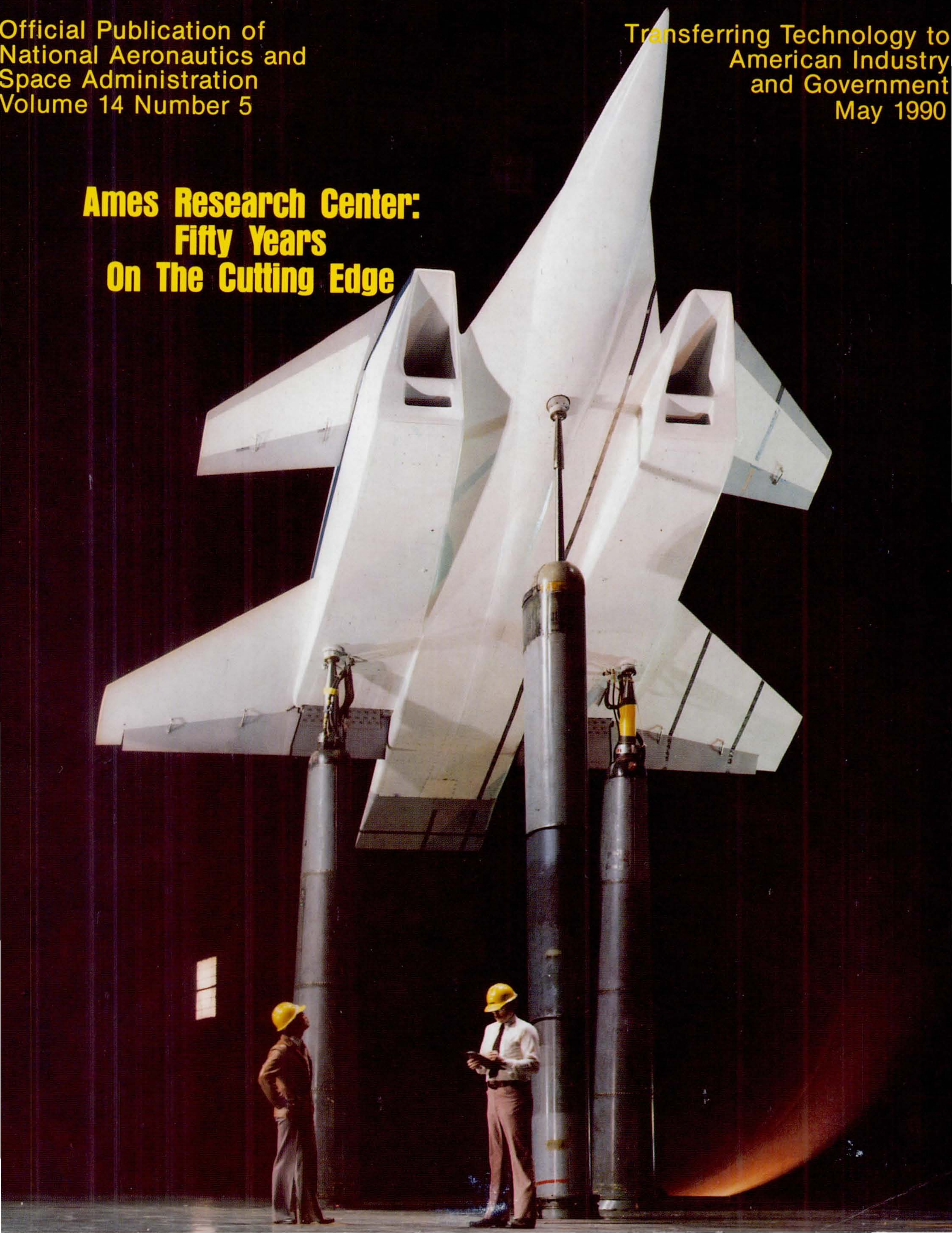

From **$77**

LD200 SERIES ECONOMICAL AC TRANSDUCERS

- Rugged Construction for Machine Tools and Vehicles
- Large Core Clearance for Easy Installation and Friction Free Movement
- Measurement Range ±0.05″ to ±0.50″

Circle reader service number **516**

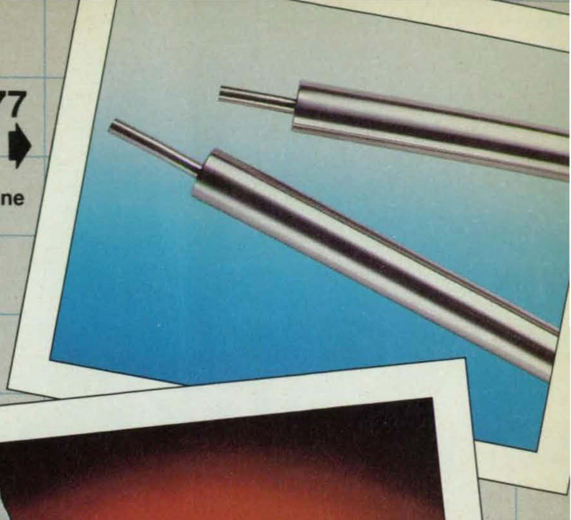

$295

MODEL LDX-3 AC LVDT SIGNAL CONDITIONER

- Powers Transducer and Provides 0 to ±5 Vdc or 0 to ±20 mA Output
- Oscillator/Demodulator Provides 0.1% Reading Accuracy
- Adjustable Zero and Span Control
- Rugged, Die-Cast Aluminum Casing

Circle reader service number **520**

From **$298**

LD300 SERIES AC LONG STROKE TRANSDUCERS

- High Accuracy, Infinite Resolution
- Rugged Stainless Steel Case with Spring Loaded Armature
- Measurement Range ±0.60″ to ±12.00″

Circle reader service number **518**

$785

MODEL DP-LVDT HIGH-PERFORMANCE DISPLAY

- Single Channel Conditioning Device Combined with a Microprocessor Controlled 5 Digit Panel Meter
- Optional Hi-Lo Alarm Relays and RS-232 Communication
- Calibration Values, and Min-Max Readings Stored in Non-Volatile Memory
- AC Transducer Excitation

Circle reader service number **517**

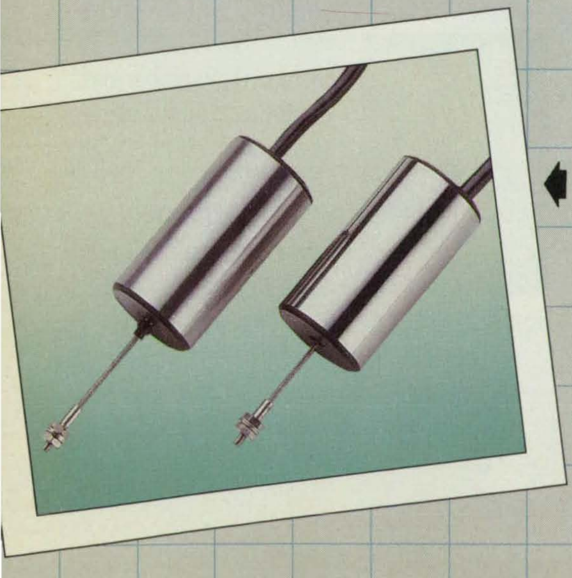

From **$198**

LD400 SERIES MINIATURE DC TRANSDUCERS

- Delrin Bearings Provide Near Frictionless Motion for Detecting the Smallest Displacement
- High Linearity and Low Mass of Moving Parts
- Measurement Range ±0.04″ to ±0.20″

Circle reader service number **519**

From **$489**

LD500 SERIES DC GAUGING TRANSDUCERS

- High Accuracy and Repeatability
- Industrial Construction with Replacement Tips and Linear Ball Bearing Actuator
- Measurement Range ±0.04″ to ±0.20

Circle reader service number **522**

OPTIMATE Data Links offer logic level compatibility, carrier sense, data quieting. In 850 and 1300 nanometer multimode, from 25 Mb/s to 220 Mb/s.

SOLID STATE RELAY

#2 IN A SERIES

Now a cheap off-the-shelf SSR that puts you in control. It lets you control the cost and the system's function in military applications.

Here's what you get.

- Short Circuit Protection
- Status Indication
- Current Overload Protection
- Optical Isolation
- TTL & CMOS Compatible Control
- Built to meet the requirements of MIL-R-28750.
- Cost Effective

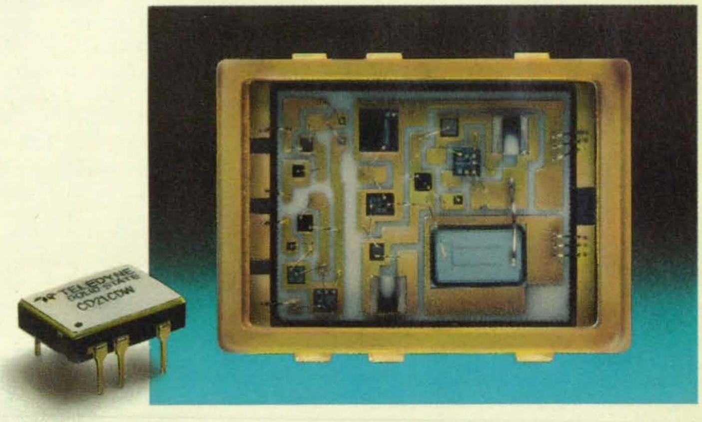

ACTUAL SIZE CERAMIC PACKAGE

PART # CD21CDW

Review the electrical characteristics and call us for immediate application assistance.*

ELECTRICAL CHARACTERISTICS (–55°C to +105°C unless otherwise noted)				
	Min	Max	Units	
Bias Voltage (V_{BIAS})	3.8	6.0	V_{DC}	See Note 1
Bias Current (I_{BIAS})		15.0	mA	$V_{BIAS} = 5V_{DC}$
Control Voltage (V_{IN})	0	18.0	V_{DC}	
Control Current (I_{IN})		250	μA	$V_{IN} = 5V_{DC}$
Turn-Off Voltage $V_{IN (OFF)}$	3.2		V_{DC}	
Turn-On Voltage $V_{IN (ON)}$		0.3	V_{DC}	
Continuous Load Current		1.2	A	–55°C to +25°C
I_{LOAD} @ 60 VDC		0.7	A	+85°C
Output Trip Current (I_{TRIP})	2.4 (Typ.)		A	+25°C, 100ms
On-Resistance (R_{ON})		0.65	Ohms	
Turn-On Time (T_{ON})		1.5	ms	
Turn-Off Time (T_{OFF})		0.25	ms	
Status Voltage (V_{STATUS})	1	18	V_{DC}	
Status Current (I_{STATUS})		2	mA	$V_{SAT} \leq 0.3V_{DC}$ See Note 2

Notes:
1. Series resistor is required for bias voltages above $6V_{DC}$. $RS = (V_{BIAS} - 6\,V_{DC})/15$ mA
2. A pull up resistor is required for the status output. $R_{STATUS} = (V_{STATUS} - 0.3)/I_{STATUS}$
3. Output will drive loads connected to either terminal (sink or source).
4. Status circuit is a built-in test feature checking the input circuitry of the relay. Status output is low (on) when the input is on.

All power FET relays may drive loads connected to either positive or negative referenced power supply lines (source or sink modes).

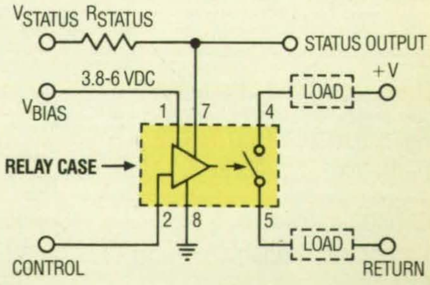

TELEDYNE SOLID STATE
A Division of Teledyne Relays

*For immediate application assistance call 1-800-284-7007.

Teledyne Solid State, 12525 Daphne Avenue, Hawthorne, California 90250.

Circle Reader Action No. 537

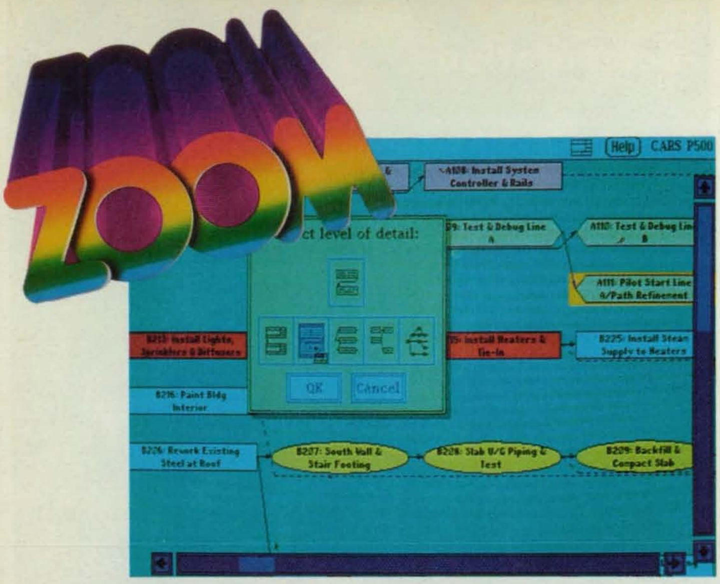

Zoom — five levels of detail for your network, from bird's-eye to close-up.

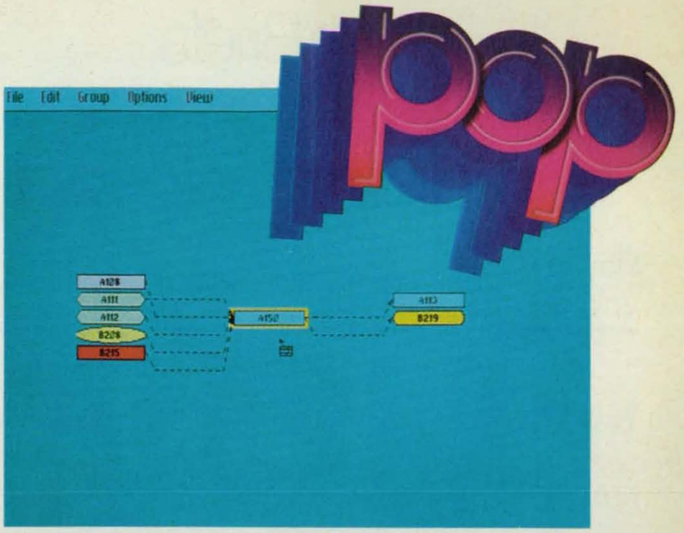

Pop — highlights all predecessor-successor relationships and lets you click your way along any activity path.

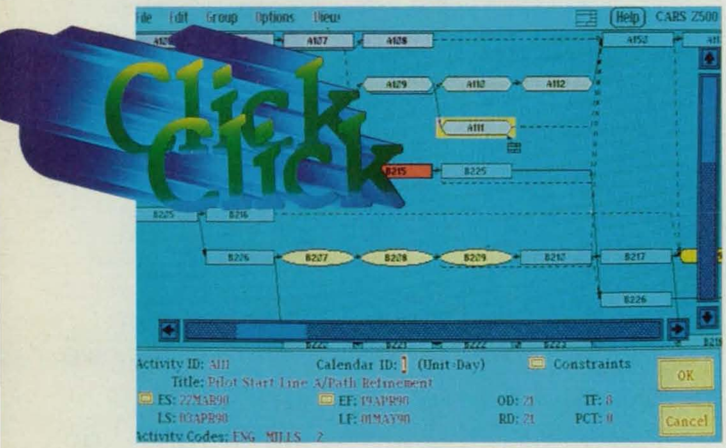

Click-Click — use double clicks to add activities, define relationships, and modify activity data.

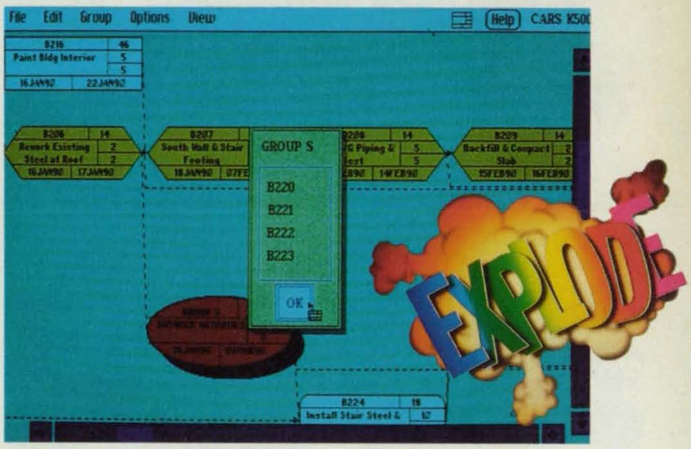

Explode — The Collapse command compresses several activities into one; Explode redisplays activities in their original positions.

Primavera introduces some important new project management terminology.

Primavera Project Planner® 4.0 works like you think. Visually. Graphically. Intuitively. As quickly as "pop", "click", "zoom"! Keeping you in touch with the big picture while giving you instant access to all the details.

Create an activity? Point, click-click.

Define a relationship? Two clicks and done.

Updates? Double click and enter progress.

P3® 4.0 gives you copy, cut and paste, group and mark, and dozens of other powerful scheduling tools.

Plus, you can output the schedule to your plotter or laser printer with a few quick keystrokes. This is *what-you-see-is-what-you-get* schedule building. No sweat, no strain.

Now, the world's best high-performance project management software is even easier to access. And it's available today, running under DOS in 640K.

Circle Reader Action No. 663

See Primavera Project Planner 4.0 in action.
Call 1-800-423-0245 today for your FREE video demo.

PRIMAVERA SYSTEMS, INC.
Project Management Software
Two Bala Plaza • Bala Cynwyd, PA 19004
(215) 667-8600 • FAX: (215) 667-7894

Please rush me my FREE video demo.

NAME ____________________

TITLE ____________________

COMPANY ____________________

CITY ____________ ST ______ ZIP ________

PHONE ____________________

NTB

NASA Tech Briefs

Transferring Technology to
American Industry and Government

May 1990
Volume 14 Number 5

Photo courtesy NASA

Scientists at NASA's Ames Research Center created this comparison of space shuttle surface presssure calculations obtained through computer simulation and wind tunnel testing. It illustrates the basic capability to reproduce wind tunnel measurements via computer. The areas of highest pressure appear white, the lowest blue. The green regions indicate statis pressure. See page 83.

SPECIAL FEATURES

TECHNICAL SECTION

ABP BPA

DEPARTMENTS

On The Cover: A V/STOL fighter model is prepared for testing in the Ames 40- by 80-Foot Wind Tunnel. The tunnel has seen several hundred aircraft and models in its test section, spanning five decades of aviation history. A special section starting on page 83 celebrates Ames' scientific and technical achievements over the last half-century.
(Photo courtesy NASA)

The second part of our report on NASA's High Speed Research Program focuses on the technological challenges in developing a next-generation supersonic transport.

Photo courtesy
McDonnell Douglas Corp.

NASA Tech Briefs, ISSN0145-319X, USPS 750-070, copyright © 1990 in U.S., is published monthly by Associated Business Publications Co., Ltd., 41 E. 42nd St., New York, NY 10017-5391. The copyrighted information does not include the individual Tech Briefs which are supplied by NASA. Editorial, sales, production and circulation offices at 41 E. 42nd Street, New York, NY 1001 5391. Subscription for non-qualified subscribers in the U.S. , Panama Canal Zone and Puerto Rico, $75.00 for 1 year; $125.00 for 2 years; $200.00 for 3 years. Single copies $10.00. Remit by check, draft, postal or express orders. Other remittances at sender's risk. Address all communications for subscriptions or circulation to NASA TEch Briefs, 41 E. 42nd Street, New York, NY 10017-5391. Second-class postage paid at New York, NY and additional mailing offices.

POSTMASTER; please send address changes to NASA Tech Briefs, 41 E. 42nd Street, Suite 921, New York, NY 10017-5391.

NASA Tech Briefs

Official Publication of
National Aeronautics and
Space Administration

ABP BPA

NASA Tech Briefs:

Published by .... **Associated Business Publications**
Editor-in-Chief/Publisher .... **Bill Schnirring**
Associate Publisher .... **Frank Nothaft**
Editor .... **Joseph T. Pramberger**
Managing Editor .... **R. J. Laer**
Assistant Editor .... **Theresa M. Detko**
Technical Advisor .... **Dr. Robert E. Waterman**
Production Manager .... **Rita Nothaft**
Traffic Manager .... **James E. Cobb**
Circulation Manager .... **Cheryl Golden**
Advertising Coordination Manager .... **Maya V. Falek**
Telecommunications Specialist .... **Evelyn Mars**
Reader Service Manager .... **Sylvia Valentin**

Briefs & Supporting Literature:
Provided to National Aeronautics and Space Administration by **International Computers & Telecommunications, Inc.**, NY, NY with assistance from **Logical Technical Services**, NY, NY
Technical/Managing Editor .... **Ted Selinsky**
Art Director .... **Luis Martinez**
Administrator .... **Elizabeth Texeira**
Chief Copy Editor .... **Lorne Bullen**
Staff Writers/Editors .... **Dr. James Boyd, Dr. Larry Grunberger, Dr. Theron Cole, Jordan Randjelovich, George Watson, Oden Browne**
Graphics .... **Vernald Gillman, Charles Sammartano**
Editorial & Production .... **Bill Little, Ivonne Valdes, Frank Ponce, Susan Finelli**

NASA:
NASA Tech Briefs are provided by the National Aeronautics and Space Administration, Technology Utilization Division, Washington, DC:
Administrator .... **Richard H. Truly**
Assistant Administrator for Commercial Programs .... **James T. Rose**
Deputy Assistant Administrator (Programs) .... **Henry J. Clarks**
Acting Director TU Division (Publications Manager) .... **Leonard A. Ault**
Manager, Technology Utilization Office, NASA Scientific and Technology Information Facility .... **Walter M. Heiland**

Associated Business Publications
41 East 42nd Street, Suite 921, New York, NY 10017-5391
(212) 490-3999 FAX (212) 986-7864
President .... **Bill Schnirring**
Executive Vice President .... **Frank Nothaft**
Vice President .... **Domenic A. Mucchetti**
Operations Manager .... **Rita Nothaft**
Controller .... **Felecia Lahey**

Advertising:
New York Office: (212) 490-3999 FAX (212) 986-7864
Director of Advertising Sales .... **James G. McGarry**
Account Executive (NY, NJ) .... **Brian Clerkin** at (201) 285-0880
Account Executive (VA, DC, MD, DE, WV) .... **John D. Floyd** at (215) 399-3265
Account Executive .... **Debby Crane** at (201) 967-9838
Account Executive (Midwest, Northwest) .... **Paul Lesher, CBC** at (708) 501-4140
Regional Sales Manager (South-Central) .... **Douglas Shaller** at (212) 490-3999
Account Executives (Eastern MA, NH, ME, RI) .... **Paul Gillespie** at (508) 429-8907; **Bill Doucette** at (508) 429-9861
Account Executives (Western MA, CT, VT) .... **George Watts** or **David Haggett** at (413) 253-9881
Account Executives (Southeast) .... **Newton Collinson** or **Jonathan Kiger** or **Lawrence Mischik** at (404) 939-8391
Account Executives (Calif., AZ, NV, NM) ....
for Area Codes 818/213/805 —**Thomas Stillman**
for Area Codes 408/415/916/209 —**Elizabeth Cooper**
and for Area Codes 619/714 —**Karen Mock** at (213) 372-2744

NTBM-Research Center
Account Supervisor .... **Lourdes Del Valle**

RESEARCH AND DEVELOPMENT

Research and Development is the foundation of Schott Glass Technologies' status as the flagship company for Schott's Optics/Electronics Division in America and as a major supplier of today's most advanced optical materials.

Scientific and industrial corporations regularly contract Schott's R & D group in Pennsylvania to develop proprietary glass compositions and to perform test melts and measurements. *Research and Development* magazine cited Schott's diverse innovative achievements with "IR-100" awards for outstanding ophthalmic, laser and fiber optic developments.

Schott's glass chemists and physicists, supported by technical expertise and today's most advanced analytical equipment, are refining many existing products and processes and are creating new directions for the electronics industry and glass-ceramics.

Our solutions are at work where demands on the materials are greatest, and we are seeking solutions to problems as yet undefined. For the latest developments in glass research, please contact us.

R&D Instrumentation (Partial Listing)

X-ray Fluorescence Spectrometry (XRF)	Fluorescence Spectrophotometer
Atomic Absorption Spectrometry with flame & graphite furnace capability	4", 12", & 24" Interferometers
A variety of spectrophotometers covering the UV, visible & IR spectral regions	Wild Spectrometers for high-precision index measurements
Internal Transmittance Spectrophotometer	Zerodur® Dilatometers
Laser Damage Tester	Instruments measuring the entire range of viscosity
	Full-service test melting

SCHOTT
GLASS TECHNOLOGIES INC.
400 York Avenue
Duryea, Pennsylvania 18642
TEL: (717) 457-7485
FAX: (717) 457-6960
On West Coast: (714) 871-0800

Circle Reader Action No. 383

High-Speed Transport Research Targets Environmental Obstacles

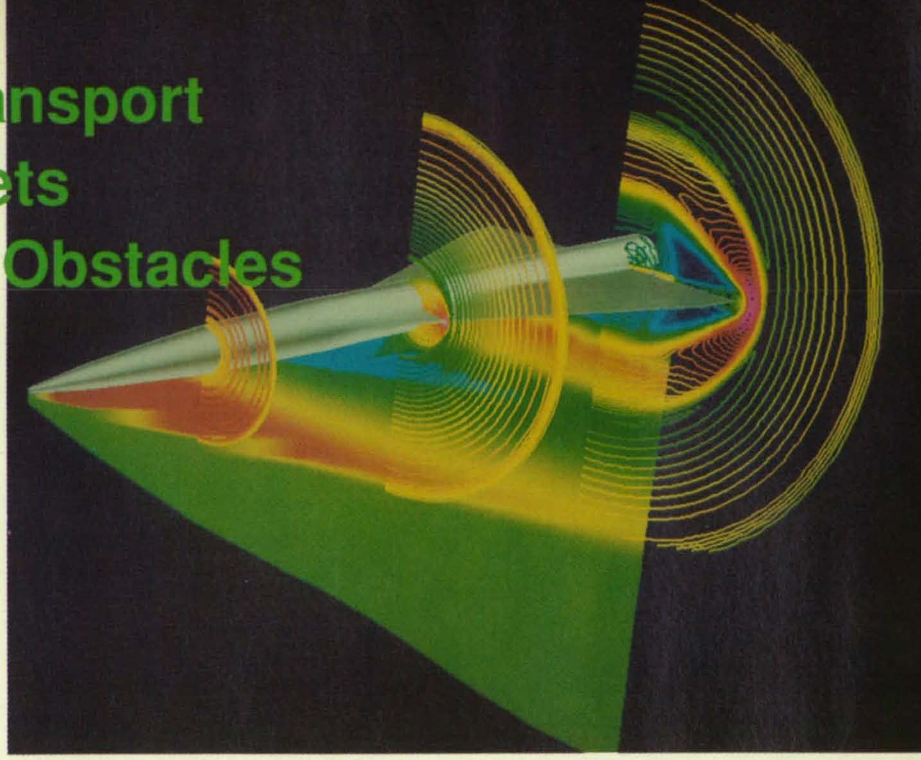

Photo courtesy NASA

The pressure field around a supersonic transport concept shows shock waves generated by the bow and wing. Computational fluid dynamics research at NASA's Ames Center is investigating the effects of aerodynamics on sonic boom and cruise efficiency.

A NASA-industry research team is intensifying its efforts to develop technologies for a next-generation supersonic airliner that would cruise in the stratosphere at speeds between Mach 2 and 3. Under a new six-year, $284 million program led by NASA's Lewis, Langley, and Ames field centers, researchers are exploring ways to resolve environmental problems—including atmospheric effects, airport community noise, and sonic boom—which could ground the high-speed civil transport (HSCT) before it gets off the drawing board.

HSCT atmospheric impact research includes long-term atmospheric chemistry assessments and low-emission combustor studies. Under contract to NASA, airframers and engine companies are determining HSCT fleet size, routes, and global stratospheric ozone effects for both unconstrained and reduced levels of nitrogen oxide (NOx) emissions. This information is being applied to atmospheric models in hopes of developing a technical basis for the establishment of emissions standards. An oversight committee of reknowned U.S. atmospheric scientists is assisting in these studies.

Beginning in 1992, NASA plans to conduct flight experiments to measure the dispersion of engine emissions and chemical perturbations along proposed flight corridors. The results will help scientists validate and improve assessment models, explained Allen Whitehead, manager of the High Speed Research Program at NASA Langley. "We need to reduce the large uncertainties in present global models," he said.

NASA and U.S. engine makers are working to reduce emissions to one-tenth uncontrolled levels. The main focus of their research is on low-emission combustor concepts. The most promising candidates are the lean premixed/prevaporized (LPP) and the rich burn/quick quench/lean burn (RQL) combustors. Although physically different, both

---

Editor's note: This is the second of two parts on NASA's High Speed Research Program.

---

combustors lower NOx emissions by reducing flame temperatures and the residence time of reacted combustion products at high temperatures.

The LPP combustor premixes fuel and air upstream of the combustion zone to completely vaporize the fluid. Burning then occurs uniformly in a stabilized combustion zone. A potential drawback is that flame flashback into the premixing zone could cause upstream burning.

The more complex RQL concept involves staged burning. Combustion is initiated in a fuel-rich zone in which fuel exceeds available air by 20 to 80 percent. Thermal NOx formation is inhibited because NOx reactions proceed more slowly than the hydrocarbon reactions, which deplete the supply of oxygen available to combine with nitrogen to form NOx. Upon completion of the rich burning phase, air is added to the partially-reacted gas and combustion is completed. "The RQL's performance is less sensitive to variations in engine conditions," said Richard Niedzwiecki, chief of the Combustion Technology Branch at NASA Lewis, "and there are indications that the combustor will not produce NOx increases with increased severity in engine operating conditions."

Computational chemistry techniques developed by Ames scientists will be used to model turbulent flow in the candidate combustor configurations and provide data needed for advanced diagnostic analysis of heated gases in Lewis Center experimental facilities. Lewis researchers have developed a square wave flame tube to study NOx formation in simulated flight conditions. Air and fuel are injected into the tube at the same temperature and pressure levels an HSCT would encounter at 60,000 feet. "We want to see if the reactive chemistry can be controlled to achieve low NOx," explained William Strack, assistant chief of the Lewis Aeropropulsion Analysis Office. With installation of appropriate modules, the rig will be able to simulate both the LPP and RQL combustor concepts. It also will be used to assess the effectiveness of NOx destructive additives.

Quieter Engines

To reduce aircraft noise to acceptable levels, HSCT researchers are investigating innovative engine configurations and sound suppression techniques. Pratt & Whitney and General Electric are developing new types of engines that change their configuration so that they act and sound more like subsonic engines at takeoff and landing. These propulsion concepts are being evaluated through wind tunnel experiments and computer simulation.

STRETCH YOUR BERT

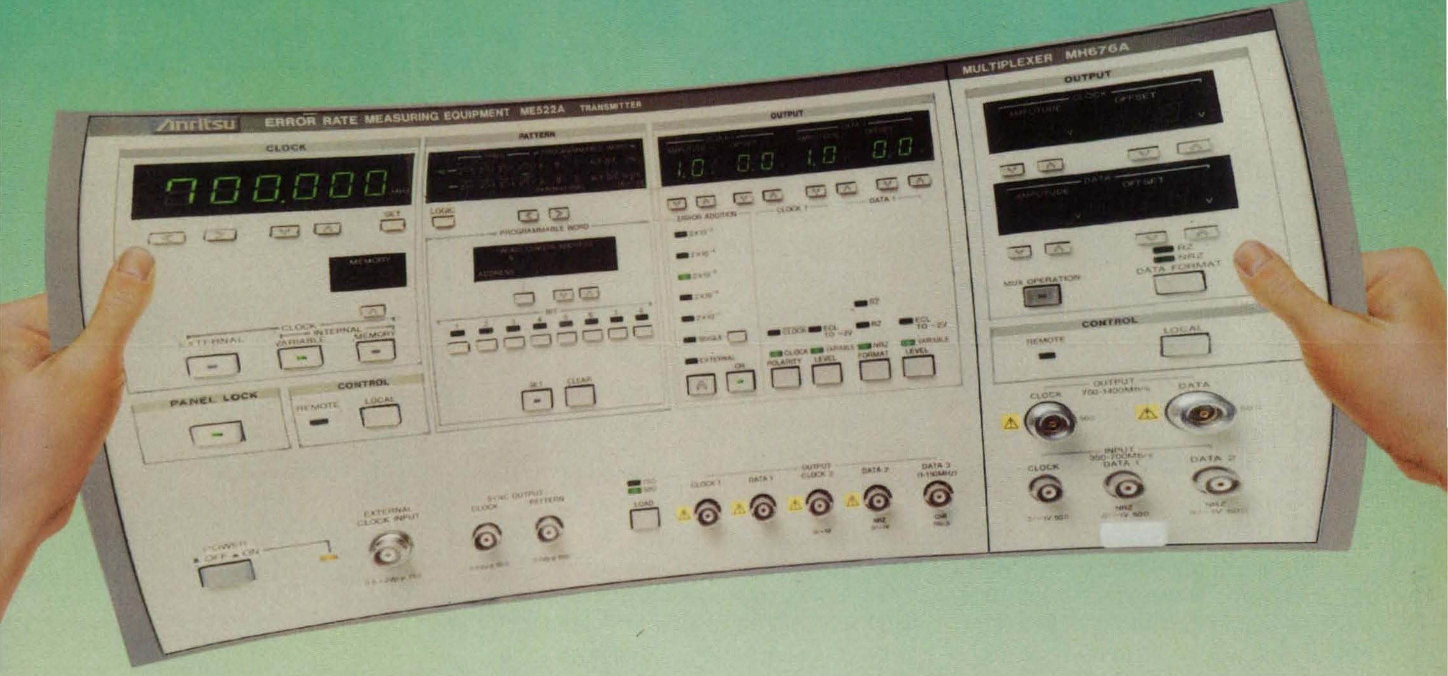

Meet Changing Requirements Of Every BER Application With Plug-In Flexibility

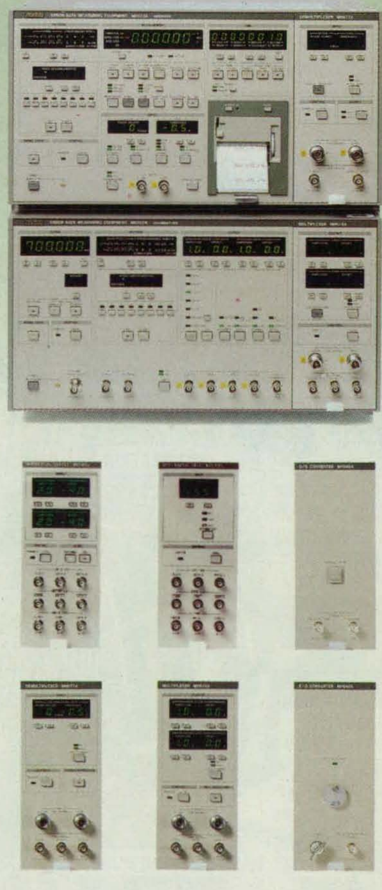

- 1 MHz to 1.4 GHz
- Synthesized Clock
- Multiple Patterns
- Multiple I/O Interfaces

The ME522A Error Rate Measurement Equipment covers a frequency range of 1 MHz to 700 MHz, and up to 1.4 GHz with plug-in MUX/ DEMUX units. It provides abundant pattern generation capability and measurement functions, including PRBS to $2^{23}-1$, three words up to 2048 bits in length, mark ratio variable patterns, alternate patterns, and isolated patterns.

The ME522A is the most flexible solution to your BER measurement requirements, from component test to systems analysis and from low frequency rates to the optical requirements of SONET.

For a demo, application assistance or literature, contact Anritsu America, Inc., 15 Thornton Road, Oakland, NJ 07436. Call 800-255-7234 or (in NJ) 201-337-1111. FAX 201-337-1033.

Anritsu

Circle Reader Action No. 407

Work is also progressing on low-noise exhaust nozzles and inlets. One of the more successful concepts for jet noise reduction is the inverted velocity profile, which consists of a coannular nozzle with the high-velocity, high-temperature stream flowing through the outer flow path and the lower velocity, cooler stream flowing through the inner path. Scale model tests have demonstrated that a 6 dB noise reduction can be achieved using this method.

NASA is looking to apply active shear flow control principles to enhance the effectiveness of HSCT noise-suppressing nozzles. Previous research has shown that the introduction of an excitation signal can increase mixing rates in an ejector or mixer, resulting in lighter, smaller nozzles. Excitation signals also can help redirect noise generated within a shear layer into sound-absorbing acoustic liners.

Airflow Demands

Inlet development for the HSCT presents a major challenge, as the inlet must be stable, provide a wide airflow range, and suppress fan noise at takeoff and approach. Moreover, it must meet these requirements with minimum weight, drag, and complexity. "A particular problem occurs in the Mach 2.1 to 2.7 range, where conventional translating centerbody inlets cannot supply the engine airflow demand during takeoff, subsonic cruise, and transonic acceleration," said Robert Coltrin, chief of the Lewis Inlets Technology Branch.

Lewis and its contractors presently are considering two advanced inlet designs that offer increased off-design airflow: the variable diameter centerbody (VDC) axisymmetric inlet and the two-dimensional (2D) expanding wedge inlet. The 2D version is simpler and features more off-design airflow capacity, but tends to be heavier than the VDC. Researchers will evaluate and modify both designs using powerful computational fluid dynamics (CFD) tools as well as part-scale models.

The Boom Box

NASA's sonic boom reduction research combines testing of low-boom aircraft designs with investigations of subjective response to boom overpressures. "Very little is known about the (subjective) response to booms or how structures react to the related impulses," said Whitehead.

Langley has built a sonic boom simulator facility, or "boom box," to measure loudness and annoyance response to signature shape and amplitude. The center plans to produce a portable version that will be placed in volunteers' homes to determine long-term and multiple-exposure response in the home environment. This sound reproduction system could be used to study response to jet engine noise as well as booms, Whitehead said.

NASA's goal is to define acceptability criteria that can be used to guide the design of low-boom aircraft shapes. Wind tunnel tests of initial low-boom models are scheduled to begin at Langley and Ames this summer. ❒

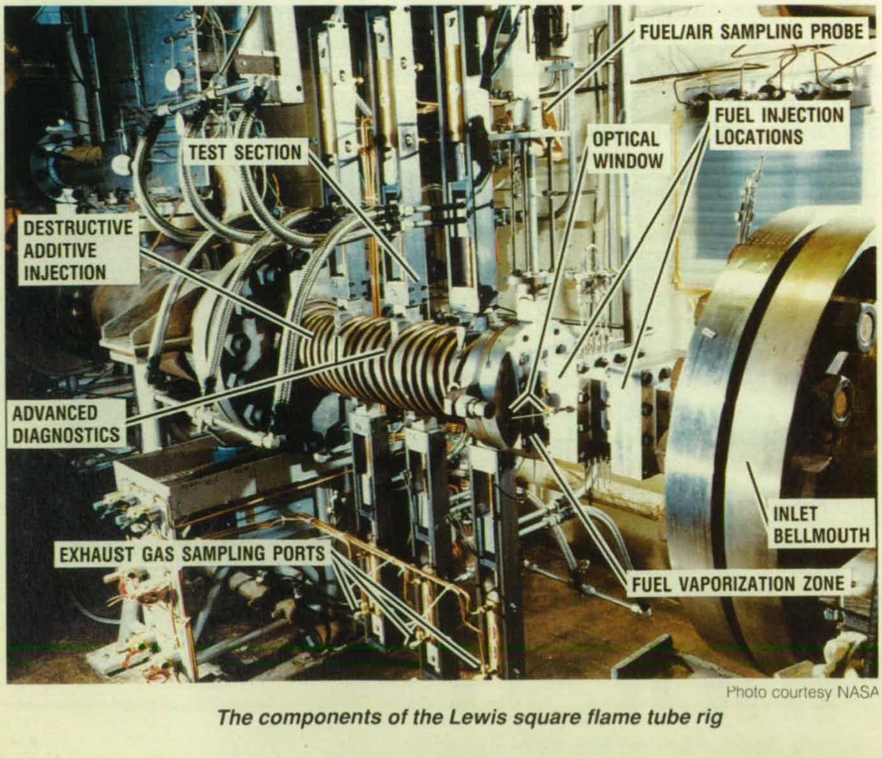

Photo courtesy NASA

The components of the Lewis square flame tube rig

THERE'S ONLY ONE THING TO SAY ABOUT INFORMATION SECURITY.

ORACLE

The term "state-of-the-art database security" can be written more concisely:

Oracle.

That's because Oracle's commitment to providing leading edge information security solutions to numerous federal agencies and military branches is well established and growing.

Already, Oracle's relational DBMS software provides high-level data integrity and security on everything from micros and minis to workstations and mainframes.

Add Oracle's reputation for exceptional quality, service and support and you'll arrive at a winning combination for high-security software.

To learn more about how Oracle can help you manage information with security and integrity, register for an Oracle seminar, or call **1-800-345-DBMS, ext. 6764** for a free brochure.

Incidentally, there's one more thing to say about information security: Authorized ADP Schedule Price List Contract No. GS00K 88 AGS 5937.

ORACLE®

FEDERAL DIVISION

Compatibility. Portability. Connectability. Capability.

Oracle Federal Division
3 Bethesda Metro Center, Suite 1400
Bethesda, MD 20814

Circle Reader Action No. 494

New Product Ideas

New Product Ideas are just a few of the many innovations described in this issue of *NASA Tech Briefs* and having promising commercial applications. Each is discussed further on the referenced page in the appropriate section in this issue. If you are interested in developing a product from these or other NASA innovations, you can receive further technical information by requesting the TSP referenced at the end of the full-length article or by writing the Technology Utilization Office of the sponsoring NASA center (see page 18). NASA's patent-licensing program to encourage commercial development is described on page 16.

Making More Efficient Use of Battery-Plate Mass

Thanks to an improved active material for the positive plate of a lead/acid electric storage battery, 65 to 68 percent of the active mass of the plate can be used to generate electric current as opposed to 25 to 40 percent by conventional plates. In preliminary tests, a cell was charged and deeply discharged more than 2,000 times with no signs of "fading."
(See page 34)

Electronically Scanned Laser Rangefinder

A proposed electronic laser scanner for guiding robotic vehicles around obstacles would sweep across its field of view without any moving parts, measuring the distances to objects between 0.5 and 20 meters away.
(See page 46)

Sensor Detects Overheating of Perishable Material

An experimental temperature sensor changes color rapidly and irreversibly when its temperature rises above a predetermined level. Such devices could be used to detect dangerous disruptions in refrigeration of foods or medicines during shipment or storage.
(See page 95)

Compliant Joints for Robots

Misalignments between tools and robotic manipulators are accommodated by newly devised compliant joints. A typical joint has some of the characteristics and appearance of both a universal-joint and a cable-spring-type flexible shaft coupling.
(See page 70)

Ethynyl-Terminated Imidothioethers and Derived Resins

Blends of ethynyl-terminated imidothioethers and ethynyl-terminated arylene ether oligomers of various molecular weights were prepared. Such blends exhibit excellent processability, good fracture toughness, resistance to solvents, and adhesive and composite properties than do comparable bismaleimides.
(See page 59)

Improved Thermal-Switch Disks Protect Batteries

Improved thermal-switch disks containing a conductive polymer help to protect electrical batteries against high currents. The polymer undergoes an abrupt increase in electrical resistance when excessive current raises its temperature above a specific point and reverts to low resistance after cooling.
(See page 24)

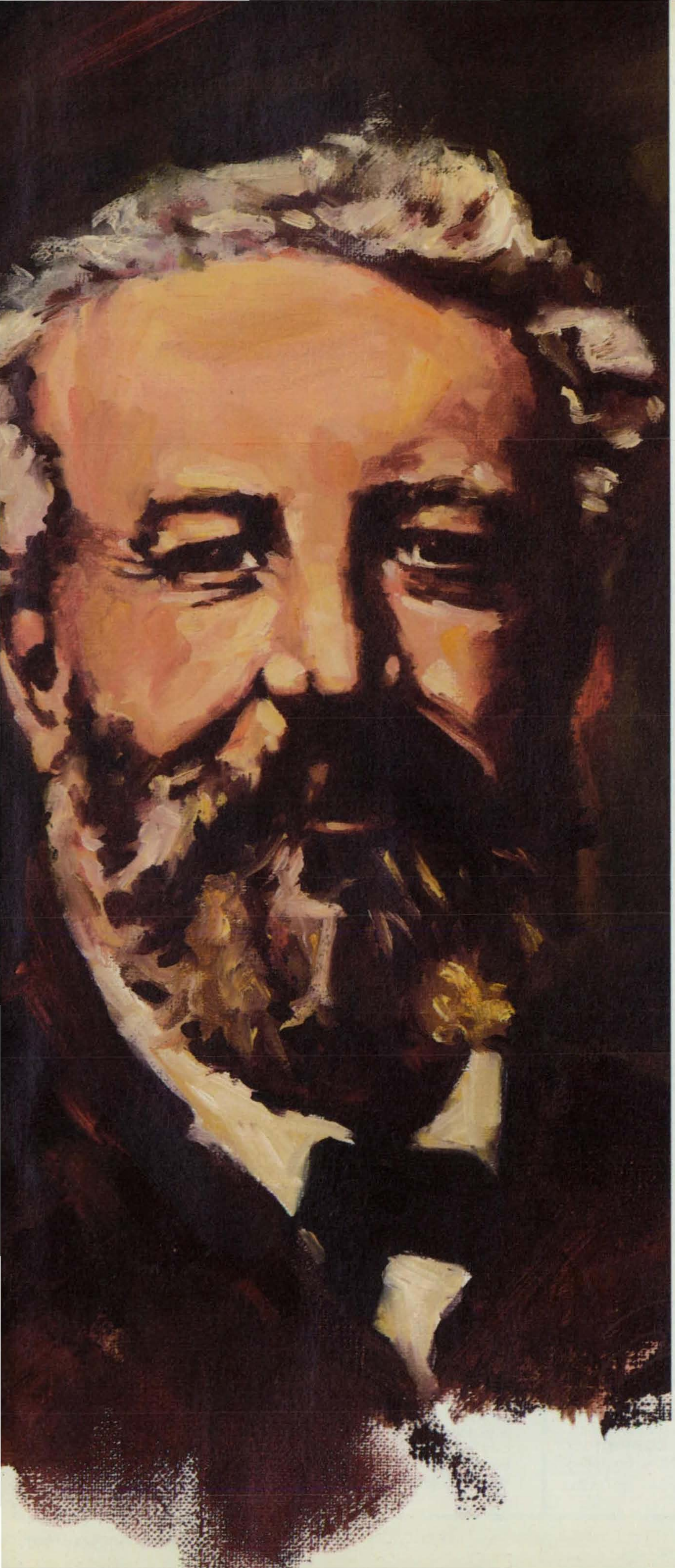

"Anything that one man can imagine, other men can make real."

Jules Verne
French Writer & Visionary
1828-1905

At Ford Aerospace, realizing customers' ideas is our business.

Flying an early bird. Our Japanese customer requires a new communications satellite. The most powerful commercial satellite ever built, tailored specifically to their needs. On a highly-accelerated schedule. We accepted the challenge and we're delivering. Our team is completing the advanced Superbird up to a year earlier than the norm.

Boosting productivity. We operate and maintain the Air Force's satellite tracking stations around the world. Requirements are increasing. So are costs. We're doing something about it. Our new Automated Remote Tracking Station could slash operating costs 60% or more. And still maintain 99.9% availability.

Securing America's future with advanced technology.

Ford Aerospace

- Command, Control, Communications and Intelligence
- Tactical Weapons Systems
- Space Systems
- Technical Services

HOW YOU CAN BENEFIT FROM NASA's TECHNOLOGY UTILIZATION SERVICES

If you're a regular reader of TECH BRIEFS, then you're already making use of one of the low- and no-cost services provided by NASA's Technology Utilization (TU) Network. But a TECH BRIEFS subscription represents only a fraction of the technical information and applications/engineering services offered by the TU Network as a whole. In fact, when all of the components of NASA's Technology Utilization Network are considered, TECH BRIEFS represents the proverbial tip of the iceberg.

We've outlined below NASA's TU Network—named the participants, described their services, and listed the individuals you can contact for more information relating to your specific needs. We encourage you to make use of the information, access, and applications services offered by NASA's Technology Utilization Network.

How You Can Utilize **NASA's Industrial Applications Centers**—A nationwide network offering a broad range of technical services, including computerized access to over 100 million documents worldwide.

You can contact NASA's network of Industrial Applications Centers (IACs) for assistance in solving a specific technical problem or meeting your information needs. The "user friendly" IACs are staffed by technology transfer experts who provide computerized information retrieval from one of the world's largest banks of technical data. Nearly 500 computerized data bases, ranging from NASA's own data base to Chemical Abstracts and INSPEC, are accessible through the ten IACs located throughout the nation. The IACs also offer technical consultation services and/or linkage with other experts in the field. You can obtain more information about these services by calling or writing the nearest IAC. User fees are charged for IAC information services.

Aerospace Research Applications Center (ARAC)
Indianapolis Center for Advanced Research
611 N. Capitol Avenue
Indianapolis, IN 46204
Dr. F. Timothy Janis, Director
(317) 262-5036

Central Industrial Applications Center/NASA (CIAC)
Rural Enterprises, Inc.
P.O. Box 1335
Durant, OK 74702
Dr. Dickie Deel, Director
(405) 924-5094

Science and Technology Research Center (STRC)
Post Office Box 12235
Research Triangle Park, NC 27709-2235
H.L. (Lynn) Reese, Director
(919) 549-0671

NASA Industrial Applications Ctr. 823 William Pitt Union
University of Pittsburgh
Pittsburgh, PA 15260
Robert G. Konecny, Acting Director
(412) 648-7000

NASA/Southern Technology Applications Center
Box 24
Progress Ctr., One Progress Blvd.
Alachua, FL 32615
J. Ronald Thornton, Director
(904) 462-3913
(800) 354-4832 (FL only)
(800) 225-0308 (toll-free US)

NASA/UK Technology Applications Program
University of Kentucky
109 Kinkead Hall
Lexington, KY 40506-0057
William R. Strong, Director
(606) 257-6322

NERAC, Inc.
One Technology Drive
Tolland, CT 06084
Dr. Daniel U. Wilde, President
(203) 872-7000

Technology Application Center (TAC)
University of New Mexico
Albuquerque, NM 87131
Dr. Stanley A. Morain, Director
(505) 277-3622

NASA Industrial Applications Center
University of Southern California Research Annex
3716 South Hope Street
Los Angeles, CA 90007-4344
Robert Stark, Director
(213) 743-6132
(800) 642-2872 (CA only)
(800) 872-7477 (toll-free US)

NASA/SU Industrial Applications Center
Southern University Department of Computer Science
P.O. Box 9737
Baton Rouge, LA 70813-9737
Dr. John Hubbell, Director
(504) 771-6272

If you represent a public sector organization with a particular need, you can contact NASA's Application Team for technology matching and problem solving assistance. Staffed by professional engineers from a variety of disciplines, the Application Team works with public sector organizations to identify and solve critical problems with existing NASA technology. **Technology Application Team, Research Triangle Institute, P.O. Box 12194, Research Triangle Park, NC 27709. *Doris Rouse, Director,* (919) 541-6980**

How You Can Access Technology Transfer Services At NASA Field Centers: **Technology Utilization Officers & Patent Counsels**—Each NASA Field Center has a Technology Utilization Officer (TUO) and a Patent Counsel to facilitate technology transfer between NASA and the private sector.

If you need further information about new technologies presented in *NASA Tech Briefs,* request the Technical Support Package (TSP). If a TSP is not available, you can contact the Technology Utilization Officer at the NASA Field Center that sponsored the research. He can arrange for assistance in applying the technology by putting you in touch with the people who developed it. If you want information about the patent status of a technology or are interested in licensing a NASA invention, contact the Patent Counsel at the NASA Field Center that sponsored the research. Refer to the NASA reference number at the end of the Tech Brief.

Ames Research Ctr.
Technology Utilization Officer: Laurance Milov
Mail Code 223-3
Moffett Field, CA 94035
(415) 604-4044
Patent Counsel: Darrell G. Brekke
Mail Code 200-11
Moffett Field, CA 94035
(415) 604-5104

Lewis Research Center
Technology Utilization Officer: Anthony F. Ratajczak (acting)
Mail Stop 7-3
21000 Brookpark Road
Cleveland, OH 44135
(216) 433-5568
Patent Counsel: Gene E. Shook
Mail Code LE-LAW
21000 Brookpark Road
Cleveland, OH 44135
(216) 433-5753

John C. Stennis Space Center
Technology Utilization Officer: Robert M. Barlow
Code HA-32
Stennis Space Center, MS 39529
(601) 688-1929

John F. Kennedy Space Center
Technology Utilization Officer: Thomas M. Hammond
Mail Stop PT-PMO-A
Kennedy Space Center, FL 32899
(407) 867-3017
Patent Counsel: James O. Harrell
Mail Code PT-PAT
Kennedy Space Center, FL 32899
(407) 867-2544

Langley Research Ctr.
Technology Utilization Officer: John Samos
Mail Stop 139A
Hampton, VA 23665
(804) 864-2484
Patent Counsel: George F. Helfrich
Mail Code 279
Hampton, VA 23665
(804) 864-3523

Goddard Space Flight Center
Technology Utilization Officer: Donald S. Friedman
Mail Code 702.1
Greenbelt, MD 20771
(301) 286-6242
Patent Counsel: R. Dennis Marchant
Mail Code 204
Greenbelt, MD 20771
(301) 286-7351

Jet Propulsion Lab.
NASA Resident Office
Technology Utilization Officer: Gordon S. Chapman
Mail Stop 180-801
4800 Oak Grove Drive
Pasadena, CA 91109
(818) 354-4849
Patent Counsel: Paul F. McCaul
Mail Code 180-801
4800 Oak Grove Drive
Pasadena, CA 91109
(818) 354-2734
Technology Utilization Mgr. for JPL: Dr. Norman L. Chalfin
Mail Stop 156-211
4800 Oak Grove Drive
Pasadena, CA 91109
(818) 354-2240

George C. Marshall Space Flight Center
Technology Utilization Officer: Ismail Akbay
Code AT01
Marshall Space Flight Center, AL 35812
(205) 544-2223
Fax (205) 544-3151
Patent Counsel: Bill Sheehan
Mail Code CC01
Marshall Space Flight Center, AL 35812
(205) 544-0021

Lyndon B. Johnson Space Center
Technology Utilization Officer: Dean C. Glenn
Mail Code IC-4
Houston, TX 77058
(713) 483-3809
Patent Counsel: Edward K. Fein
Mail Code AL3
Houston, TX 77058
(713) 483-4871

NASA Headquarters
Technology Utilization Officer: Leonard A. Ault
Code CU
Washington, DC 20546
(202) 453-8377
Assistant General Counsel for Patent Matters: Robert F. Kempf, Code GP
Washington, DC 20546
(202) 453-2424

A Shortcut To Software: **COSMIC®**—For software developed with NASA funding, contact COSMIC, NASA's Computer Software Management and Information Center. New and updated programs are announced in the Computer Programs section. COSMIC publishes an annual software catalog. For more information call or write: **COSMIC®**, 382 East Broad Street, Athens, GA 30602 *John A. Gibson, Dir.,* (404) 542-3265

If You Have a Question . . . **NASA Scientific & Technical Information Facility** can answer questions about NASA's Technology Utilization Network and its services and documents. The STI staff supplies documents and provides referrals. Call, write or use the feedback card in this issue to contact: **NASA Scientific and Technical Information Facility,** Technology Utilization Office, P.O. Box 8757, Baltimore, MD 21240-0757. *Walter M. Heiland, Manager,* (301) 859-5300, Ext. 242, 243

ANOTHER ASTRO-MED FIRST IN 8-CHANNEL RECORDERS

LASER PRINTER RESOLUTION!

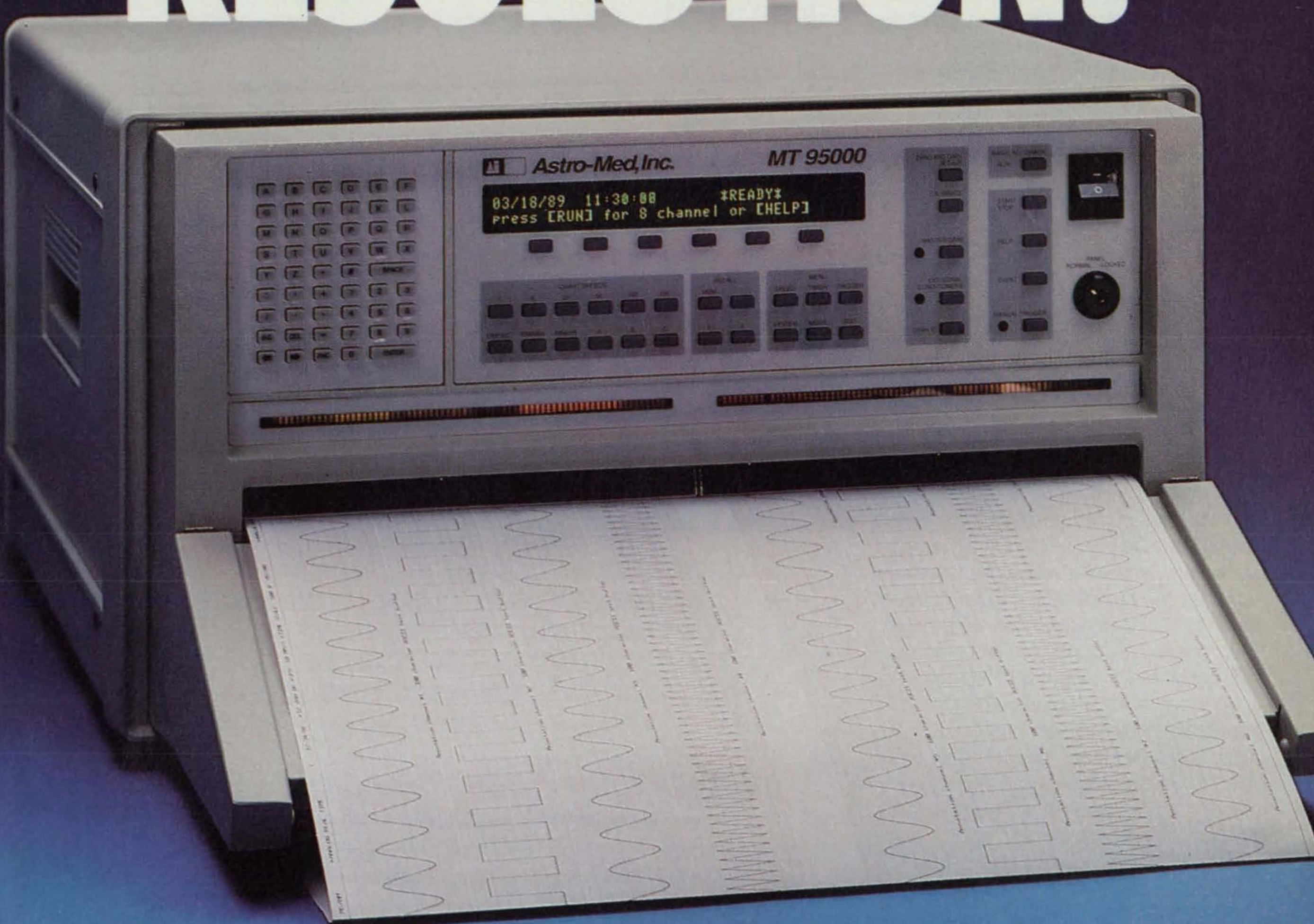

- **Laser Quality Writing—300 dpi**
- **20 kHz Frequency Response**
- **Automatic Self-Calibration—Traceable to NBS**
- **Expandable to 16 Channels**
- **Data Capture with 200 kHz Sample Rate Per Channel**
- **Built-In Programmable Signal Conditioners**

From its laser-sharp charts to its unparalleled frequency response, this remarkable new 8-channel recorder brings you the technology of the Twenty-First Century today! It outperforms even Astro-Med's MT-9500, which in 1987 was heralded as the first breakthrough in 8-channel recorders in 20 years. It has 50% more resolution, 4 times higher frequency response, and 8 times more memory than the MT-9500. With automatic self-calibration traceable to NBS, expandability to 16 channels, and a host of other important features. We call it the MT-95000, a product so unique that it is protected by U.S. Patent No. 4,739,344.

Phone, Fax or Write for details!

Astro-Med, Inc.®

Astro-Med Industrial Park, West Warwick Rhode Island 02893
Telephone (401) 828-4000 • Toll Free 800-343-4039
Telex No. 710-382-6409 • Fax (401) 822-2430

Circle Reader Action No. 405

Superlattice Long-Wavelength Infrared Sensors

A superlattice of LaN and Si could detect at wavelengths up to 12 μm.

NASA's Jet Propulsion Laboratory, Pasadena, California

If LaN can be grown epitaxially on silicon, as appears likely, the sensitivity of silicon-based photodetectors could be extended farther into the infrared wavelength region with high quantum detection efficiency by the use of LaN/Si superlattices (see figures). In principle, by appropriate choice of the thicknesses of layers, the effective band-gap energy of a superlattice structure could be set to any desired value between that of the band gaps of the two materials.

The effective band gap determines the long-wavelength cutoff of the detector; photons of energy lower than the band-gap energy cannot be detected because they cannot cause photoexcitation of carriers across the gap. The band gaps of LaN (a semimetallic compound) and silicon are 0 and 1.1 eV, respectively. As a practical matter, variations in thicknesses of the layers will set some lower limit to the achievable band gap. However, gaps as small as about 0.1 eV, representing a cutoff wavelength of 12 μm, should be feasible. In contrast, present silicon-based intrinsic sensors cut off at wavelengths of 2 μm or less.

Infrared detectors made of HgTe/CdTe superlattices have been proposed previously; there has been considerable work on such devices. However, it is extremely difficult to grow such materials epitaxially on silicon. Compatibility with silicon is desirable for image-array applications because it would enable the integration of closely spaced infrared sensors with charge-coupled-device (CCD) or metal oxide/semiconductor field-effect transistor (MOSFET) multiplexing read-out circuitry on the same silicon chip.

Most likely, the CCD's or MOSFET's would be fabricated first, leaving windows of bare silicon in which the LaN/Si superlattices would be grown by molecular-beam epitaxy, the low growth temperatures of which would prevent damage to the CCD's or MOSFET's. Alternatively, the superlattices might be grown first. However, the superlattices might not survive the fabrication of the CCD's or MOSFET's.

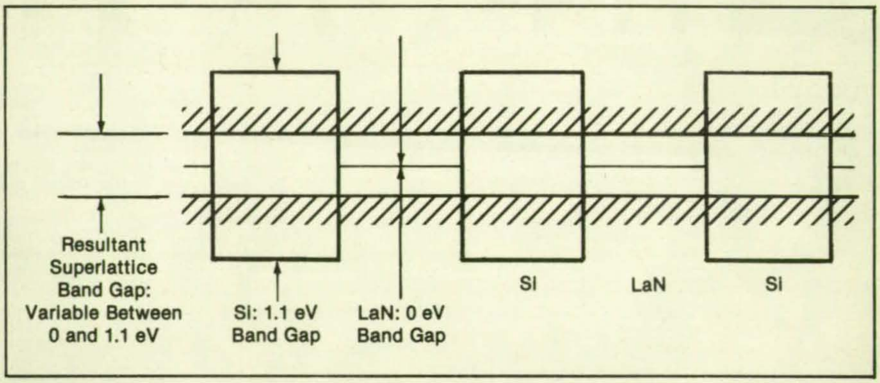

Figure 1. The **Energy-Band Diagram of LaN/Si Superlattice** shows that the band gap of the superlattice is intermediate to those of the Si and the LaN.

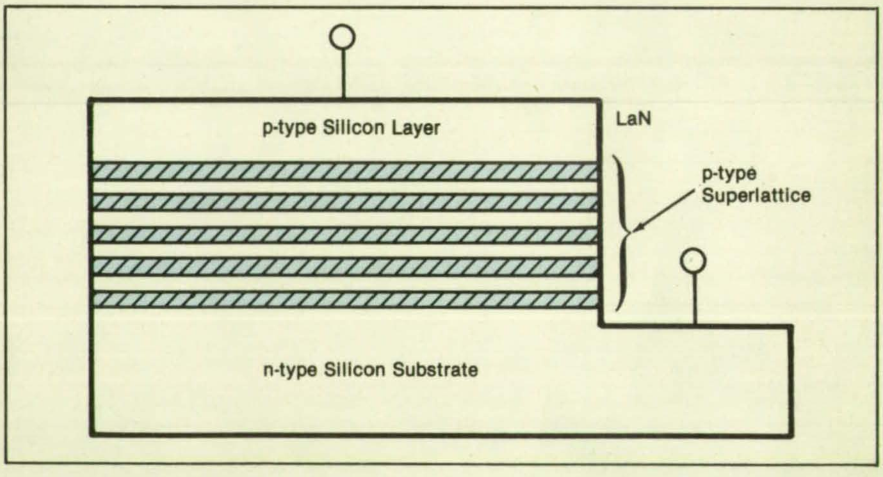

Figure 2. This **LaN/Si Superlattice** would function as a photodiode.

LaN might be deposited in a molecular-beam-epitaxy system by laser ablation of LaN or by evaporation of pure La from an electron-gun source or an effusion oven in the presence of either gaseous nitrogen or a jet of atomic nitrogen. For evaporation of silicon for epitaxy on LaN, an electron-gun evaporator could be used.

Compounds of the form RN (where R is a rare earth) have lattice parameters smaller than those of silicon, while the lattice parameters of RAs and RP are larger than those of silicon. All of these compounds have the NaCl crystalline structure. Although it would be possible to alloy these materials to match the lattice parameter of silicon exactly, it may not be necessary because LaN has a lattice constant only 2.6 percent smaller than that of silicon. Thus, it may be possible to use LaN without alloying it with LaAs or LaP, thereby avoiding both the toxicity of As and P and the potential problem of autodoping of the silicon with As and P. On the other hand, better chemical stability may be possible with compounds other than LaN, as LaN is somewhat water soluble.

This work was done by Robert W. Fathauer of Caltech for **NASA's Jet Propulsion Laboratory**. *For further information, Circle 132 on the TSP Request Card.* *NPO-17713*

Nicolet 400.

The only DSO with an expandable 64K-256K per channel memory.

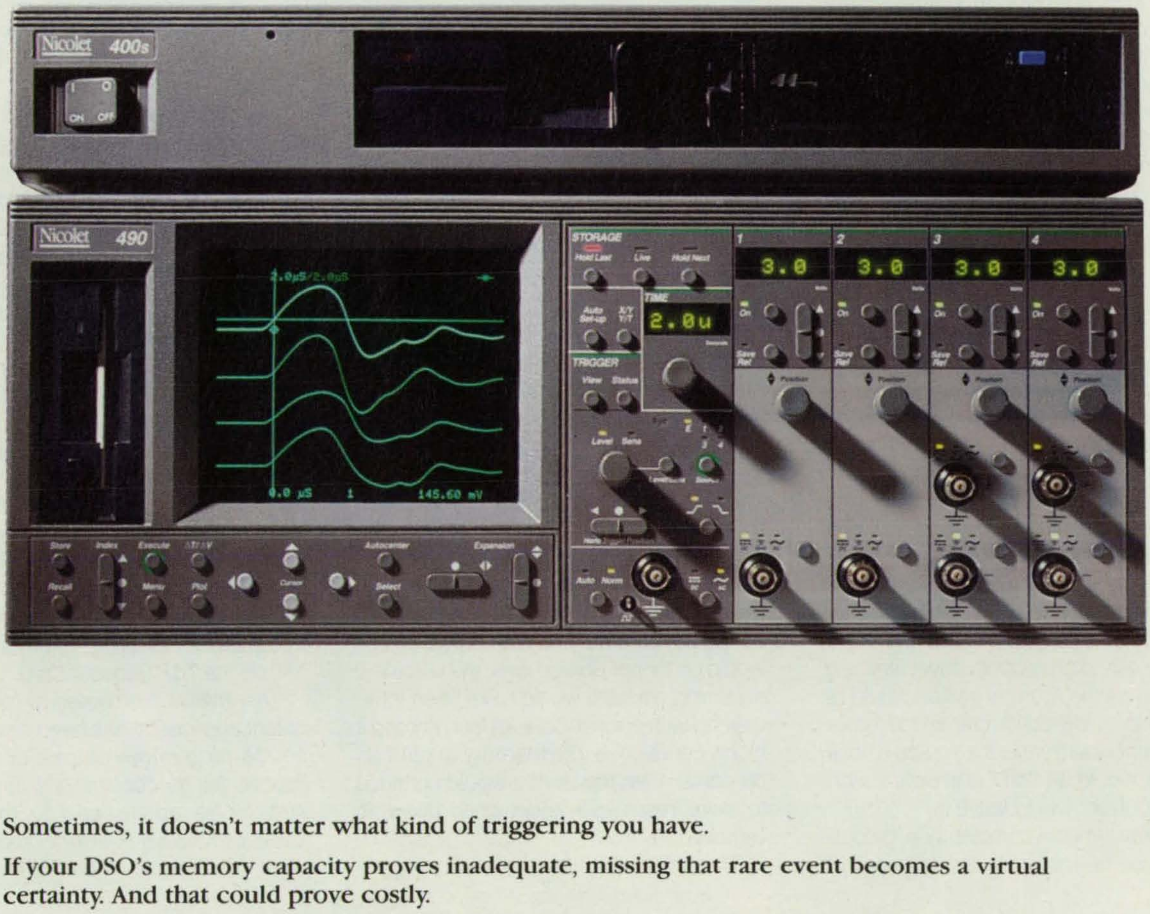

Sometimes, it doesn't matter what kind of triggering you have.

If your DSO's memory capacity proves inadequate, missing that rare event becomes a virtual certainty. And that could prove costly.

This is precisely why we designed the high precision Nicolet 400 DSO Series with expandable 64K-256K memory per channel. (That's 5 to 10 times more than the nearest competition.) And an optional 44MB removable hard disk, also only from Nicolet: to make sure the 400 you buy doesn't draw a blank when you might need it most.

With seven different models and over 200 configurations, you're able to choose the number of channels, memory, speed and resolution right for you. Each 400 features a LEARN mode to help automate test sequences, along with FFT and averaging for complete waveform processing. Even an optional dual timebase, or powerful *Nicolet-Windows*™ PC software for instant remote control.

So learn more about the 400 soon. Send for details now, or call 1-800-356-3090.

Nicolet Test Instruments Division

5225 Verona Road, Madison, WI 53711-4495
608/273-5008 or 800/356-3090

Nicolet

INSTRUMENTS OF DISCOVERY

Circle Reader Action No. 696

Nonvolatile Ionic Two-Terminal Memory Device

A proposed device would be electrically programmable and erasable.

NASA's Jet Propulsion Laboratory, Pasadena, California

A conceptual solid-state memory device would be nonvolatile and erasable and would have only two terminals instead of the usual three. The proposed device is based on two effects: thermal phase transition and reversible intercalation of ions.

Devices of this type would be usable in digital computers and neural-network computers, much as random-access memories are used today. In neural networks, many small, densely packed switches would function as erasable, nonvolatile synaptic elements.

A single switching element would consist of electrical terminals separated by two parallel conduction paths — one through corrosion-resistant metal, a resistor, and an electrical switching element; the other through a thermal switching element, corrosion-resistant metal, an ion source, and an ionic conductor connected to the electrical switching element of TiO_2, V_2O_5, or WO_3 (see figure). The electrical conductance of the electrical switching element would depend on the degree of its intercalation — that is, the extent to which sodium is combined chemically with the refractory-metal oxide. The conductance of the thermal switch would depend on its temperature; it would be made of one or more vanadium oxide(s) or organic semiconductor(s), which undergo a change in phase to a state of high conductivity when heated above room temperature.

When the device is in an initial low-conductance, quiescent state, the terminals should be nearly electrically isolated from each other because the electrical switch would not be intercalated and, therefore, would be only slightly conductive. Similarly, inasmuch as the thermal switch would be cool and in its low-conductance (off) state, little current would enter the source of ions, so it, too, would be "off," and only a slight leakage current would leave it.

However, when a sufficiently large positive voltage is applied to the terminals, a small current should enter the thermal switch, enough to heat it to its high-conductance "on" state. Current from the thermal switch would then stimulate a flow of sodium ions through the ion conductor into the electrical switching element. (The source of ions would be a highly intercalated material like $NaTiO_2$ or $NaWO_3$: electron current causes such materials to give off their sodium ions.) Enriched by the sodium ions, the electrical switching element would become highly conductive (turn "on") and connect both terminals through the resistor.

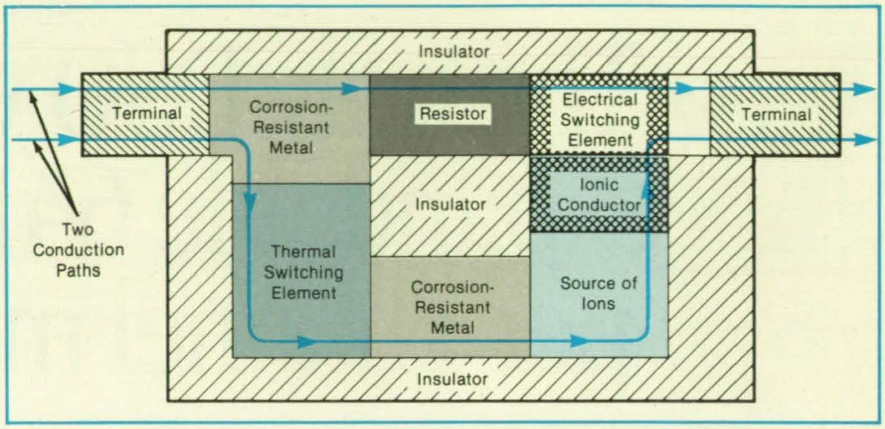

The **Transfer of Sodium Ions** between the source of ions and the electrical switching element would increase or decrease the electrical conductance of that element, thus turning the switch "on" or "off."

The high voltage on the terminals would thus have written a "one" or "zero" in the device. Removal of the writing voltage would not erase the memory. Even though the thermal switch would return to its low-conductance state and the source of ions would no longer donate ions, the electrical switching element would have been intercalated with enough sodium ions to keep it highly conductive. The memory would thus be nonvolatile; the device would continue to store information even when power is removed.

The information would be read by applying a voltage lower than the writing voltage but of the same polarity. If the electrical switching element were "on," a significant current — limited by the resistor — would pass through it. If the electrical switching element were "off," only leakage current would pass.

The information would be erased by applying a voltage larger than the writing voltage but of opposite polarity. Ionic current would pass from the electrical switching element through the ion conductor to the source of ions. Sodium ions would thereby be drained from the electrical switching element, which would revert to its poorly conducting state and remain there when the erasing voltage is removed.

This work was done by Roger M. Williams of Caltech for **NASA's Jet Propulsion Laboratory**. *For further information, Circle 140 on the TSP Request Card.*

This invention is owned by NASA, and a patent application has been filed. Inquiries concerning nonexclusive or exclusive license for its commercial development should be addressed to the Patent Counsel, NASA's Resident Office-JPL [see page 16]. Refer to NPO-17621

Recovering Energy From a Rapidly Switched Gate

The gate capacitance would be charged and discharged efficiently.

NASA's Jet Propulsion Laboratory, Pasadena, California

A circuit has been proposed to recover the energy usually lost in charging and discharging the internal gate capacitance of a field-effect transistor during high-frequency switching.

The scheme includes a pulse-forming circuit that would generate a rectangular waveform with zero-level notches near the beginning and end of the "on" period. An inductor would resonate the internal gate capacitance so that the energy could be recovered during the notches (see figure).

Synchronized by a conventional gate-drive signal v_{in}, the pulse-forming circuit would drive complementary metal-oxide/semiconductor transistors Q_1 and Q_2 to produce the notched gate-drive waveform v_x for field-effect transistor Q_3. The zero-level notches would have equal durations ΔT; the notches at the beginning and end of the "on" period would be preceded and


TEAM WORK
THE COOPERATION OF 5 COUNTRIES HAS ASSURED EFFICIENCY ON THE GROUND AND RELIABILITY IN THE AIR: AIRBUS WAS DESIGNED AND EQUIPPED THROUGH THE COOPERATION AND PARTNERSHIP OF 4 EUROPEAN COUNTRIES AND THE U.S.A. THE ENGINES AND AVIONICS FOR EXAMPLE, ARE PARTLY DESIGNED AND BUILT IN COOPERATION WITH THE AMERICANS. AIRBUS ANSWERS THE PRECISE REQUIREMENTS OF AMERICAN, PAN AM, NORTHWEST, EASTERN, CONTINENTAL, AIR CANADA AND CANADIAN INTERNATIONAL, WHO FLY AND WILL FLY THEIR COLORS. THE QUALITY OF THE WORK AND THE ORIGINALITY OF THE CREATIVE EFFORT KEEPS US UP THERE — MEET THE TEAM.
aerospatiale
AEROSPATIALE INC. 1101, 15TH STREET NW WASHINGTON DC 20005
PHONE: 202 293 0650
PUBLICIS ZB-A1

followed, respectively, by rectangular pulses also of duration ΔT.

In the following analysis, the effect of resistance in the gate circuit is neglected. The inductor would be chosen so that ΔT would be one-sixth of the period of the series resonance between the inductor and the internal gate capacitance; that is, $\Delta T = (\pi/3)\sqrt{LC}$, where L = the inductance, and C = the capacitance. During the initial turn-on period 1, v_x would equal the supply voltage V_{CC}, causing the gate-drive current i_L in the inductor to rise sinusoidally, as during the first 60° of the resonant cycle. During the notch interval 2, v_x would be zero, causing i_L to decay sinusoidally, as during the period of 120° to 180° of the resonant cycle. At the end of interval 2, i_L would be zero; that is, all the energy formerly stored in L would then be stored in C, and the field-effect transistor would be fully turned on, with gate voltage $v_g = V_{CC}$.

Near the end of the "on" period, the process would be reversed. During notch interval 3, C would begin to discharge by a 60° sinusoidal growth of i_L in the opposite direction. The final pulse of $v_x = V_{CC}$ during interval 4 would reverse this sinusoidal growth, bringing i_L back to zero. Thus, at the end of the "on" period, all the energy previously stored in L and C would have been returned to the power supply.

This work was done by Wally E. Rippel of Caltech for **NASA's Jet Propulsion Laboratory**. *For further information, Circle 87 on the TSP Request Card.*

In accordance with Public Law 96-517, the contractor has elected to retain title to this invention. Inquiries concerning rights for its commercial use should be addressed to

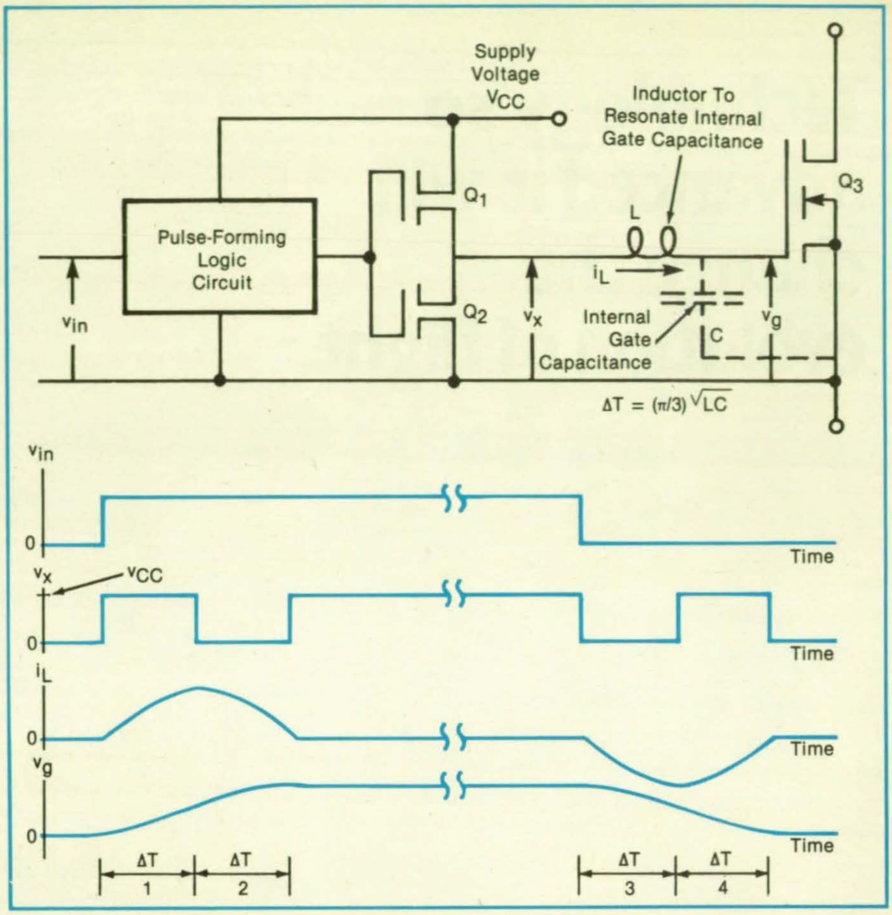

Notches in the Gate-Drive Waveform v_x act in concert with the series resonance of L and C to charge and discharge C efficiently and rapidly.

Edward Ansell
Director of Patents and Licensing
Mail Stop 305-6
California Institute of Technology
1201 East California Boulevard
Pasadena, CA 91125

Refer to NPO-17221, volume and number of this NASA Tech Briefs *issue, and the page number.*

Improved Thermal-Switch Disks Protect Batteries

Insulating washers hold disks in place to prevent additional short circuits.

Lyndon B. Johnson Space Center, Houston, Texas

Improved thermal-switch disks help to protect electrical batteries against high currents like those due to short circuits or high demands for power in the circuits supplied by the batteries. By protecting against overcurrents, the thermal-switch disks also protect batteries against excessive temperatures. For example, short-circuit tests of commercial alkaline cells have resulted in temperatures above 150 °C.

The disks (Polyswitch or equivalent) contain a conductive polymer that undergoes an abrupt increase in electrical resistance when excessive current raises its temperature (or the ambient temperature rises) above a specific point. After cooling, the polymer reverts to low resistance. Thus, unlike conventional fuses, the disks can be reused.

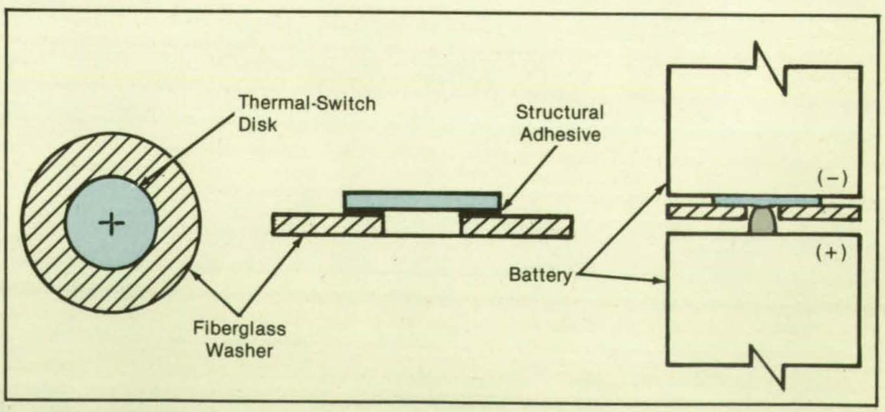

The **Thermal-Switch Disk** is centered by an insulating fiberglass washer.

A disk is placed between the central positive button contact of one cell and the negative contact surface of the next cell in series. A disk of the conventional design consists of a layer of polymer coated on both faces with stainless steel. Its current rating depends on its diameter and thickness. Because it is expensive to make the changes in machinery necessary to change

the thickness, the current rating is usually set in manufacturing by the choice of diameter.

Whether or not the diameter of the disk is as large as that of the battery compartment, the metal faces of the disk can make a short circuit with the conductive wall of the battery compartment if the disk is dislodged from its nominal position by vibration or shock. Furthermore, if the disk has a very small diameter, dislodgment may or may not cause a short circuit, but in any case can result in loss of the protective function.

In the improved thermal switch (see figure), the disk is mounted centrally on an electrically insulating fiberglass washer and bonded to it by a Hysol (or equivalent) structural adhesive. The hole in the washer accommodates the positive button contact of one cell, while the negative end of the other cell makes flush surface contact with the disk. The outer diameter of the washer is slightly less than that of the battery compartment. Thus, the washer holds the disk in position, preventing both the loss of the protective function and short circuits to the wall.

This work was done by Eric Darcy and Bobby Bragg of **Johnson Space Center**. *No further documentation is available.*

This invention is owned by NASA, and a patent application has been filed. Inquiries concerning nonexclusive or exclusive license for its commercial development should be addressed to the Patent Counsel, Johnson Space Center [see page 16]. Refer to MSC-21428.

Integrated Electro-optical Laser-Beam Scanners

Scanners using solid-state devices would be compact, consume little power, and have no moving parts.

Lyndon B. Johnson Space Center, Houston, Texas

Integrated all-solid-state electro-optical laser-beam scanners have been proposed for such diverse applications as nonimpact laser printing, color imaging, ranging, bar-code reading, and robotic vision. The new scanners would be more compact, weigh less, and consume less power than mechanical laser-beam scanners do. They would also be more reliable because, unlike mechanical scanners, they would contain no moving parts. Moreover, the new scanners would offer beam-deflection angles larger than those of acousto-optic scanners.

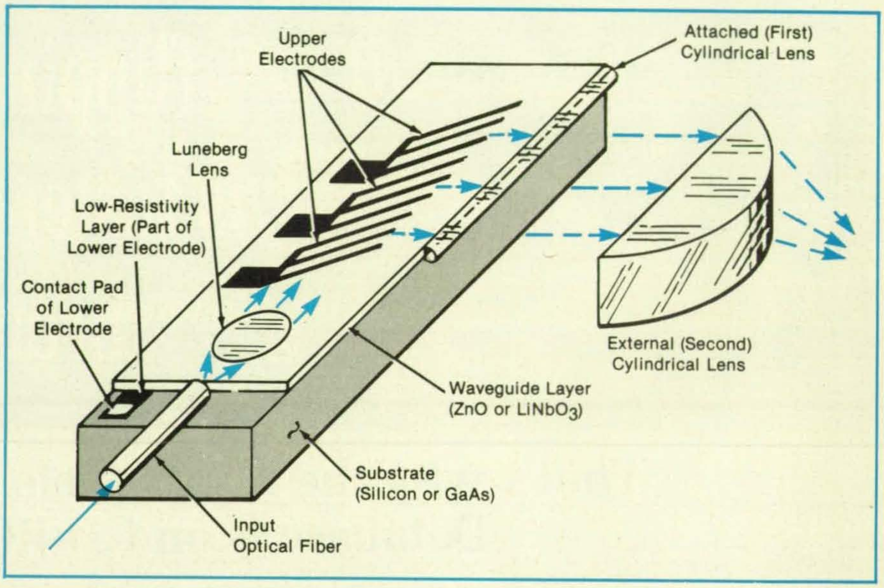

The **Integrated Electro-optical Laser Scanner**, in conjunction with the external lens, would point the outgoing beam of light in any of a number of different directions, depending on the number of upper electrodes.

The figure illustrates, partially schematically, a scanner of the new type. The integrated electro-optical components would be fabricated on a substrate, which would preferably be made of silicon or of gallium arsenide. Ancillary integrated electronic circuits for processing the beam-scanning signals could also be fabricated on the substrate. A lower electrode consisting of a low-resistivity heavily-doped layer and a small metal contact pad would be formed on top of the substrate.

A waveguide layer would be deposited on top of the lower electrode. This layer would be made of zinc oxide or lithium niobate, either of which might be chosen because it exhibits the electro-optical effect and has an index of refraction greater than that of the substrate, lower electrode, and any cladding material that is to be deposited on top of it. Upper electrodes in the form of gratings tilted at 45° to the axis of the incoming beam would be deposited on top of the waveguide layer. An optical fiber would transmit the light from the laser to the scanner. A V-groove in the substrate would align the fiber with the midplane of the waveguide layer and along the axis. A Luneberg lens integral with the waveguide would collimate the light emerging from the fiber and direct it along the axis toward the grating electrodes.

The application of a suitable voltage to an upper electrode would generate a diffraction grating in the waveguide layer via the electro-optical effect. The grating spacing would be chosen so that the light would be diffracted perpendicularly from the axis of the device. The diffracted light would be focused by a cylindrical lens as it emerged from the side of the device. A second, external cylindrical lens perpendicular to the first one would point the output along a direction that would depend on the position of the diffracted beam and, therefore, on the position of the upper electrode that is energized at the moment. Thus, if the device includes many upper electrodes, the beam could be pointed to any of a large number of angles separated by small increments, effectively scanning over a wide angular range.

This work was done by Warren T. Boord of APA Optics, Inc., for **Johnson Space Center**. *For further information, Circle 42 on the TSP Request Card.*

In accordance with Public Law 96-517, the contractor has elected to retain title to this invention. Inquiries concerning rights for its commercial use should be addressed to

Edward Ansell
Director of Patents and Licensing
Mail Stop 301-6
California Institute of Technology
1201 East California Boulevard
Pasadena, CA 91125

Refer to MSC-21498, volume and number of this NASA Tech Briefs *issue, and the page number.*

Optoelectronic Integrated Circuits for Neural Networks

Many threshold devices would be placed on a single substrate.

NASA's Jet Propulsion Laboratory, Pasadena, California

Integrated circuits containing optoelectronic threshold (i.e., amplifying and switching) elements are being developed for use as planar arrays of artificial neurons in research on neural-network computers. These arrays would be mounted with volume holograms recorded in photorefractive crystals (e.g., $LiNbO_3$), which would serve as dense arrays of variable interconnections between the neurons (see Figure 1).

The integrated circuits could be made by existing GaAs technology. The initial design concept calls for a monolithically integrated circuit chip (2 by 2 cm in size) containing a square array of 100 by 100 neuron elements. Each element would contain an on-chip light source (laser or light-emitting diode) driven by a saturating amplifier (field-effect or bipolar transistor), which in turn would be driven by a photodetector. Alternatively, the saturating amplifier and photodetector could be combined in a phototransistor.

Figure 2(a) illustrates the cross-section of a candidate configuration for one element, which is currently pursued. In this version, light-emitting diodes were integrated with Darlington pairs of double-heterojunction bipolar phototransistors. A fabricated 10-by-10 array of optical neuron elements is shown in Figure 2(b).

In the future, the light source would be a surface-emitting laser diode with etched mirrors. Laser diodes of this type are easier to make than are the ones that emit perpendicularly to the plane. The exact shapes and dimensions of the features in this structure must be chosen to minimize coupling on the chip between the laser in each such element and the detector in the same or any other element. A highly reflective coating would be applied to at least one of the facets of the laser to reduce its threshold current and crosstalk.

The fabrication process has been designed to have few steps, to increase the yield on the wafer. However, the yield is not critical, in the sense that a circuit chip designed for use in a neural network can function properly even if it contains some defective neurons.

It will be important to reduce the consumption of power in each neuron. This could be accomplished by optimizing the thickness, composition, and doping of the epitaxial layers; reducing the width of the active laser region; and increasing the reflectivities of the laser mirrors. Furthermore, a semiconductor laser can be designed to minimize its heat dissipation at a given output power.

It has been estimated that each element would be on about half the time and would be required to emit up to about 100 μW of radiation. Assuming 10-percent efficiency, this amounts to an average dissipation of about 0.5 mW per element, or 5 W over the entire array in addition to the power dissipation due to the laser threshold current.

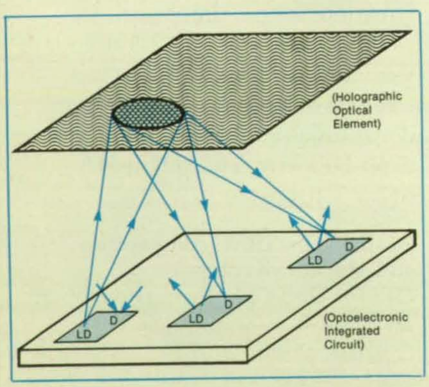

Figure 1. An **Optoelectronic Integrated Circuit** would be a planar array of optical "neuron" elements, each containing an on-chip light source and a photodetector. The holographic optical element would define the interconnections between the neurons.

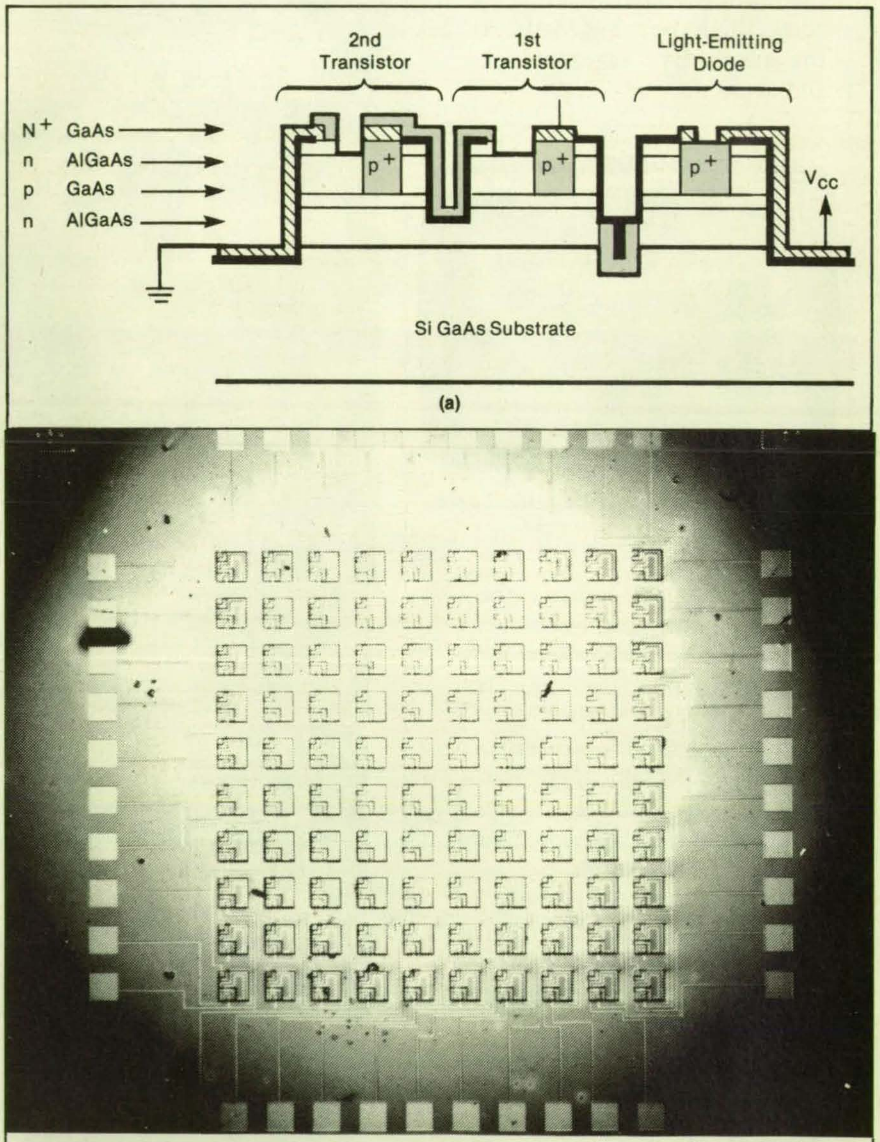

Figure 2(a). The **Cross Section of a Currently Pursued Configuration** for a one-neuron element consists of a light-emitting diode and a Darlington pair of double-heterojunction bipolar phototransistors. Part (b) shows a 10-by-10 array of monolithically integrated optical neuron elements.

However, with suitably sparse coding, this power requirement could be further reduced.

This work was done by D. Psaltis, J. Katz, Jae-Hoon Kim, S. H. Lin, and A. Nouhi of Caltech for **NASA's Jet Propulsion Laboratory**. *For further information, Circle 129 on the TSP Request Card.*
NPO-17652

Cheap Corner Reflectors for Radar

Retroreflectors are made from readily available materials at a small fraction of their usual cost.

NASA's Jet Propulsion Laboratory, Pasadena, California

Corner reflectors for radar can be constructed easily and inexpensively. Made of plastic pipe and wire mesh, the reflectors can be built at a cost of about $20 a piece for materials (1988 prices). In contrast, conventional all-aluminum reflectors can cost $600 to $1,000 a piece.

A corner reflector is retroreflective; that is, a radar signal that strikes any of its three mutually perpendicular surfaces is reflected back to the source. Corner reflectors are used as targets for the calibration of radars and as markers to identify points in radar imaging. Because the corner reflectors are typically deployed in groups of 10 or more, the new design can reduce costs significantly.

The materials for the new reflectors can be found in hardware and building-supply stores. No special skills or tools are needed for assembly. Panel frames are built from schedule 40 polyvinyl chloride (PVC) pipe and standard fittings, bonded together with joint cement. A panel frame may be triangular or square (see figure) and may range in size from 0.2 to 2.5 m on a side.

The frame is covered with wire mesh such as poultry wire, hardware cloth, or expanded metal. For efficient reflection, the holes in the mesh should be smaller than one-fourth the radar wavelength. Self-tapping screws and plastic cable ties hold the mesh to the frame. Fabric-backed aluminum tape covers the rough edges of the mesh.

Three covered panels are assembled with bolts so that their edges overlap. With reasonable care, the panels can be positioned so that they are mutually perpendicular to within 1°.

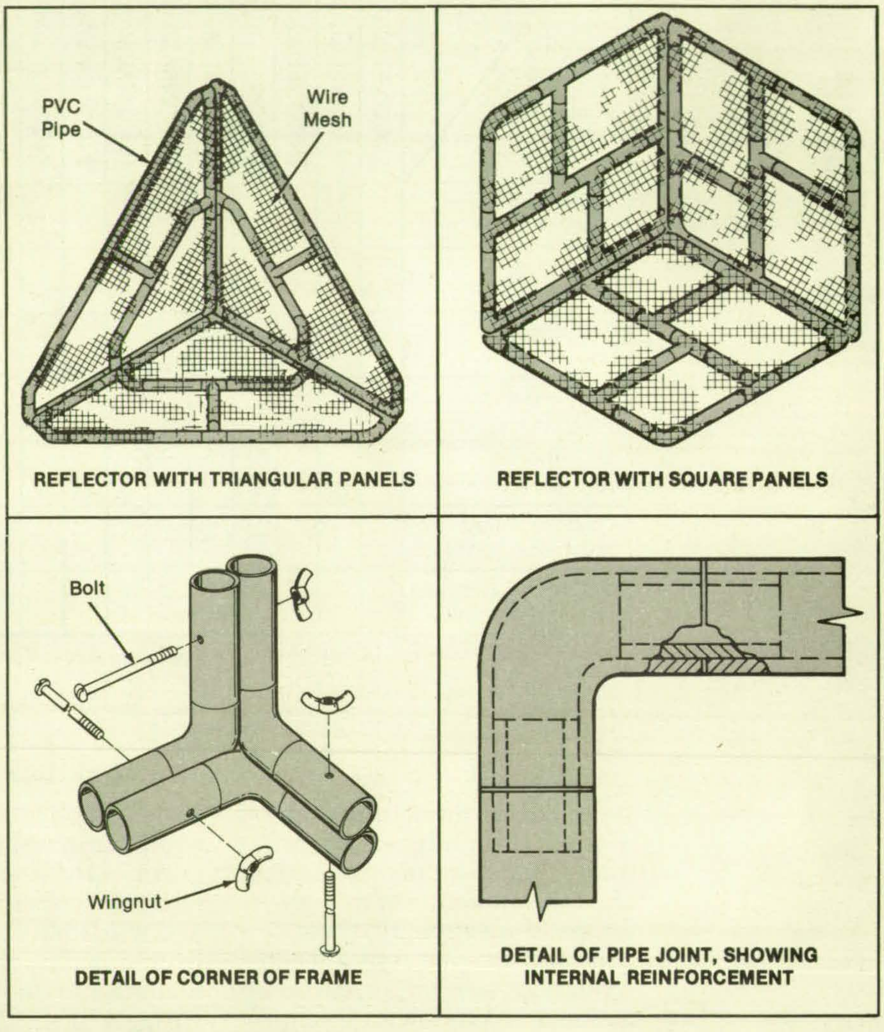

Wire Mesh on Plastic Pipe forms retroreflective panels of triangular or square shape. Panels are joined by bolts and wingnuts. Overlapping panel edges ensure mutual perpendicularity.

This work was done by E. R. Caro and L. J. Olivieri of Caltech for **NASA's Jet Propulsion Laboratory**. *For further information, Circle 95 on the TSP Request Card.*
NPO-17658

Optically-Tuned Far-Infrared Device

The spacing of a visible interference pattern determines the frequency of infrared radiation.

NASA's Jet Propulsion Laboratory, Pasadena, California

A variable photoconductivity grating formed by the interference of two visible laser beams that intersect on the surface of a proposed AlGaAs device would substitute for the fixed metal grating used in a typical existing device. The proposed device would provide higher output-power density and greater tunability than those available in the metal-grating devices.

The frequency of the two-dimensional plasmons in the device (and hence of the far-infrared radiation) is a function of the spatial periodicity of the plasmons, the surface density of electrons, the dielectric constant of the AlGaAs, and other parameters. The spatial period of the plasmons is constrained to that of the grating, whether the grating is metal or spatially modulated photoconductivity. In a conventional silicon metal-oxide/semiconductor field-effect transistor (MOSFET) device with a fixed metal grating, tuning is achieved by varying the gate voltage, which affects the surface density of electrons. However, the channel pinchoff phenomenon, common to all FET devices, limits the electric field that can be usefully applied between the drain and the

How to improve your station in life.

It's easy.

From now until June 30, 1990, just trade in your VAXstation™ 2000 workstation and Digital will give you \$2,000 off the purchase price of our VAXstation 3100 and VAXstation 3100 SPX workstations.

When you do, you're getting a lot more than just money off.

The VAXstation 3100 workstation delivers 3 to 4X the performance of the 2000. And the VAXstation 3100 SPX family delivers up to 10X the performance of entry-level VAXstation 3100 systems.

	VAXstation 2000	VAXstation 3100	VAXstation 3100 SPX
VUPs	1	4	4
Memory	6-14 MB	8-32 MB	8-32 MB
Disk Capacity	70-1.3 GB	104-1.3 GB	104-1.3 GB
Resolution	1024 x 864	1024 x 864	1024 x 864 or 1280 x 1024 (with Trinitron® displays)
Planes	1, 4, 8	1, 8	1, 8

All VAXstation 3100 workstations let you run DECwindows™ software. DECwindows gives you a consistent user interface for accessing applications on your network whether they're running on VMS,™ UNIX®/ULTRIX™ or MS-DOS.® You choose what you want and it shows up on screen the way you want.

And, even though the VAXstation 3100 and VAXstation 3100 SPX workstations are upgrades, you can use all the same software you've been using on the 2000. With no rewriting.

Take the all-important first step toward improving your station in life. Call 1-800-343-4040, ext. 874 to take advantage of this special \$2,000 offer.

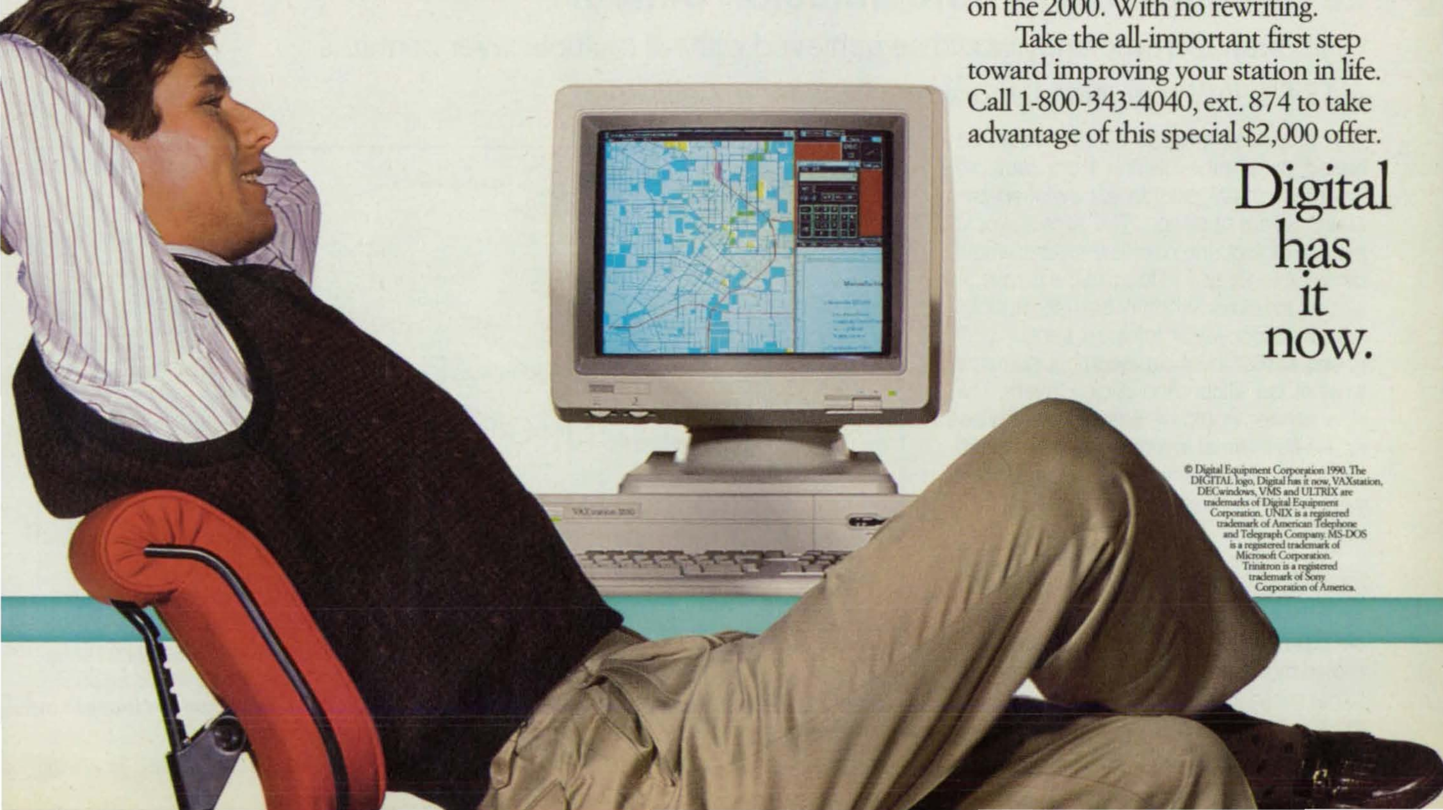

Digital has it now.

source; and this in turn limits the power density.

In the proposed device, the wavelength of the lasers (e.g., 623.8 nm for He/Ne lasers is short enough that the laser light would be strongly absorbed, generating electron/hole pairs in a pattern corresponding to the maximums and minimums of the interference pattern. The spatial modulation of conductivity thus produced would couple two-dimensional plasmons to the far-infrared radiation.

The spatial period of the grating could be varied by changing the wavelength of the illumination or the angle between the beams that control the frequency of the far-infrared radiation. The grating period Λ is $(\lambda/2)\sin(\theta/2)$, where λ is the laser wavelength and θ is the angle between the laser beams. Typically, Λ would be of the order of 10 μm. The efficiency of coupling between the plasmons and the far-infrared radiation would increase with the power of the lasers. The dissipation of heat from the absorption of the laser beams would be negligible.

This work was done by Joseph Katz of Caltech for **NASA's Jet Propulsion Laboratory**. *For further information, Circle 86 on the TSP Request Card.*

In accordance with Public Law 96-517, the contractor has elected to retain title to this invention. Inquiries concerning rights for its commercial use should be addressed to

Edward Ansell
Director of Patents and Licensing
Mail Stop 305-6
California Institute of Technology
1201 East California Boulevard
Pasadena, CA 91125

Refer to NPO-17160, volume and number of this NASA Tech Briefs *issue, and the page number.*

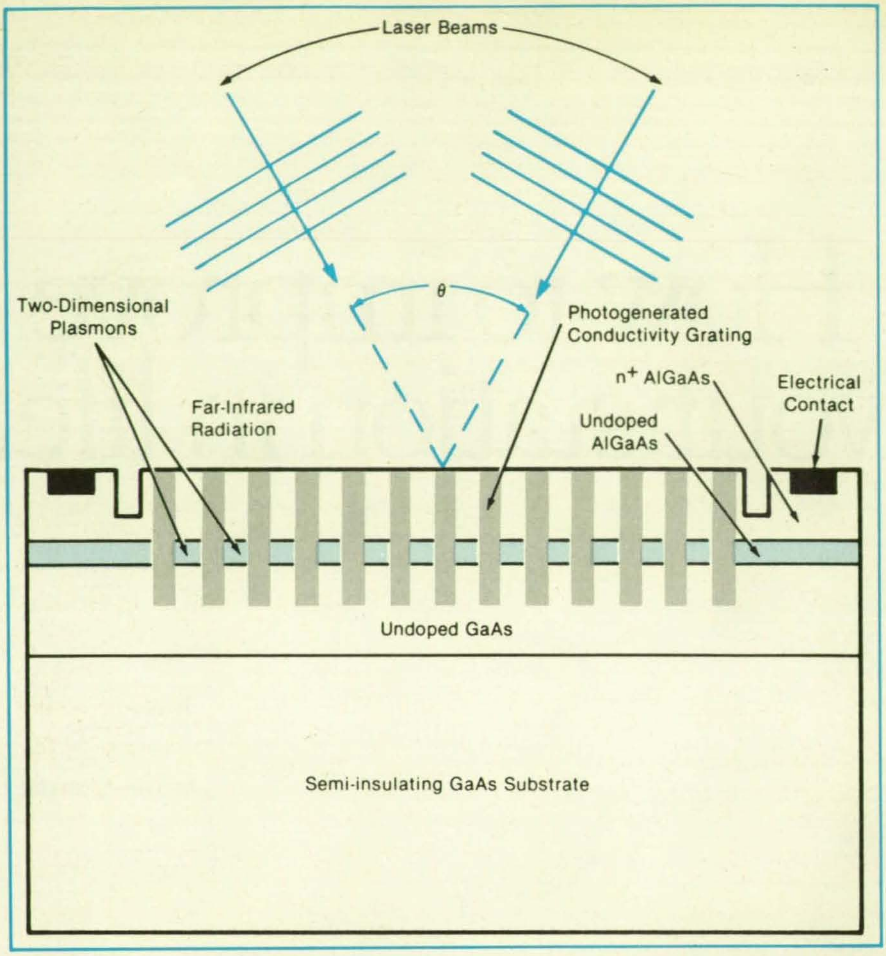

A **Tunable Source of Far-Infrared Radiation** would use an adjustable interference pattern produced by two coherent interfering visible laser beams to create a photoconductivity grating that would control the frequency of the radiation produced.

Layered Internal-Photoemission Sensor

High quantum efficiency would be achieved without multiple layer contacts.

NASA's Jet Propulsion Laboratory, Pasadena, California

A proposed infrared sensor would be based on photoemission from multiple layers of metal silicide sandwiched between layers of silicon. The sensor would provide high quantum efficiency and would be suitable for use in focal-plane arrays. A similar stacked-Schottky-barrier, mutiple-silicide/silicon-layer infrared sensor proposed earlier involved electrical contacts to all of the silicon and silicide layers. The new sensor would be easier to make because its internal layers would be allowed to "float" electrically, contact being made with only the two outer semiconductor layers.

The device would have a configuration partly reminiscent of that of a positive/intrinsic/negative diode, except that the middle layer of intrinsic silicon would be interrupted by multiple layers of cobalt disilicide (other metal silicides might also be used). It would be operated with reverse bias. Inci-

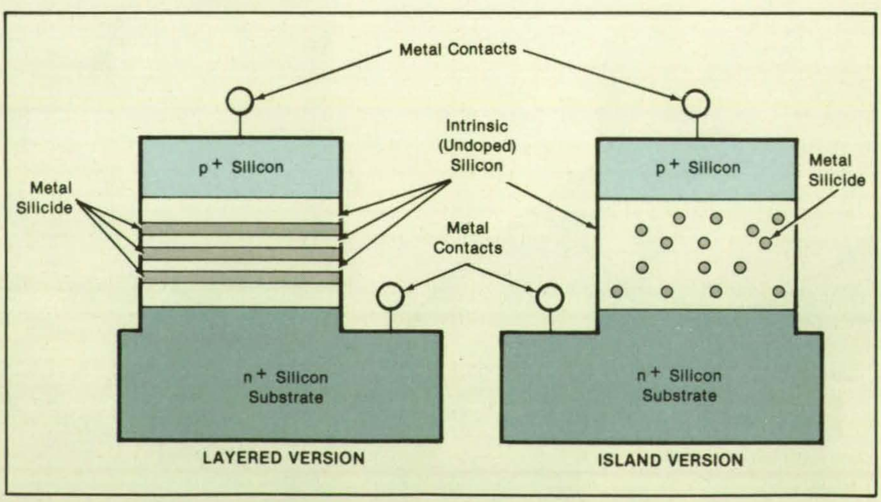

The **Layered Internal-Photoemission Sensor** would have a positive/intrinsic/negative structure modified by the inclusion of layers or islands of a metal silicide. Holes would be photoexcited from the silicide regions and swept to detection by the reverse-bias electric field in the intrinsic silicon.

DADiSP 2.0

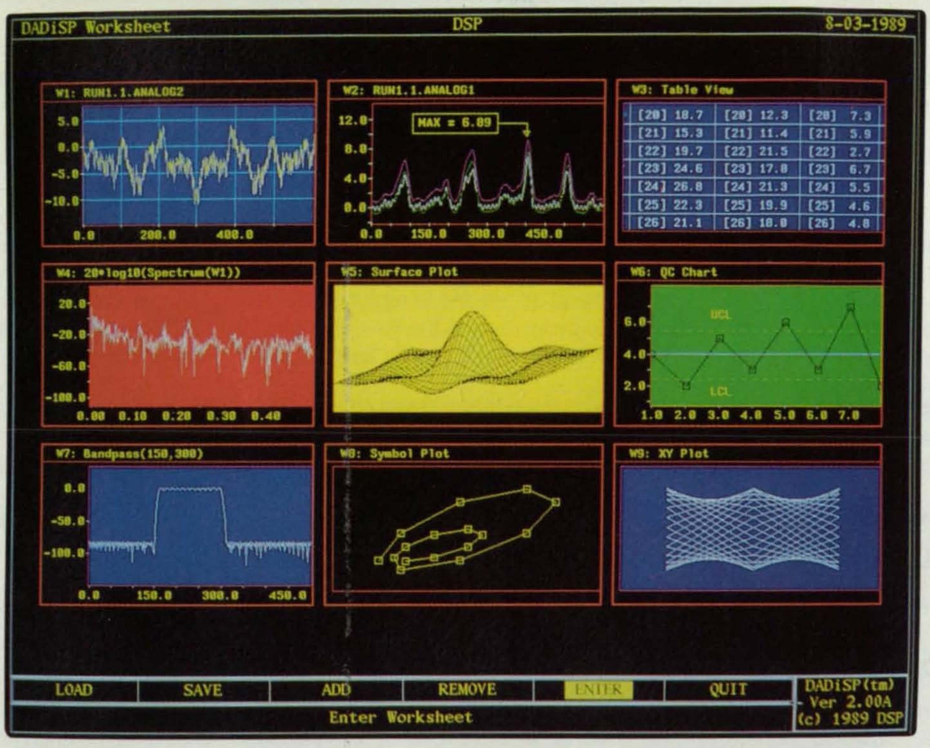

DADiSP. The Big Picture in Signal Processing

DADiSP — interactive graphics and data analysis software for scientists and engineers. DADiSP 2.0 delivers unprecedented power, through easy-to-use menus. Choose from hundreds of analysis functions and graphic views — from tables to 3-D. Simultaneously display multiple windows, each with different data or analyses, for unlimited perspective on your toughest data analysis problems.

Build your own analysis worksheets — build and display an entire signal processing chain, *without programming*. And DADiSP's powerful graphic spreadsheet automatically recalculates and updates the entire chain if you change your data or a processing step.

Do serious signal processing...the way you always pictured it! FFTs, digital filter design, convolutions, waterfall plots, and more — all at the press of a key.

Let your instruments do the talking — use DADiSP-488 to bring data from your instruments directly into a DADiSP window for immediate viewing and analysis.

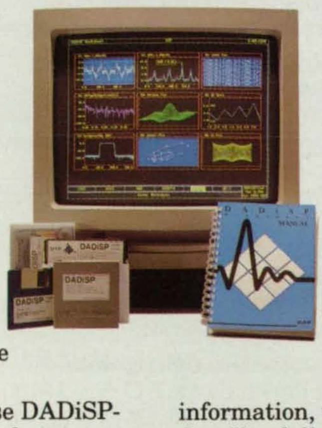

Flexible, expandable, customizable — annotate your graphs and send them to printers, plotters, or publishing packages. Create your own macros, automate routine tasks, and run any program written in any language from within DADiSP. *DADiSP even lets you build your own menus.*

A proven standard — already used by thousands of engineers and scientists worldwide, in a whole range of applications like medical research, chemistry, vibration analysis, communications, manufacturing quality control, test & measurement, and more. DADiSP supports the IBM PC and PS/2, SUN, DEC VAX, HP 9000 and Concurrent families of personal computers and workstations.

GET THE PICTURE!
CALL TODAY 617-577-1133

Ask for our Evaluation Disk. For more information, write to DSP Development Corporation, One Kendall Square, Cambridge, MA 02139, or FAX: 617-577-8211.

DSP Development Corporation

Australia-Interworld Electronics, 03 521-2952; England-Adept Scientific, (0462) 683355; Biosoft, (0223) 68622; Finland-Turion, 0-372-144; France-SM2I, (1) 34810178; Sacasa, 69077802; West Germany-Datalog, (02166) 46082; Stemmer Electronik, 089-809 02-0; Israel-Racom Electronics, 03-491-922; Italy-BPS Computers, (02) 61290221; Japan-Astrodesign, 044-751-1011; Netherlands-Computer Engineering Roosendaal, 01650-57417; New Zealand-GTS Engineering, (09) 392 464; Sweden-Systek, 013 110140; Switzerland-Urech & Harr AG, 61 611325; Taiwan-Advantech, 2-351-2117

Circle Reader Action No. 652

dent infrared photons would create hot holes in the silicide layers. At shorter wavelengths, hot electrons would be created in addition to the hot holes. To be detected as photocurrent, the holes and electrons have to cross over into the silicon.

Because the mean free path of a hot hole in the silicide is much shorter than the absorption length for infrared radiation, the silicide layers have to be thin (< 10 nm) to assure that most of the holes reach the silicon. In turn, the thinness of the silicide layers requires a multiplicity of such layers to convert most of the incident infrared photons into photoexcited charge carriers. The fact that the layered internal-photoemission sensor contains multiple layers potentially allows this device to have a higher quantum efficiency than standard internal photoemission sensors based on Schottky diodes.

Although the silicide layers must be thin, they should be at least 2 nm thick to avoid significant quantization of the energy levels in them. Such quantization is undesirable because it could give rise to thickness-dependent nonuniformities that would degrade the performance of a focal-plane array.

The charges in the silicide regions would become unbalanced by the photoexcitation process. However, the energy levels of the silicide and silicon regions would bend as needed to replenish these charges by increasing the flow of charge carriers not created directly by photoexcitation.

In an alternative configuration, also shown in the figure, silicide islands would be embedded in the intrinsic silicon layer. The considerations for the dimensions and separations of the silicide islands are similar to those for silicide layers. A device with this alternative configuration has been successfully demonstrated. The structure was grown by molecular beam epitaxy, and contains three layers of $CoSi_2$ particles. While $CoSi_2$ does not have a long cutoff wavelength relative to many other silicides, it does grow epitaxially on silicon with relative ease. The quantum efficiency of this device is comparable to or greater than that of a standard Schottky diode, and devices with larger numbers of particles are expected to show increased quantum efficiency.

This work was done by Robert W. Fathauer of Caltech for **NASA's Jet Propulsion Laboratory**. *For further information, Circle 141 on the TSP Request Card. NPO-17751*

Making More Efficient Use of Battery-Plate Mass

Conductive fibers and enhanced porosity increase efficiency and discharge-cycle life.

NASA's Jet Propulsion Laboratory, Pasadena, California

An improved active material for the positive plate of a lead/acid electric storage battery is made with additional porosity to give the electrolyte access to a larger plate-surface area. As a result, 65 to 68 percent of the active mass of the plate can be used to generate electric current. In conventional plates, the efficiency of utilization is only 25 to 40 percent. Batteries with the new plate material also offer an extremely long cycle life. In preliminary tests, a cell was charged and deeply discharged more than 2,000 times with no signs of "fading"; that is, loss of energy-storage capacity.

In effect, the plate is manufactured in a condition like that normally encountered in failure; that is, covered with lead sulfate. This material is selected for its large molecular volume. Because the density of the material increases during charging, additional pores open up in the material.

The lead sulfate is precipitated by acidification in a solution of lead nitrate with excess sulfuric acid in water. The precipitate is filtered and washed thoroughly to remove the nitrate. Enough sulfuric acid is added to turn the precipitate into a paste, which is blended with about 5 to 10 percent by weight of glass fibers coated with electrically conductive tin oxide. The mixture is then applied to the positive side of a bipolar plate to form the positive electrode.

This work was done by John J. Rowlette of Caltech for **NASA's Jet Propulsion Laboratory**. *For further information, Circle 62 on the TSP Request Card.*

In accordance with Public Law 96-517, the contractor has elected to retain title to this invention. Inquiries concerning rights for its commercial use should be addressed to

Edward Ansell
Director of Patents and Licensing
Mail Stop 305-6
California Institute of Technology
1201 East California Boulevard
Pasadena, CA 91125

Refer to NPO-17435, volume and number of this NASA Tech Briefs *issue, and the page number.*

Enhanced Data-Acquisition System

The time-consuming, costly digitization of analog signals on magnetic tape would be eliminated.

Lyndon B. Johnson Space Center, Houston, Texas

A proposed data-acquisition system would provide nearly immediate access to data in incoming signals by digitizing them and recording them both on magnetic tape and on an optical disk. The system is intended to replace the Space Shuttle data-acquisition system, in which signals are recorded on magnetic tape in analog form for subsequent digitization and analysis via a time-consuming and expensive process. The concept of the system is not limited to the Space Shuttle, however, and may be of interest in industrial and scientific applications in which it is necessary to digitize, store, and/or process large quantities of experimental data.

The system would include a commercial portable data-acquisition subsystem that accepts signals from as many as 128 channels (see figure). The incoming signals would be digitized with a resolution of 12 or 16 bits at as many as four simultaneously and independently selectable sampling rates, with an overall rate of 250,000 samples per second. A filter between the inputs and the analog-to-digital converter would reduce noise and prevent aliasing. As each input channel is sampled, the auto-balance value of that channel would be injected into its signal prior to digitization, thus providing exceptional accuracy in all readings.

The system would include IEEE488 and RS-232-C interfaces, enabling it to operate with almost any host central processing unit. The system could run continuously or be triggered by selected input pulses; for example, signals that turn engines on. Some other notable features of the system would include internal or external synchronization, front-panel keyboard and display, redundant battery power to protect the clock and calendar functions, direct connection to low-level transducers, operation as either an autonomous unit or as part of a larger system, automatic restart after failure of power, and shock/vibration mounting.

Digitized data would be stored temporarily in a main (buffer) memory of 2 to 16 megabytes, then transferred to the digital tape and/or optical disk, each of which could hold up to 2 gigabytes. The data thus recorded could be read out in digital or analog form for subsequent processing.

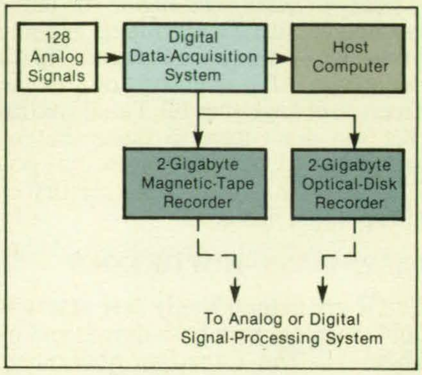

The **Enhanced Data-Acquisition System** would digitize up to 128 analog incoming signals and record them on magnetic tape and/or an optical disk. The tape and/or disk could later be played back to reconstruct the signals in analog or digital form for analysis.

This work was done by Roy W. Mustain of Rockwell International Corp. for **Johnson Space Center**. *For further information, Circle 143 on the TSP Request Card. MSC-21598*

Simplified Correlator for Ranging Codes

The received signal is processed with fewer arithmetical operations.

NASA's Jet Propulsion Laboratory, Pasadena, California

An improved correlating subsystem of a pseudorandom-code ranging system is made possible by the advent of fast, custom-made, very-large-scale integrated circuits. In contrast with its predecessors, the correlator performs far fewer arithmetical operations, contains much less specialized analog and digital circuitry, and can be used with a large number of different codes.

In a ranging system of this general type, the range is calculated from the delay between a received signal modulated by a binary pseudorandom or square-wave code and a replica of the code generated at the receiver. The first step in the estimation of the delay τ is to try various candidate values $\hat{\tau}$ and compute the cross-correlation integral

$$I_{\hat{\tau}} = \int_0^T y(t)c(t-\hat{\tau})dt$$

where t = time, $y(t)$ = the received modulation plus noise, $c(t)$ denotes a component of the code signal, and T is an observation interval that depends on the signal-to-noise ratio and the required accuracy. The value of $\hat{\tau}$ that maximizes I_τ is accepted as the best estimate of $\hat{\tau}$.

Typically, a code consists of repeated sequences of p bits that last t_0 each. For the purpose of estimating $\hat{\tau}$, each bit period is divided into k subintervals (k is usually 1 or 2 but could be any integer). A receiver determines a set of $N = pk$ candidate values $\hat{\tau}_i = it_0/k$, where $i = 0$ to $N-1$. A typical observation time T is M code periods; that is, $T = Mpt_0$.

The relative simplicity of the new correlator is achieved by exploiting the periodicity of the code to transform the correlation integral into

$$I_{\hat{\tau}_i} = \sum_{j=0}^{pk-1} c_{j-i}A_j$$

where A_j represents the accumulated integrate-and-dump value of the jth-bit subintervals of $m = 0$ to $M-1$ code periods; namely,

$$A_j = \sum_{m=0}^{M-1} \int_0^{t_0/k} y[t+(j+mpk)t_0/k]dt$$

The correlator, shown in the figure, includes pk accumulators for the $\{A_j | j = 0, 1, \ldots pk-1\}$ values. The output of the integrator during each bit subinterval is added only into one of the accumulator channels, switched by the accumulator index j, each t_0/k seconds. Because of this simplification, only one adder is required for all the accumulators. For each integrator sample, the corresponding accumulator is fetched, added to the sample, and restored into

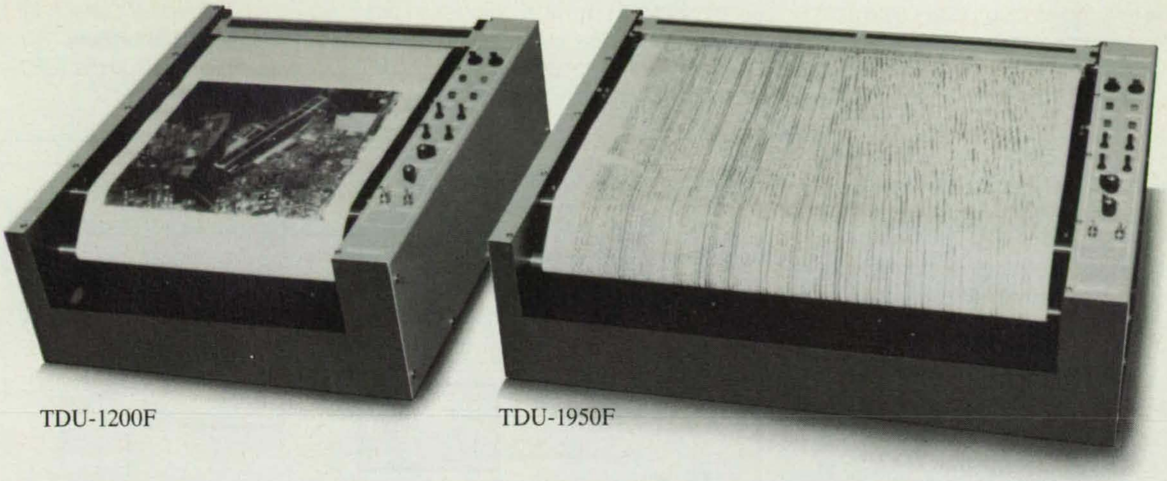

TDU-1200F TDU-1950F

We're widening the scope of hard copy recording.

TDU-1200

TDU-850

Raytheon has added a series of wide "flatbed" models to its quality line of thermal hard copy recorders. The new TDU-1950F and TDU-1200F units, in 19.5 inch (49.5 cm) and 12 inch (30 cm) configurations, respectively, provide enhanced vertical integration of data for a broad range of specialized applications.

The flatbed models join Raytheon's established family of "free fall" thermal recorders – the TDU-850, with an 8.5 inch (21 cm) printing width, and the TDU-1200, with a 12 inch (30 cm) printing width.

Raytheon's thermal recorders produce high resolution copy at high speeds and can generate full tonal images up to 256 multi-shade levels of true grey. Alternately, they can display digital data in crisp graphic or alphanumeric form using an optional IEEE 488 interface.

Traditional uses include CRT hard copy, military surveillance, spectrum analysis, LOFAR gram displays, ultrasonic production control, and facsimile transmissions. New and evolving applications include support for computer assembly testing and chromosome analysis in genetic research.

TDU's print on paper, plastics or transparencies. They feature clean, odor-free, maintenance-free operation.

Make hard copy easy with today's most versatile and reasonably priced thermal recorders. Call or write Marketing Manager, Production Components, Raytheon Company, Submarine Signal Division, 1847 West Main Road, Portsmouth, RI, USA 02871-1087. Phone 401 847-8000.

Raytheon

Circle Reader Action No. 512

memory. Access to each accumulator is sought only once each pt_0 interval.

The accumulators are in jeopardy of overflow only $1/p$ as much of the time as in the conventional design. Consequently, each accumulator can be shorter by $\log_2(p)$ bits than those of the conventional design.

The address generator is merely a counter clocked at the bit subinterval symbol rate and reset at the beginning of each period of the receiver code. This is the only code-dependent signal that enters the digital portion of the correlator. Except for the number of accumulators, the digital portion of the correlator assembly is independent of the code.

Code multiplications need not be made until after the complete accumulation of A_j values has been read into the computer of the ranging assembly. Then the same set of A_j serves in the calculation of all of the $I_{\hat{\tau}_i}$. The vector **I** containing the $I_{\hat{\tau}_i}$ is related to the vector **A** of accumulator values A_j by the equation

$$\mathbf{I} = \mathbf{C}\mathbf{A}$$

where **C** is the $N \times kp$ matrix of binary code values, $c_{i,j} = c_{j-i}$. Since the receiver code(s) are stored solely in the computer memory, as **C**, since the vector **I** is computed separately from the accumulation process, and since this computation must be performed only infrequently, there is a greater degree of flexibility and generality in the simpler design than existed in the previous ranging assemblies.

This work was done by R. C. Tausworthe and J. R. Smith of Caltech for **NASA's Jet Propulsion Laboratory**. *For further information, Circle 19 on the TSP Request Card. NPO-17415*

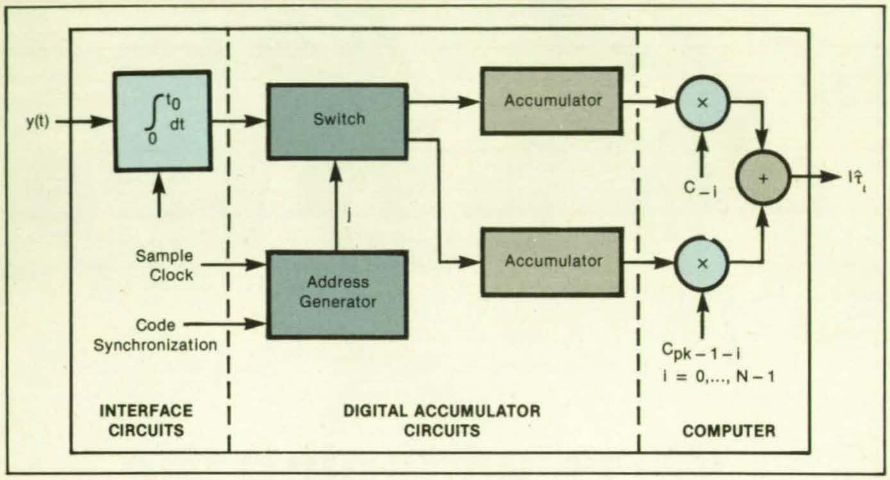

In the **Simplified Correlator**, no code-dependent multiplications or additions are performed before accumulation.

Optical Detection of Deformations of an Antenna

Aim would be corrected in response to changes in shape.

NASA's Jet Propulsion Laboratory, Pasadena, California

A proposed control subsystem would generate small aiming-bias signals to correct for deviations of the 70-m-diameter reflector of a microwave antenna from its ideal shape. The subsystem would take optical measurements to determine the deformations produced by such environmental factors as wind, gravity, and thermal differentials. Using these measurements, the subsystem would estimate the misalignment of the radiation pattern caused by the deformations. Signals to correct for the estimated misalignment would be added to the angle-command signals of the main antenna-aiming system.

The antenna includes an intermediate reference structure, which is presumed to be rigid and aimed correctly. Some of the deformations are assumed to occur in the main paraboloidal reflector. The rest of the deformations are assumed to occur in the quadripod legs that support the hyperboloidal subreflector. These deformations would be manifested as shifts in the position and orientation of the subreflector (see Figure 1).

The antenna would be instrumented with a network of time-of-flight laser ranging devices and retroreflectors (see Figure 2). Now undergoing development, this network is capable of multiple simultaneous measurements with submillimeter accuracies, at a rate of 10 sets of measurements

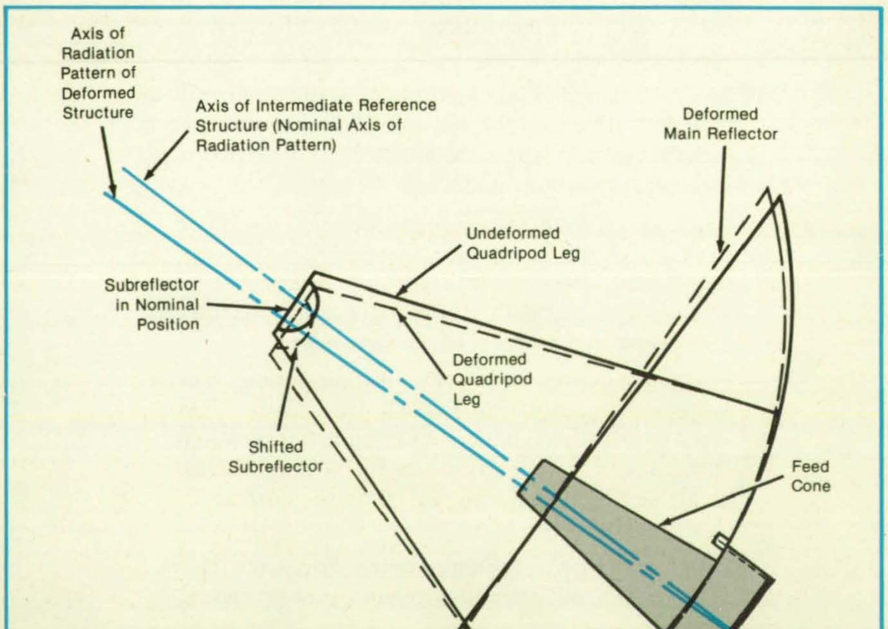

Figure 1. The **Principal Deviations** of the antenna from its ideal shape are deformations in the main reflector and shifts in the position and orientation of the subreflector.

Finally, a comprehensive reference guide for applying and specifying cryogenic temperature sensors.

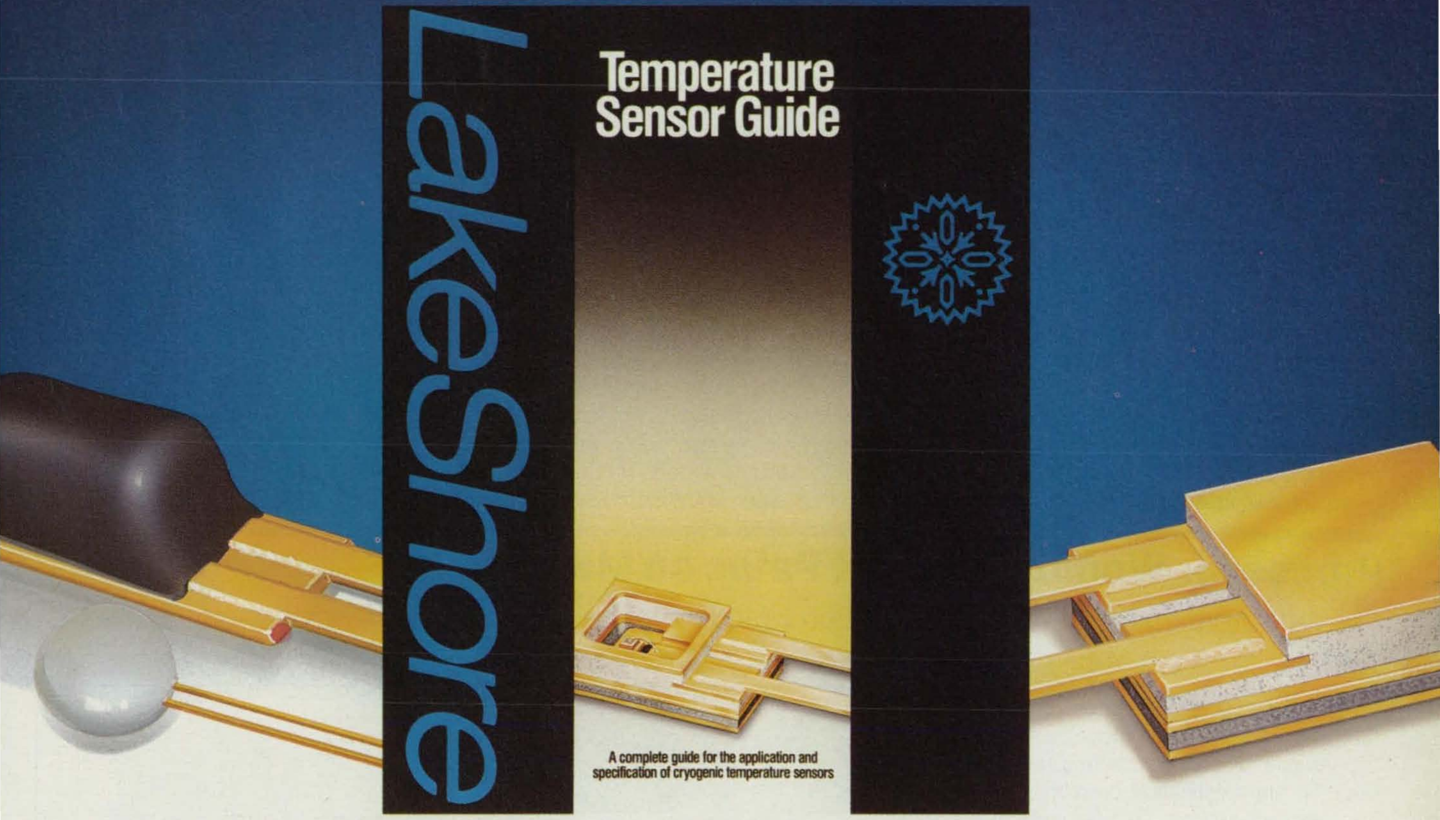

FREE Temperature Sensor Guide

Call 614-891-2243

The new Lake Shore Temperature Sensor Guide contains over 50 pages of specification, application and performance details for virtually every type of cryogenic temperature sensor.

The guide contains sensor reference tables and application notes with information on physical properties, recommended temperature range of use, magnetic field dependence, calibrations, precision options, installation and measurement techniques and more.

Temperature sensors profiled in the guide include: silicon and gallium-aluminum-arsenide diodes, platinum resistance thermometers, germanium and carbon-glass resistors, rhodium-iron resistors, capacitance sensors, Hall sensors and thermocouples.

This comprehensive guide includes convenient "how to order" information for cryogenic temperature sensors and a broad range of cryogenic accessory products. It is a must for anyone involved in low temperature research. For your **FREE** copy call **614-891-2243** or circle and return the reader response card in this magazine.

LakeShore
CRYOTRONICS, INC.

64 E. Walnut Street, Westerville, OH 43081 USA Tel: 614-891-2243 Telex: 24-5415 CRYOTRON WTVL FAX: 614-891-1392

Circle Reader Action No. 579

per second. The measurement data would be used in a two-dimensional triangulation analysis to determine shifts in the positions of the retroreflectors (and of the antenna substructures to which they are attached) with respect to the intermediate reference structure.

The proposed configuration of the network would yield the maximum amount of useful data for the number of measurements made. The portion of the network devoted to the main reflector would be arranged to maximize sensitivity to horizontal forces (e.g., crosswinds) and to vertical forces (e.g., gravitation). The portion devoted to the subreflector would be arranged for sensitivity to translations and rotations that affect the radiation pattern.

The measurements would be affected by variations in the index of refraction of air, which depend on atmospheric pressure, carbon dioxide content, temperature, relative humidity, and other related quantities. To minimize errors from this source, principal environmental parameters would be measured at the antenna. Small-scale fluctuations in the index of refraction that are caused by turbulence would contribute to random errors and would not be correctable.

An analysis of errors yields a 35-μm root-mean-square (rms) overall resolution in the determination of the antenna geometric boresight, based on a 25-μm rms random error in the range measurements and 25-μm rms random noise due to local variations in the index of refraction. This translates to an error of 3 millidegrees in the determination of the direction in which the antenna is actually aimed. This result is based on a worst case combination of measurement errors and is considered to be conservative by a factor of about 4.

This work was done by L. L. Schumacher and H. C. Vivian of Caltech for **NASA's Jet Propulsion Laboratory**. *For further information, Circle 139 on the TSP Request Card. NPO-17677*

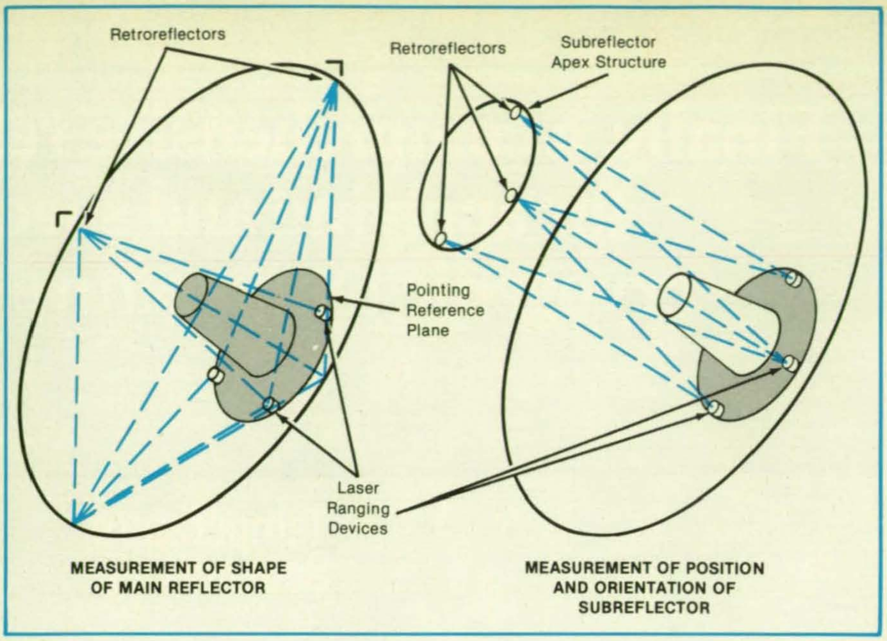

Figure 2. **To Measure Deviations** like those shown in Figure 1, laser ranging devices are placed at the base of the feed on the rigid intermediate reference structure, while retroreflectors are placed on the parts that deviate from their assigned positions relative to the intermediate reference structure.

Processor Would Find Best Paths on Map

The path from an origin to any destination would have the lowest possible cost.

NASA's Jet Propulsion Laboratory, Pasadena, California

A proposed very-large-scale integrated (VLSI) circuit image-data processor would find the path of least cost from a specified origin to any destination on a map. The least-cost-path problem occurs in research, in military maneuvers (e.g., finding the best path across terrain), and in planning the routes of vehicles.

A cost would be assigned to the traversal of each picture element of the map. Each picture element would be represented by a microprocessor (which could be analog or partly analog and partly digital) connected to the microprocessors of the four nearest-neighbor picture elements. One picture element would be designated as the origin; its microprocessor would send out a constant maximum signal to its nearest neighbors (see Figure 1).

The microprocessor of every other picture element would take whichever of the signals from its nearest neighbors is the maximum one, scale it down according to the cost assigned to that picture element, and transmit the resulting signal to its nearest neighbors. Thus, a wavefront of processing would ripple out from the origin as signals are modified and transmitted from element to element. After the system

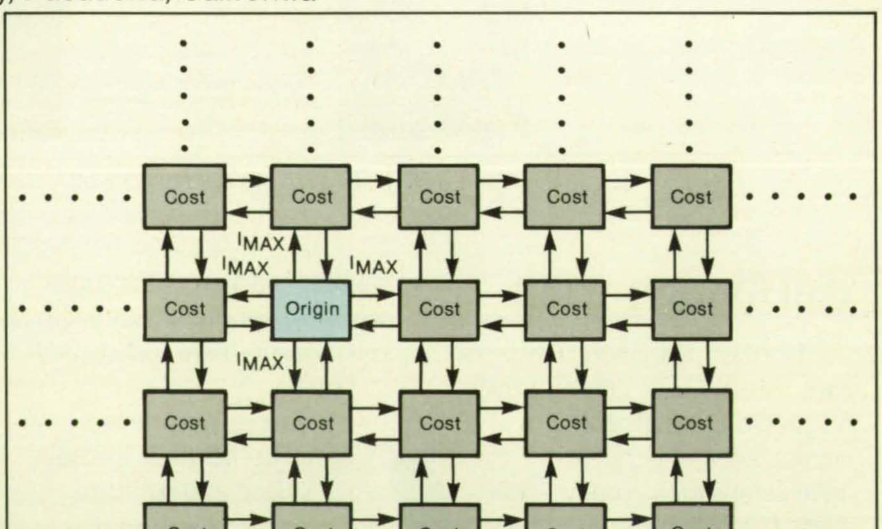

Figure 1. A **Cost of Traversal** is assigned to each picture element of a map. The path of least cost from the originating picture element to every other picture element is computed as the path that preserves as much as possible of the signal transmitted by the originating picture element.

settled down, the level of the signal at each picture element would correspond to the total cost of the best (lowest cost) path from the origin to that element.

To identify the best path after this wave of processing, it would be necessary to backtrack from the destination to the origin. This could be done by polling the destination microprocessor to determine from which neighboring microprocessor it is receiving the maximum (best path) input. The polling procedure would be repeated recursively until the best path is traced back to the origin.

The operation of each picture-element microprocessor is shown in more detail in Figure 2. The circuit would include a maximum circuit, a scaling circuit, a cost memory, and digital pixel-processor interface circuitry. The maximum circuit would take the signals from the north, south, east, and west neighbors and determine which is the maximum. The circuit would also determine the direction from which the maximum signal comes, as required for the backtracking operation.

The scaling circuit would reduce the signal by some function of the cost programmed into the cost memory. Scaling would be performed in such a way that a circuit with low cost of traversal would not significantly attenuate the path-cost signal propagated through it. Scaling could be multiplicative or additive, depending on the desired cost function. The resulting signal would be routed to all four neighbors.

The costs could be programmed in several ways. It may be desirable to optically project the map onto the VLSI chip: costs would be encoded as light intensity and detected by photosensors. Costs could also be programmed element by element; for example, using capacitors to store voltages corresponding to the costs. These voltages could be periodically refreshed by use of external random-access memory and a digital-to-analog converter.

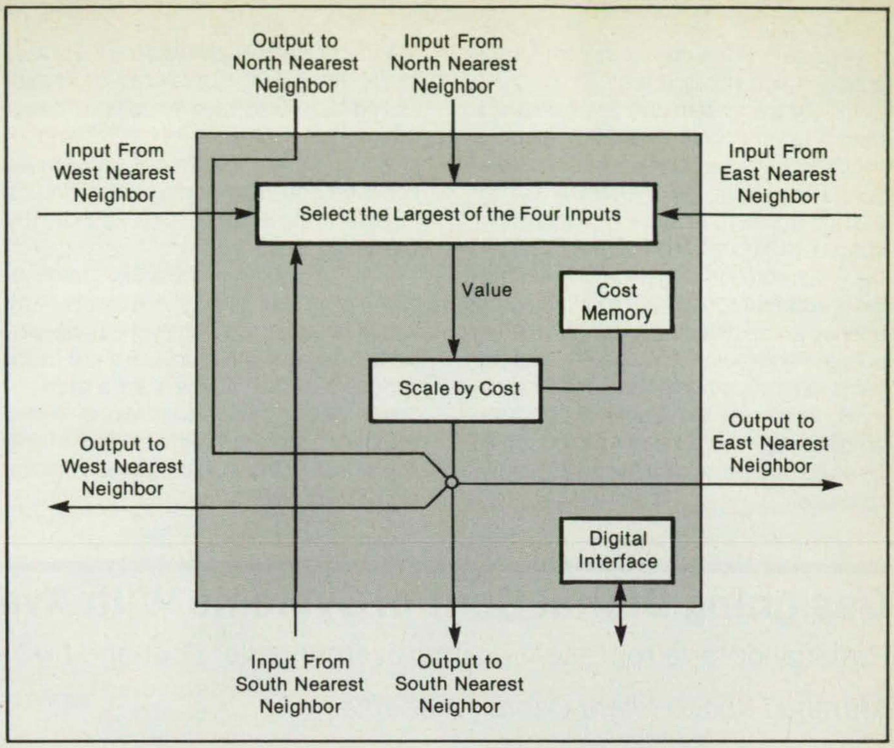

Figure 2. The **Dedicated Microprocessor** at each picture element stores the cost of traversal and performs its share of the computations of the paths of least cost.

This work was done by Silvio P. Eberhardt of Caltech for **NASA's Jet Propulsion Laboratory**. *For further information, Circle 6 on the TSP Request Card.*

This invention is owned by NASA, and a patent application has been filed. Inquiries concerning nonexclusive or exclusive license for its commercial development should be addressed to the Patent Counsel, NASA's Resident Office-JPL [see page 16]. Refer to NPO-17716

System Detects Vibrational Instabilities

Sustained vibrations at two critical frequencies trigger diagnostic response or shutdown.

Lyndon B. Johnson Space Center, Houston, Texas

A vibration-analyzing electronic system detects instabilities of combustion in a rocket engine. The concept of the system can be adapted to other detection and/or control schemes that involve the simultaneous real-time detection of signals above or below preset amplitudes at two or more specified frequencies. Potential applications include rotating machinery and encoders and decoders in security systems.

The vibrations that characterize instabilities in the particular engine have frequencies of 5.9 and 12 kHz. Because the amplitudes at these critical frequencies are superimposed upon the overall vibration spectrum that covers a range of frequencies, simple monitoring the root-mean-square (rms) amplitude of the overall vibration signal does not reveal the instabilities. It is necessary to tune out the components at other frequencies and prevent false alarms. In addition to performing these functions, the vibration-analyzing system

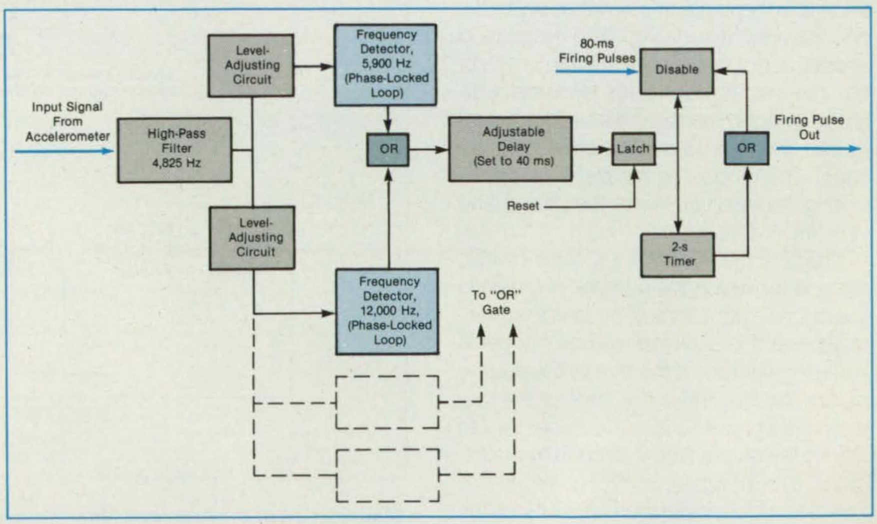

The **Vibration-Analyzing System** controls the pulse-mode firing of an engine and identifies vibrations above a threshold amplitude at 5.9 and/or 12kHz.

acts as part of the control system for the engine during vibration tests.

Initially, the system (see figure) allows a train of externally-generated 80-ms pulses to control the firing of the engine. The vibrations of the engine are detected by a piezoelectric accelerometer. A high-pass filter attenuates frequencies below 4,825 Hz in the input vibration signal to minimize mixing effects that could make spurious contributions to the detected amplitudes at the critical frequencies. The filtered input signal is fed through amplitude-adjusting circuits, which set the trigger acceleration amplitudes (in this case, rms amplitude 40 times normal Earth gravity) at the critical frequencies.

When the amplitude exceeds the preset levels, the signal is analyzed by phase-locked-loop integrated circuits to determine whether components at 5.9 and 12 kHz are present. (Additional frequencies could be added by adding other circuits "tuned" to those frequencies, as shown by the dotted lines.)

If either or both of the critical frequencies are present, then an adjustable delay circuit determines whether the preselected frequencies and amplitudes are maintained for at least 40 ms. If so, a latch circuit is set to disable the train of 80-ms pulses and replace it with a single 2-s firing pulse. During this long pulse, the vibration signal is analyzed by an external recording device to determine whether the instability is sustained once it is detected. If it is sustained, then a flashing red light alerts the operators to the instability and continues flashing until the system is reset or turned off.

This work was done by Richard J. Bozeman, Jr., of **Johnson Space Center**. *For further information, Circle 34 on the TSP Request Card.*

This invention is owned by NASA, and a patent application has been filed. Inquiries concerning nonexclusive or exclusive license for its commercial development should be addressed to the Patent Counsel, Johnson Space Center [see page 16]. Refer to MSC-21408

Designing Digital Control Systems With Averaged Measurements

Rational criteria represent an improvement over "cut-and-try" approach.

Marshall Space Flight Center, Alabama

A recent development in the theory of control systems has yielded improvements in the mathematical modeling and design of digital feedback controllers that use time-averaged measurements. This is an important development because the digital outputs in many practical systems are time-averaged measurements of the quantities of interest between the designated sampling instants. Previously, most theoretical treatments were based on the often-incorrect assumption that the sampled outputs are instantaneous measures of those quantities at the sampling instants.

In conventional practice, one ignores the averaging effect in formulating the initial mathematical model of the plant to be controlled. One designs the feedback controller, then simulates the closed-loop system to determine whether the performance is acceptable. If it is not acceptable, one iterates the design and simulation phases until it is. However, by using one of the new formulations for systems with time-averaged measurements, the designer can take the averaging effect into account when modeling the plant, thus eliminating the need to iterate the design and simulation phases.

The best formulation for a given plant is the one for which the number of states in the discrete equations of state is the least. In general, this is the formulation that yields n states, where n is the size of the square matrix that describes the state of the system. In this formulation, it is necessary to modify the output time-averaged measurements by subtracting correction terms that are delayed, transformed versions of the input control vector (see figure).

When it is impossible or undesirable to modify the averaged measurements, then one should use whichever of the other formulations yields the fewest states. Thus, if the plant has fewer averaged measurements than control inputs, one should choose the formulation that yields $n+p$ states (where p = the number of averaged measurements). If the plant has fewer control inputs than averaged measurements, then one should choose the formulation that yields $n+r$ states (where r = the number of control inputs). If $p = r$, then the choice is arbitrary.

This work was done by Michael E. Polites and Guy O. Beale of **Marshall Space Flight Center**. *For further information, Circle 38 on the TSP Request Card.*
MFS-28362

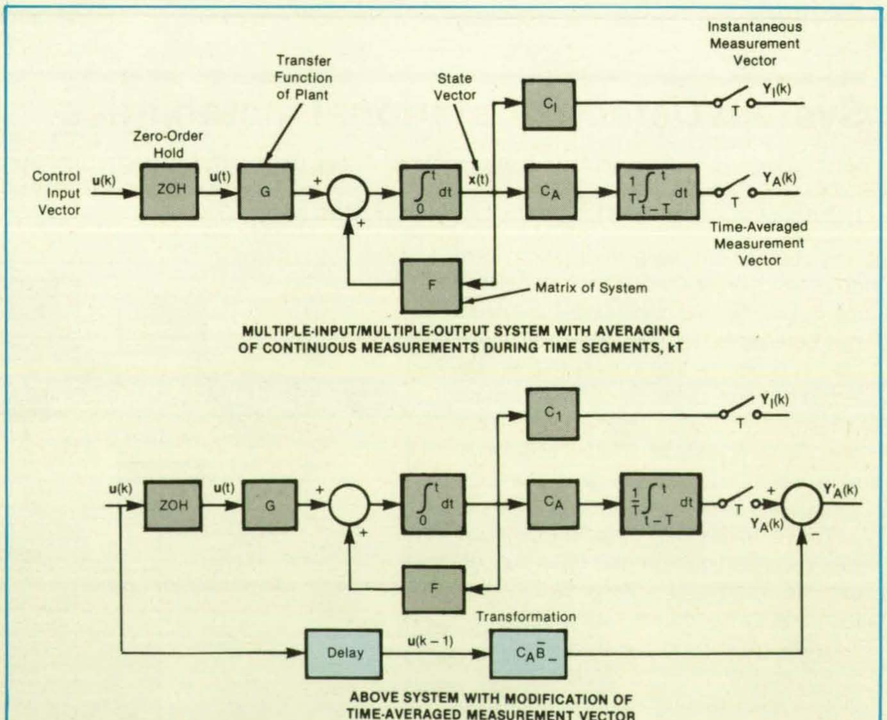

Modification of the Averaged Measurement Vector by a delayed, transformed input control vector is one of several ways of accounting for the time-averaging effect in mathematical modeling and design.

Digital Controller for Emergency Beacon

Identification codes would guide rescuers in the appropriate types of responses.

Lewis Research Center, Cleveland, Ohio

A prototype digital controller is intended for use in a 406-MHz emergency beacon. Now undergoing development according to international specifications, the 406-MHz emergency beacon system will include satellites that will provide worldwide monitoring of beacons, with Doppler tracking to locate each beacon within 5 km.

The digital controller turns the beacon on and off and generates binary codes that identify the source (e.g., ship, aircraft, person, or vehicle on land). The codes are transmitted by phase modulation. Knowing the code, a monitor can attempt to communicate with the user of the beacon to verify the emergency. If unable to communicate with the user, the monitor can at least use the code information to dispatch a rescue team appropriate to the type and location of the carrier.

In addition to the international specifications for frequency, code, and modulation, the beacon has to satisfy such practical requirements as relatively low cost, a small number of parts, and low power (because power is to be supplied by a battery). These requirements are met by a design that incorporates three integrated-circuit chips: an 80C51 microcontroller, a 256 × 4 programmable read-only memory (PROM), and a 1K × 4 PROM (see figure).

The 80C51 microcontroller includes 4K of onboard PROM, 128 bytes of onboard random-access-memory (RAM), two internal timers, and a transmitting-and-receiving port for asynchronous communications. The PROM and RAM hold the software. One timer is used to generate the transmission bit rate while the other timer generates the asynchronous-communication baud rate. The 80C51 provides the signals for reading the two PROM's external to itself. It also provides up to 24 input/output ports and 2 ports for interruption by external sources.

The 256 × 4 PROM stores such beacon-specific data as the identification of the user and the country of origin. The 1K × 4 PROM encodes the switch settings that specify the emergency code.

To eliminate the need for extra integrated circuits that would otherwise be needed to multiplex the "PROM enable" signal, the design includes an unusual addressing scheme: Both PROM's are always read together. Each PROM includes a 4-bit-wide data bus. Two PROM's are put in parallel to form an 8-bit data bus compatible with the 80C51. The addressing system of the 80C51 expects the lower 8 of 16 address bits to be latched during each read/write cycle because the lower 8 address bits and the data bus are multiplexed. To eliminate the need for an integrated circuit for latching, the beacon-specific-data PROM is addressed using the upper 8 address bits.

The main program consists of an interruption-handling routine and the following major modules: initialization of the central processing unit, RS-232 communications, generation of messages, Biphase-L transmission, and jitter delay (to prevent synchronization of separate beacons). The main program and the RS-232 communication module are written in a high-level language. Because of the extremely detailed manipulation of bytes and bits involved in the remaining modules, they are written in Assembly language.

This work was done by William D. Ivancic of **Lewis Research Center**. *Further information may be found in NASA TM-100859 [N88-26566], "COSPAS/SARSAT 406-MHz Emergency Beacon Digital Controller."*

Copies may be purchased [prepayment required] from the National Technical Information Service, Springfield, Virginia 22161, Telephone No. (703) 487-4650. Rush orders may be placed for an extra fee by calling (800) 336-4700.

This invention is owned by NASA, and a patent application has been filed. Inquiries concerning nonexclusive or exclusive license for its commercial development should be addressed to the Patent Counsel, Lewis Research Center *[see page 16]*. *Refer to LEW-14857*

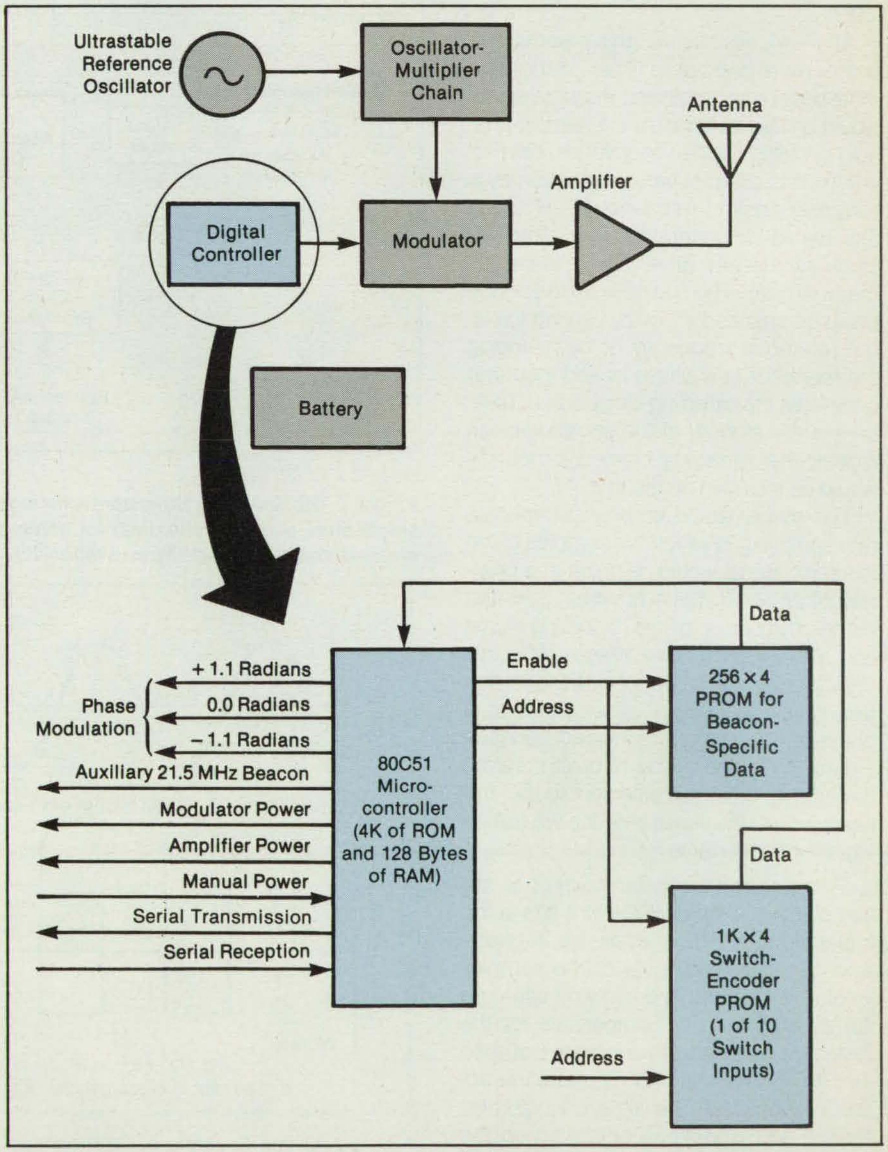

The **Digital Controller** makes the emergency beacon a versatile piece of equipment that can be programmed to transmit such useful information as the user's identity, the location, and the type of emergency.

Sampling Downconverter for Radio-Frequency Signals

Phase and delay errors would be reduced greatly.

NASA's Jet Propulsion Laboratory, Pasadena, California

A proposed GaAs integrated-circuit for a receiver of radio signals at gigahertz frequencies would sample an incoming signal in phase and in quadrature, digitize it, and down-convert it to baseband in a single step. The circuit would incorporate both digital and analog components in a design that offers improved stability, versatility, and sampling bandwidth. Because most of the processing of the signal would be performed digitally and the analog filters could be given very wide bandwidths, the instrumental phase and delay errors could be reduced greatly in comparison with those of all-analog versions. The design eliminates the need for several components found in conventional analog designs, including mixers, postmixer filters, and a 90° phase shifter.

After processing through a preamplifier, one or more band-pass filters, and one or more wideband amplifiers, the input signal would be fed to an ultrafast sample-and-hold circuit in the downconverter (see Figure 1). This sampler would be driven by a sampling clock of frequency $2f_s$, which in turn would be generated by a sampling-clock synthesizer driven by a reference-clock signal. The sampling frequency could be changed either by varying the input reference frequency or by changing the multiplier in a phase-locked loop that generates the sampling-clock signal. To increase the stability of the sampling-clock signal, the sampling-clock synthesizer would be included on the chip.

The circuit would employ commensurate sampling, in which the samples of the incoming signal would be taken at a clock rate of $2f_s = 4f_c/(2n+1)$, where f_c = the carrier frequency of the incoming signal and n is a nonnegative integer. With this choice of sampling frequency, the samples taken at alternate clock cycles would be in phase and in quadrature, respectively (see Figure 2). To satisfy the Nyquist criteron, the analog filters are selected so that the bandwidth of the signal entering the sampling downconverter is f_s.

The piecewise-constant output of the sampler would be digitized to 4 bits in the initial version. The successive in-phase and quadrature outputs of the sampler would be reversed in polarity on alternate samples of each to compensate for the reversals in polarity of the input signal, then sent to an in-phase and a quadrature adder, respectively. The adders would perform a sum-and-dump operation on the initial high-rate samples. The summing interval would be selectable in the range from 1 to 64 points when the initial sample rate is a simple multiple of the desired output rate. With a settling of 1, the sampled data can be passed at full rate to allow subsequent circuitry to apply customized processing. In an alternate mode that will produce an arbitrary output rate, activation of the adder can be controlled by an externally supplied adder clock.

The in-phase and quadrature samples would be taken at slightly separated times. However, at the high sampling rates contemplated (e.g., 1.2 GHz), this separation would be small (833 ps) and would introduce negligible errors in some applications if ignored. Where the separation could not be ignored, it could be corrected in subsequent processing, inasmuch as the separation remains constant and is known accurately.

This work was done by J. B. Thomas, B. Rayhrer, and L. E. Young of Caltech for **NASA's Jet Propulsion Laboratory**. *For further information, Circle 4 on the TSP Request Card.*

This invention is owned by NASA, and a patent application has been filed. Inquiries concerning nonexclusive or exclusive license for its commercial development should be addressed to the Patent Counsel, NASA's Resident Office-JPL [see page 16]. Refer to NPO-17530

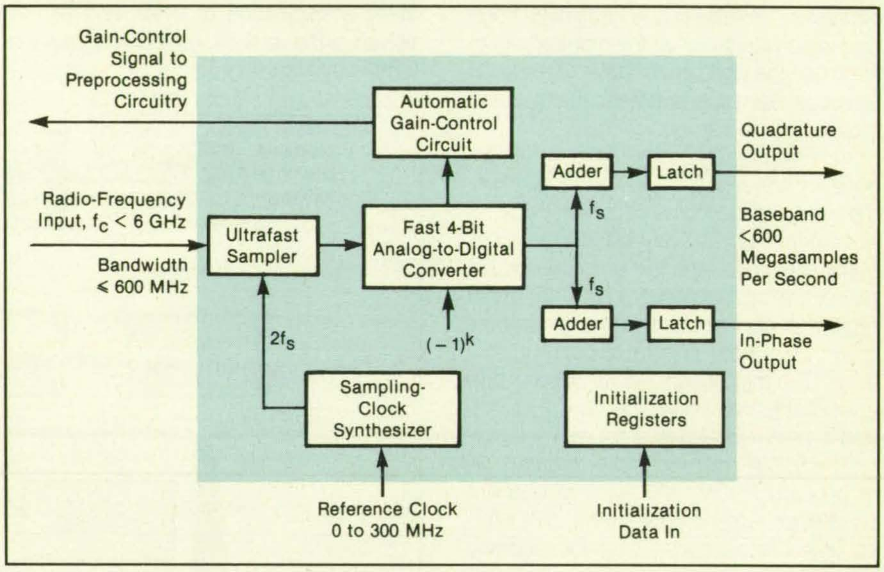

Figure 1. The **Sampling Downconverter** would perform sampling and down conversion in a single step, eliminate the need for some conventional analog components, and offer increased stability, versatility, and reliability.

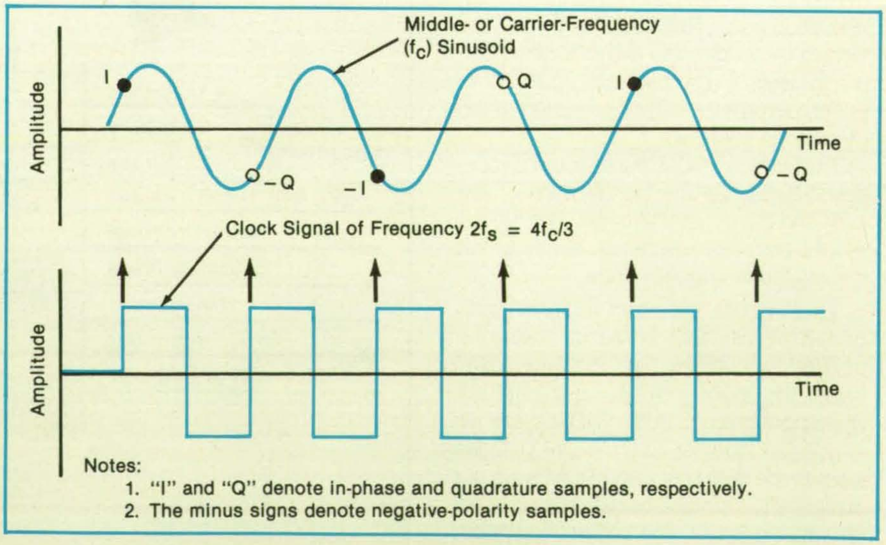

Figure 2. In this **Example of Commensurate Sampling**, the sampling clock runs at three-quarters of the carrier or middle frequency of the signal to be sampled. The successive leading edges of the positive-going clock pulses trigger alternate positive and negative in-phase and quadrature samples separated by three-quarters of the carrier-signal period.

Frequency-Domain Signal Processor for Laser Velocimeter

The dynamic range and accuracy are increased.

Langley Research Center, Hampton, Virginia

A new signal processor for laser-velocimeter (LV) applications overcomes the major limitations of present signal processors. The system requires no input-signal conditioning other than that provided by amplifiers, and it operates in the instantaneous mode at signal levels from bursts containing as few as 150 photons down to the photon-resolved regime in the averaging mode.

The residual turbulence intensity is 0.2 percent, with little dependence on the signal-to-noise ratio. Therefore, this system has the capabilities of a high-speed burst counter over a greater dynamic range of input-signal levels while providing a more accurate measurement of the signal frequency. It has a residual or false turbulence-intensity value (turbulence-intensity measurement value due to instrument noise obtained with a constant input-signal frequency) approximately one-fifth that of a high-speed burst counter, and this value is obtained with as few as 500 photons per burst and remains essentially constant at higher signal levels.

The frequency-domain LV signal processor (see figure) consists of a nonlinear analog-to-digital converter, data-storage shift registers, a bank of digital elliptical filters, a controlling microprocessor, and miscellaneous frequency- and signal-gain-control circuits. These functional elements are divided into two groups: (1) the high-speed transient-recorder group containing the nonlinear analog-to-digital converter and data-storage shift registers and (2) the low-speed data-processing group containing the filter bank and controlling microprocessor.

The transient-recorder group captures and stores a digitized version of an LV signal burst when the integrated, digitized photomultiplier output signal crosses a threshold level, indicating the presence of the signal burst. The captured signal burst is then transferred to the data-processing group, where it is put into a bank of seven digital elliptical band-pass filters. The signal passing through each of the seven filters is statistically analyzed, using zero-crossing detection and/or energy distribution to yield the frequency of the signal contained within the signal burst. This digital value is then made available to the external data-acquisition hardware or computer system.

The frequency-domain LV signal processor is designed to have two phases of operation. The first is the instrument-setup phase, wherein the reference clock frequency and filter selection are established, and the second is the data-acquisition phase. Following the completion of the data-acquisition phase, the external computer system completes the data-acquisition process by converting the measured frequencies to absolute frequency values through multiplication of the data by the reference clock frequency. Interarrival times (times between adjacent signal bursts) are obtained by using the external data-acquisition system to measure the time between the command pulses from the signal-integration circuit. Therefore, the same data-acquisition scheme cur-

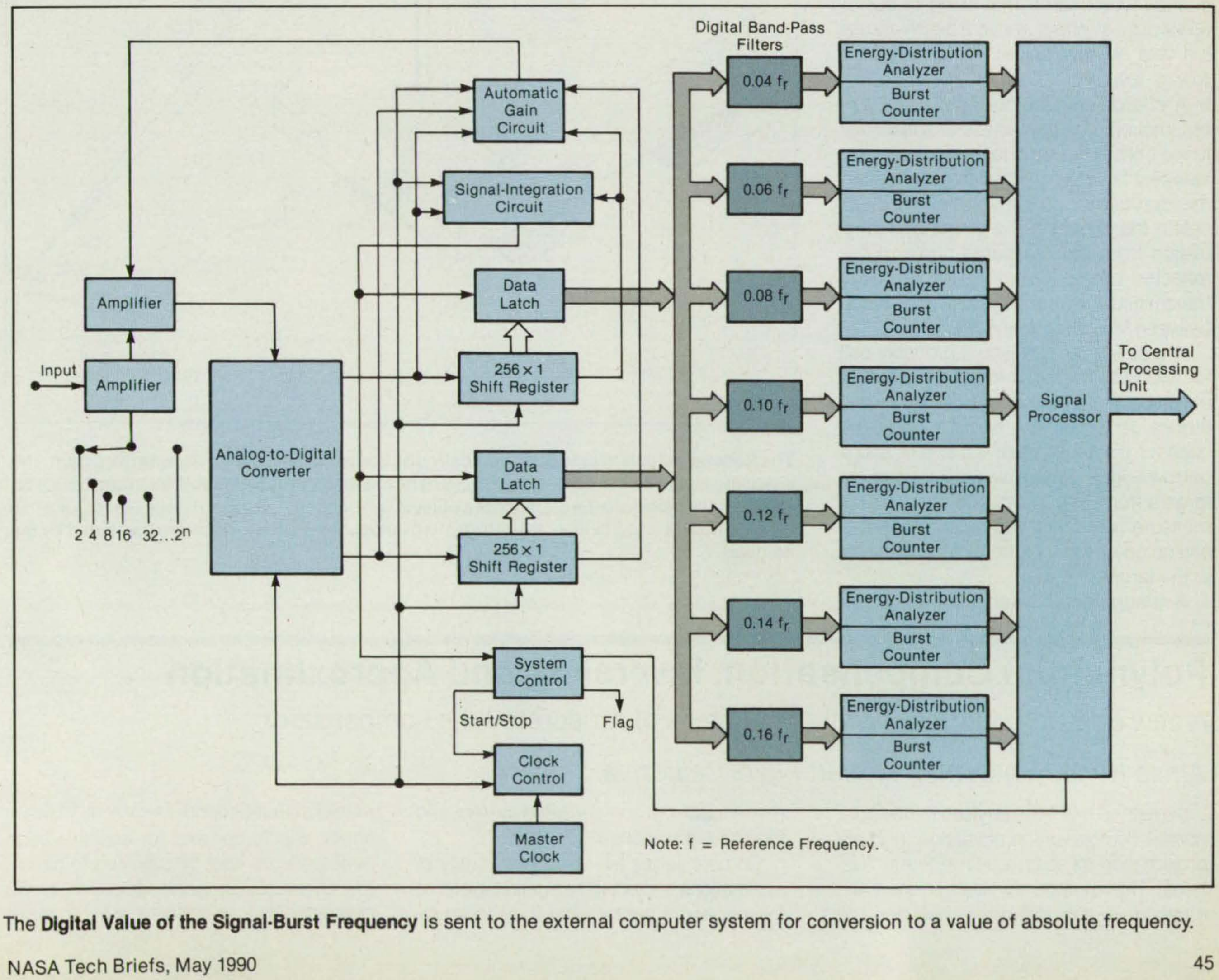

The **Digital Value of the Signal-Burst Frequency** is sent to the external computer system for conversion to a value of absolute frequency.

rently used for high-speed burst-counter measurements is maintained with the frequency-domain LV signal processor.

This work was done by James F. Meyers and James I. Clemmons, Jr., of **Langley Research Center** *and John W. Stoughton, Sharad V. Kanetkar, and Andreas E. Savakis of Old Dominion University. Further information may be found in NASA TP-2735 [N87-27994], "Frequency Domain Laser Velocimeter Signal Processor."*

This invention is owned by NASA, and a patent application has been filed. Inquiries concerning nonexclusive or exclusive license for its commercial development should be addressed to the Patent Counsel, Langley Research Center [see page 16]. Refer to LAR-13552

Electronically Scanned Laser Rangefinder

A system would measure distances to objects in front of a vehicle.

NASA's Jet Propulsion Laboratory, Pasadena, California

A proposed electronic laser scanner would sweep across its field of view without any moving parts, measuring the distances to objects between 0.5 and 20 meters away. The scanner would guide a robotic vehicle around obstacles.

In a conventional laser scanner, the laser is moved by panning and tilting mechanisms to steer the beam. The equipment is bulky and complex and consumes substantial power. The proposed scanner would scan electronically rather than mechanically. It would be immune to the wear, stress, and breakage to which mechanical scanners are subject.

An array of laser diodes, each oriented in a precise angular increment from its neighbor, would be turned on and off in sequence (see figure). This mode of operation would, in effect, move a beam across the field of view, column by column and row by row.

A charge-coupled-device (CCD) camera, mounted on the vehicle at a fixed distance from the array of laser diodes, would intercept beams reflected from targets. A microprocessor on the vehicle would calculate the distance of a target by triangulation from the measured angle of the reflected beam, the known angle of the transmitted beam, and the known distance between the camera and the array.

A practical design would probably call for two CCD cameras to obtain accurate measurements over a large range of distances. A wide-angle camera would be used for distances from 0.5 to 5 m and a narrow-angle camera would be used for targets from 5 to 20 m. The accuracy of measurements with the dual cameras is estimated at 1 to 3 percent of the distance to the target.

A triangulation calculation would be done for each scanned row in the array. The composite scans for each row would show all targets in the field of view. Currently available CCD cameras can produce full composite scans many times per second, so that the relationship of the vehicle to objects in its path can be updated frequently.

This work was done by Katsutnori Shimada of Caltech for **NASA's Jet Propulsion Laboratory**. *For further information, Circle 17 on the TSP Request Card. NPO-17571*

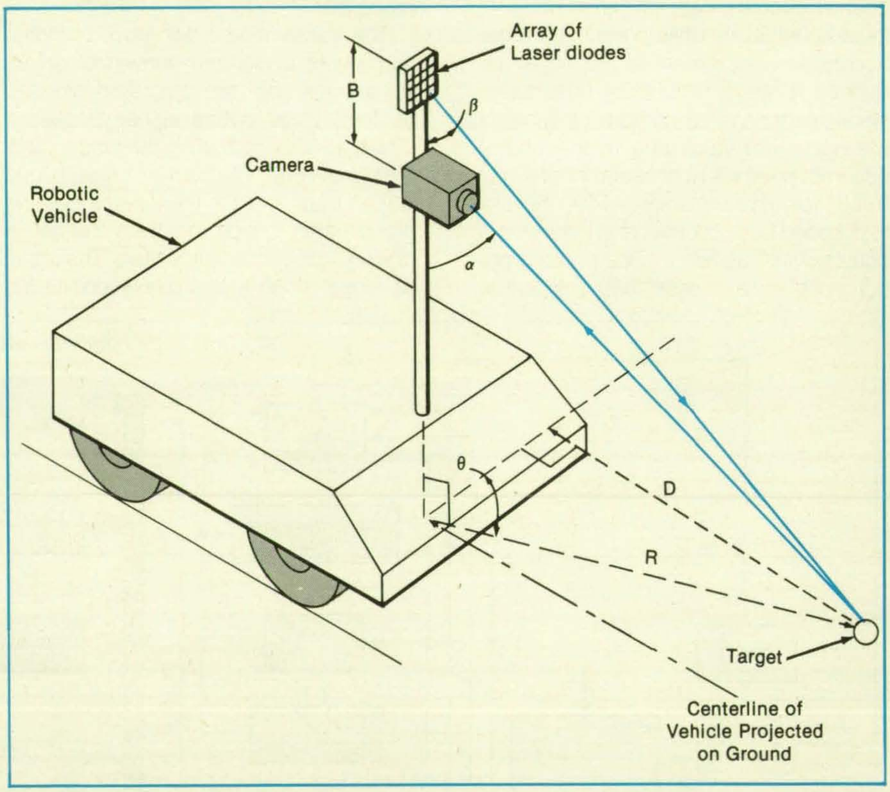

The **Robotic Vehicle Would Scan** vertically and horizontally to detect objects in its path. The scanning would be done electronically, with no mechanical movement. A microprocessor on board would calculate the distances to objects by triangulation. Specifically, R and D are calculated from B and β (which are known in advance) and α and θ (which are measured by the camera).

Polynomial Compensation, Inversion, and Approximation

A new criterion is introduced for the design of a discrete-time compensator.

Ames Research Center, Moffett Field, California

A method has been devised for the polynomial compensation, inversion, and approximation of discrete-time linear systems. The method involves a quadratic measure of the difference between the response of the compensated system and the desired response.

Compensators are used in a variety of applications, including navigation systems for spacecraft, aircraft, and ships and automated manufacturing equipment. There is an increasing demand for adaptive compensators that can be adjusted to cancel the effects of temporal variations in the characteristics of systems; e.g., changes in the distributions of loads on planes and ships and changes in the environment (e.g., winds, currents, and waves). The concepts introduced in the method make it possible to design adaptive compensators with the same techniques used in the design of adaptive linear filters.

The general problem is the transformation of a given linear system into one having desired properties by cascading it with another linear system. This problem has been known in the design of control systems as cascade compensation. The problems of the inversion and approximation of systems can also be formulated as system-transformation problems by properly defining the roles of the systems involved.

An exact causal transformation from the given to the desired system may not exist or may not be feasible because of complexity, and an approximate transformation of relatively low complexity may be desired. However, finding an approximation within the class of rational linear systems of a given order is, typically, a difficult parameter-optimization problem involving local extrema.

In the derivation of the new method, the transformations of discrete-time, multivariable linear systems are treated by convolving these systems with systems that have finite weighting patterns or, equivalently, polynomial transfer matrices. The given and the desired systems are represented in state space. The coefficients of the normal equation and of the approximation error are obtained in closed explicit forms, and it can be shown that they are the weighting patterns of certain linear systems. These systems can, in turn, be used in the recursive solution of the polynomial coefficients by a multivariable version of the Levinson procedure.

The figure shows the impulse responses obtained in the application of the new method in the compensation of a system that has a transfer function given by

$$\Omega(z) = \frac{(z+0.2)(z-0.5\pm 0.2j)(z+0.02\pm 0.1j)}{(z-0.2)(z+0.1)(z+0.6\pm 0.3j)(z-0.1\pm 0.3j)}$$

In this example, a polynomial compensator is used to approximate the desired system

$$\Pi(z) = \frac{1}{(z+0.3521)\ (z-0.8521)}$$

The criterion introduced in this method is an exact analog of the least-squares criterion in array processing and in the rejection of interference (in which an additional objective is to reduce the difference between a filtered version of the received signal and a known reference signal). The connection established by this analogy between the discipline of the design of compensators and that of adaptive linear filtering makes it possible to transfer ideas and techniques from the latter to the former. In particular, the great wealth of adaptive recursive least-squares filtering techniques can be applied to the design of fast adaptive compensators.

This work was done by Yoram Baram of **Ames Research Center**. *For further information, Circle 160 on the TSP Request Card.*
ARC-12174

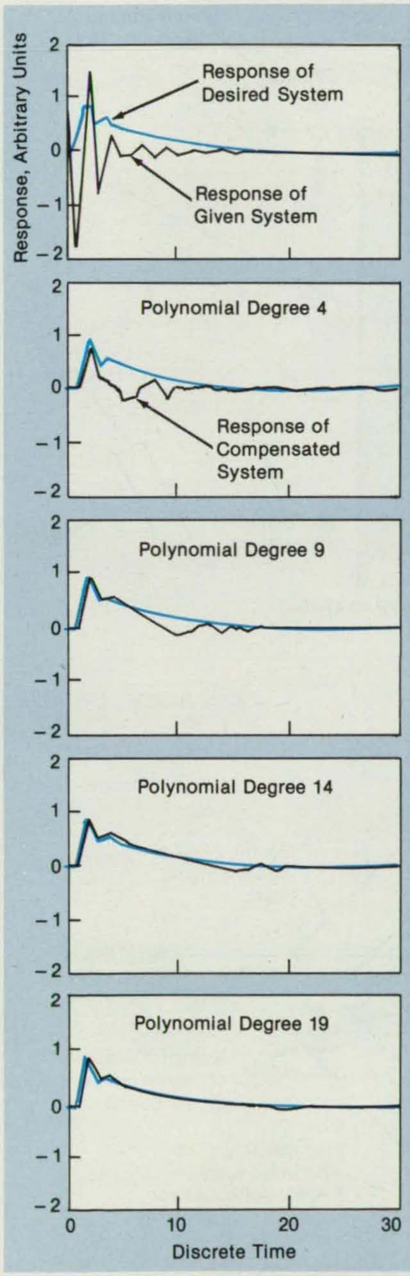

The **Impulse Response** of the compensated system improves as the degree of the polynomial increases. The compensator emphasizes the matching of the large initial response.

Physical Sciences

Hardware, Techniques, and Processes

Books and Reports

Optical Modulation via the Photorefractive Effect

Rotation of polarization and use of an analyzer yield large variations in intensity.

NASA's Jet Propulsion Laboratory, Pasadena, California

Experiments show that one beam of light can be used to change the intensity of another beam via the photorefractive effect in GaAs. The results of the experiments agree closely with predictions of the theory of the photorefractive effect. Furthermore, according to the theory, this modulation scheme should work with other photorefractive materials of similar crystallographic symmetry.

The configuration is shown schematically in the figure. An incident coherent signal beam (the beam to be modulated) and an incident reference beam (the modulating beam) intersect in the GaAs crystal, which is oriented so that the bisector of the angle of intersection of these beams is perpendicular to the surface. The incident beams are polarized along the $\langle 001\rangle$ crystalline axis. The interference vector lies along the $\langle\bar{1}\bar{1}0\rangle$ crystalline axis.

The internally-generated space-charge electric field is also aligned with the $\langle\bar{1}10\rangle$ axis and gives rise to two principal dielectric axes via the electro-optical effect. The component of the electric field of the incident beams that lies along each such axis experiences a change in the index of refraction opposite to that experienced by the component along the other axis. In other words, these two components pass through two different index-of-refraction gratings of equal modulation depth and 180° apart in phase.

The index-of-refraction gratings are 90° out of phase with the pattern of interference between the incident beams, and each grating causes the transfer of optical energy from one beam to the other. The position of the gratings with respect to the interference pattern determines the direction of transfer. The net effect is that in traveling through the crystal, one of the components of the signal beam grows somewhat due to constructive interference while the other component is diminished by destructive interference. Thus, the polarization is rotated through a small angle ψ, as shown in the lower part of the figure. (The polarization of the reference beam is rotated by the same amount in the opposite direction.)

An analyzer (that is, a sheet of polarizing

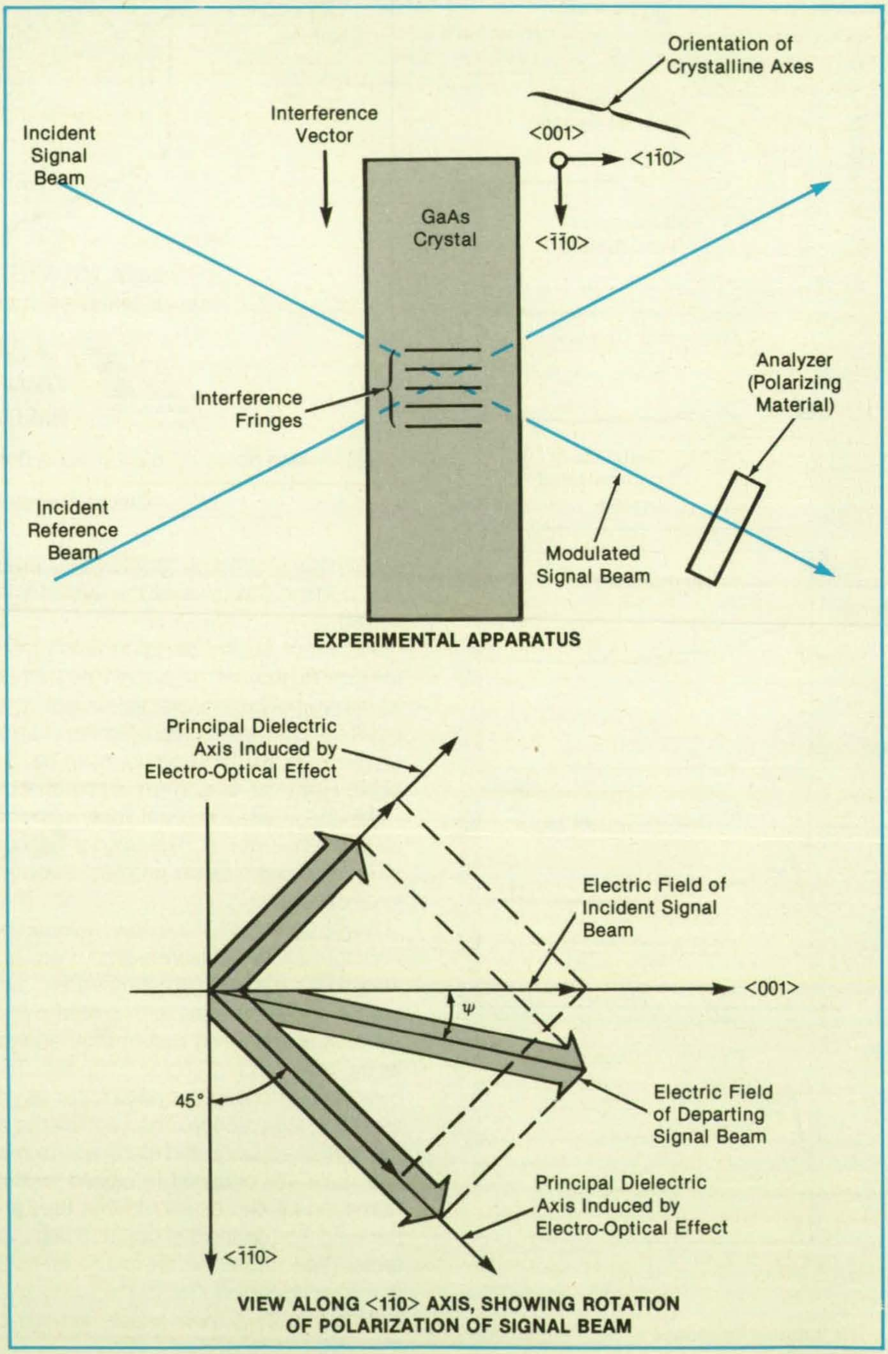

Two Incident Laser Beams Interact via the photorefractive effect in a suitably oriented crystal of GaAs or electro-optically similar material. Each beam causes the polarization of the other beam to rotate. The rotation (in effect, the modulation) can be detected by passing the modulated beam through an analyzer.

NASA invites you to the high-tech show of 1990!

WHERE INDUSTRY CAN

access technology *from NASA and its contractors*

meet NASA technology transfer experts

find new partners *for R&D projects*

learn what's in the pipeline *from current NASA programs*

look at the future *of applied space-based research*

share the experiences *of current spinoff companies*

ALL ABOUT TECHNOLOGY 2000

High-tech innovation — from the revolutionary to the incremental, from the million dollar idea to the .05% reduction in cost — is what **TECHNOLOGY 2000** is all about. Join NASA and NASA Tech Briefs Magazine as they launch the first annual exposition and conference of NASA technology and technology transfer.

In two jam-packed days, government and corporate trailblazers will bring you up to date on the latest innovations in telecommunications, robotics, computational fluid dynamics and other areas — with a focus on potential commercial applications.

Between and after these sessions, you will visit the idea-stocked exhibit area, making contact with experts from all nine NASA research centers as well as many of the leading-edge companies around the country. You will have ample opportunity to meet these leaders, to develop personal contacts with potential R&D partners, and to learn what's directly ahead in a variety of high-tech fields.

Many firms have picked up NASA's ideas and run with them - creating new processes and products both large and small. Others have used space-based technology to hone their internal operations or improve their manufacturing systems. All have fulfilled NASA's stated goal of making American industry more competitive.

You too can benefit from this wealth of government-sponsored research. Join NASA, its leading contractors and spinoff companies at **TECHNOLOGY 2000.**

THE SPONSORS

TECHNOLOGY 2000 is sponsored by **NASA, NASA Tech Briefs Magazine**, and the **Technology Utilization Foundation,** a not-for-profit organization dedicated to technology transfer.

EXHIBITS

Exhibits will be open from 11 a.m. to 5 p.m. on Tuesday and Wednesday, November 27 and 28.

WHO SHOULD ATTEND

Top management, research directors, project leaders, senior/design engineers, scientists and technology transfer agents from public and private organizations. The industries represented include: aerospace, electronics, computers, industrial equipment, defense, communications, bio-medical, materials, power, transportation and chemicals.

THE PROGRAM

NASA management has invited space agency researchers and key industry leaders to address **TECHNOLOGY 2000** audiences. **Several concurrent sessions are planned for the 9 - 11 a.m. and 3 - 6 p.m. time slots on both Tuesday and Wednesday, November 27 and 28.** The tentative program includes symposia on:

MATERIALS SCIENCE
SENSOR TECHNOLOGY
ROBOTICS AND ARTIFICIAL INTELLIGENCE
SOFTWARE ENGINEERING
LASERS/OPTOELECTRONICS
COMPUTATIONAL FLUID DYNAMICS
TELECOMMUNICATIONS
BIO-MEDICINE

A final program, including specific topics and speakers, will be sent to all registrants as soon as possible; they may then choose which sessions they wish to attend.

THE LOCATION

All sessions will be held at the Washington Hilton Hotel and Towers, 1919 Connecticut Ave., N.W., Washington D.C. 20036. The hotel is conveniently located near the DuPont Circle stop on the Metro Red Line, and offers indoor parking.

REGISTRATION AND FEES

The full registration fee is $150, and includes symposia and exhibits for both days. For those who can attend for only one day, registration for technical sessions and exhibits is $100. Attendees may visit the exhibit area only at a cost of $20/day.

Clip the coupon opposite and return with your payment to: Technology Utilization Foundation, 41 East 42 Street, Suite 921, New York, N.Y. 10017 (212)490-3999

HOTEL ACCOMMODATIONS

Reservations must be made directly with
The Washington Hilton, Reservations Department ,
1919 Connecticut Ave., N.W. ,Washington, D.C. 20036
(202)483-3000

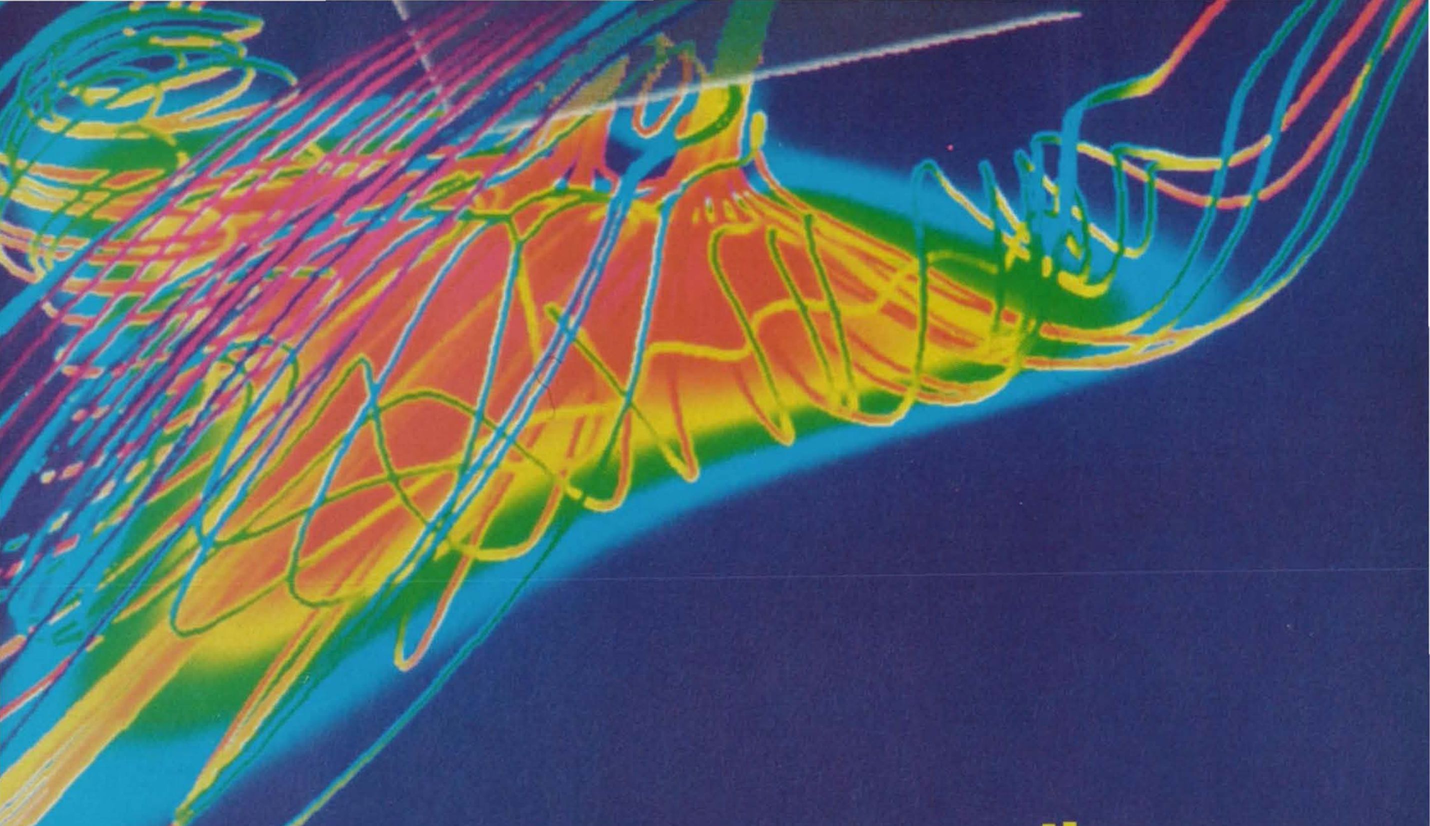

material) is placed in the signal beam on the output side with its axis of polarization oriented to suppress some or all of the signal beam in the absence of the reference beam. Then as the reference beam increases in intensity, the output polarization rotates, and the portion of the signal beam that passes through the analyzer increases in intensity. In the experiments, which were conducted with a helium/neon laser operating at a wavelength of 1.15 μm, the modulation reached a level of 500 percent, limited only by the finite extinction ratio of the analyzer.

This work was done by Li-Jen Cheng and A. Partovi of Caltech and E. Garmire of the University of Southern California for **NASA's Jet Propulsion Laboratory**. *For further information, Circle 162 on the TSP Request Card.*
NPO-17460

Generating Second Harmonics in Nonlinear Resonant Cavities

Single-axial-mode lasers pump very-low-loss doubling crystals.

Langley Research Center, Hampton, Virginia

There has been increased interest in the development and applications of solid-state lasers pumped by diode lasers. One important application is in the generation of visible radiation by doubling of frequency. Since the power levels of diode-pumped continuous-wave lasers are relatively low, the efficient generation of second harmonics requires some methods of increasing the intensities in the doubling crystals.

Although internal second-harmonic-generating lasers typically yield good conversion efficiencies, they usually oscillate in several axial modes, resulting in large fluctuations in the amplitudes of the second harmonics. Experiments in the generation of second harmonics with the help of external resonant cavities have indicated the importance of using both lasers that are stable in frequency to maintain the resonance condition, and very-low-loss external cavities and doubling crystals for large fundamental enhancements.

An important advance in making resonant generation of second harmonics possible for diode-laser-pumped solid-state lasers has been the recent development of monolithic nonplanar ring geometries in neodymium:yttrium aluminum garnet (Nd:YAG) lasers that produce frequency-stable single-mode outputs. The other important advance was the development of high-quality MgO:LiNbO$_3$ as an electro-optically nonlinear material. Accordingly, a series of experiments was devised to improve the doubling efficiency of low-power lasers, and particularly of diode-laser-pumped continuous-wave Nd:YAG lasers.

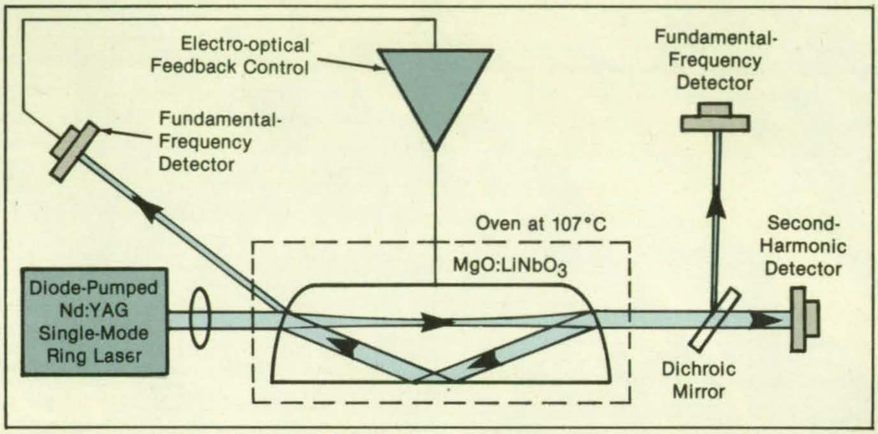

In the **Experimental Ring Doubler**, the single-ended output is detected through the dichroic mirror. The reflected fundamental-frequency beam used for locking is measured directly, eliminating the need for the Faraday isolator that would be required if this were a standing-wave doubler.

A Nd:YAG nonplanar ring oscillator was used in three experiments. MgO:LiNbO$_3$ was selected as the nonlinear material for these experiments because of its low loss and large nonlinear coefficient for noncritical phase-matched doubling of the frequency of radiation of a wavelength of 1,064 nm. A monolithic cavity was desired for these experiments to ensure the lowest possible cavity losses and good frequency stability. The resonators were formed by polishing curved ends on the MgO:LiNbO$_3$ crystal and then depositing thin films directly on these curved surfaces.

The experiments were performed on three separate monolithic resonators: a standing-wave doubler and two external-ring resonant doublers. The figure shows the experimental setup for the external-ring-resonant-doubler experiments. The frequency of the laser was controlled by adjusting the temperature of the laser crystal. The ring geometry eliminates the need for a Faraday isolator because the incident fundamental-frequency beam is reflected and refracted obliquely from the slanted surface of the external cavity. The reflected portion of this power is detected and used for locking the ring doubler by use of the dither-and-lock-in-detection technique. The dither-and-lock-in-detection servo proved to be very robust, tracking the effect of the thermal drift, and the system maintained lock and good second-harmonic-power stability for arbitrarily long periods.

In one experiment, 56 percent efficiency was achieved in the resonant generation of second harmonics by use of an external cavity with a diode-laser-pumped, continuous-wave, single-axial-mode Nd:YAG laser. A theory of external doubling with a resonant fundamental was developed and compared with experimental results for three monolithic cavities of nonlinear MgO:LiNbO$_3$. This technique is being used to pump an optical parametric oscillator, which can be used for remote wind measurements. The doubler laser can also be used as a frequency standard for laboratory calibration of "wavemeters" (for use in accurate measurements of the frequencies of lasers).

This work was done by William J. Kozlovsky, C. David Nabors, and Robert L. Byer of Stanford University for **Langley Research Center**. *No further documentation is available.*

In accordance with Public Law 96-517, the contractor has elected to retain title to this invention. Inquiries concerning rights for its commercial use should be addressed to
Jon Sandelin
Office of Technology Licensing
Stanford University
857 Serra St., Second Floor
Stanford, CA 94305-6225
Refer to LAR-14051, volume and number of this NASA Tech Briefs *issue, and the page number.*

Classification of Radar Scatterers Via Polarimetric Data

Scattering mechanisms are identified via polarization signatures.

NASA's Jet Propulsion Laboratory, Pasadena, California

An algorithm automatically classifies the radar-backscattering mechanisms in images produced by a synthetic-aperture-radar polarimeter. The algorithm uses the full polarimetric data from each picture element. These data can generally be expressed in terms of a complex 2 by 2 scattering matrix equivalent to three independent amplitudes and three independent phases that represent the relationships between the horizontally- and vertically-polarized components of the transmitted and backscattered signals.

The algorithm constructs the Mueller matrix, which is a 4 by 4 matrix derived from products of scattering parameters and their complex conjugates. It classifies the scattering mechanism of each picture element by comparing the polarization properties expressed in its Mueller matrix with the polarization properties expressed in the Mueller matrices of mathematical models of three simple types of scatterers: a slightly rough surface, a dihedral corner reflector, and an area (e.g., a forest) that exhibits a large amount of diffuse scattering (see figure).

In an experimental application to a polarimetric radar image of the San Francisco Bay area in California, the algorithm classified scattering by the ocean as similar to that predicted by the model of the slightly rough surface. Scattering by the urban area was classified as being similar to that predicted by the model of the dihedral corner reflector. Scattering by the Golden Gate Park was classified as being similar to that predicted by the model of the forest. The large diffuse component in the backscattering from an area in San Francisco where the streets made an angle of about 45° with the line of sight of the radar caused that area to be classified as having a radar appearance similar to that of forest. The algorithm also classified the scattering by a lighthouse in the ocean and boats on the surface of the ocean as being similar to that predicted by the model of the dihedral corner reflector, making it easy to identify such an object against the background of the surrounding ocean.

The algorithm was also applied to vegetated areas. Scattering from clear-cut areas and agricultural fields was found to be mostly similar to that predicted by the model of the slightly rough surface. In areas covered by trees, there was a mixture of picture elements for which the scattering was similar to that predicted by all three models. As the angle of incidence increased, more picture elements were classified as forested areas because the random scattering from the canopies became stronger relative to the scattering attributable to dihedral corner reflectors and slightly rough surfaces. This is a consequence of the thicker effective canopy through which the doubly reflected signals and the direct backscatter from the ground have to pass through before reaching the receiver.

Other results show that the return from an area with dead trees cn ground saturated with water is different from the return from a normal area covered with trees. Also, the results show that in areas with lakes surrounded by forests, a strong double-bounce effect is observed on the far shores of the lakes because of reflections from the surfaces of the lakes onto the trees on the shore, followed by reflection from these trees back to the receiver.

This work was done by Jakob J. Van Zyl of Caltech for **NASA's Jet Propulsion Laboratory**. *For further information, Circle 9 on the TSP Request Card.* *NPO-17373*

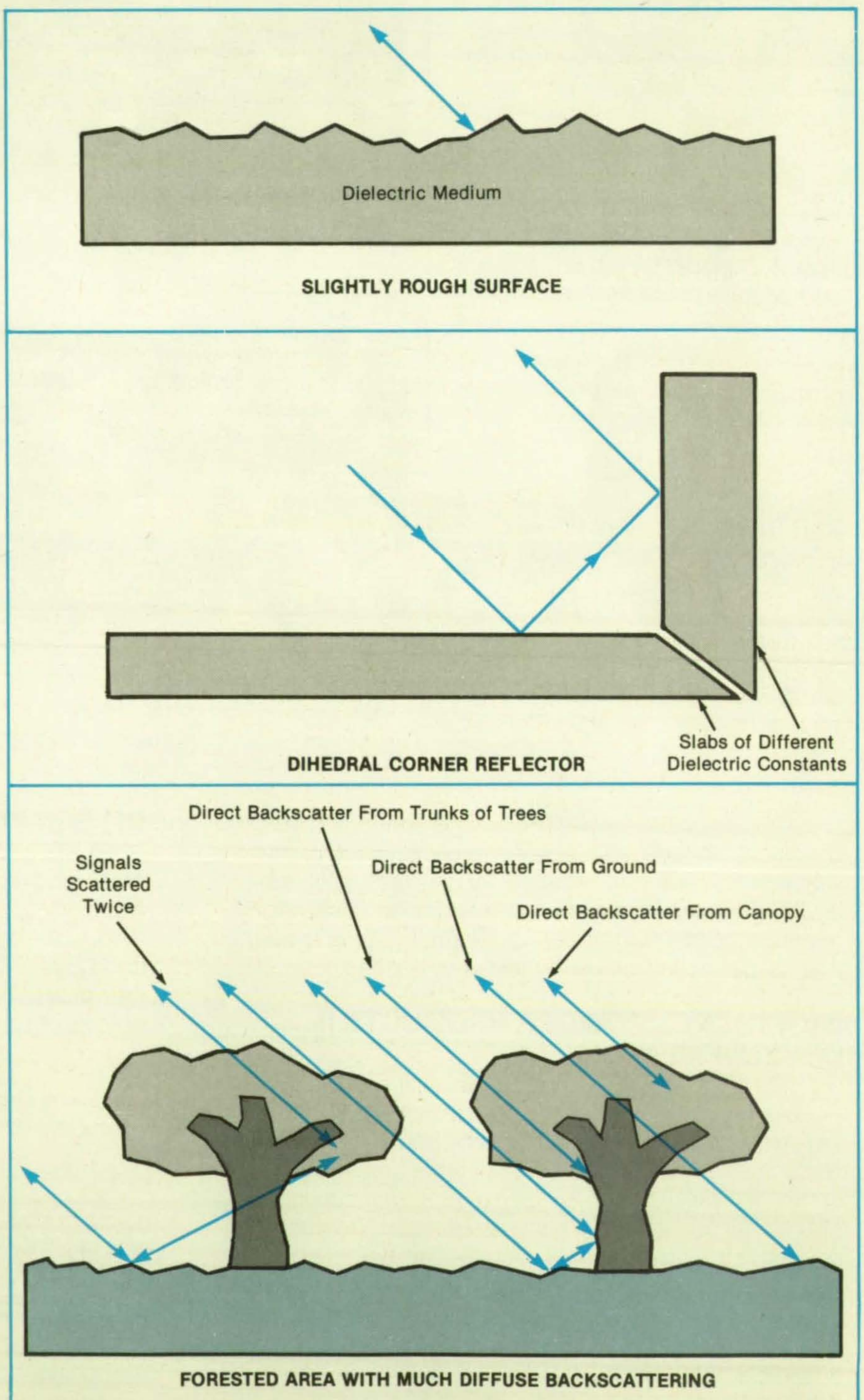

The **Type of Scatterer** in each picture element of a polarimetric radar image is identified by the similarity of its radar-backscattering polarization properties to the radar-backscattering polarization properties of one of these mathematical models.

Molecular Electronic Shift Registers

Electrical charges would be transferred along chains of repeating molecular units.

NASA's Jet Propulsion Laboratory, Pasadena, California

Molecular-scale shift registers may eventually be constructed as parts of high-density integrated memory circuits. In principle, the variety of organic molecules makes possible a large number of different configurations and modes of operation for such shift-register devices. Several classes of devices and implementations in some specific types of molecules have been proposed. All are based on the transfer of electrons or holes along chains of repeating molecular units.

Figure 1 illustrates a device of one of the conceptual classes. Each repeating unit would include three molecular groups (α, β, and γ) that would serve as electron-localization sites. A "1" (or "0") would be written by reducing (or not reducing) the first repeat unit in the chain, which would be in contact with an electrode. Exposing the chain to short, intense bursts of light would shift the written state one unit to the right. The potential of the electrode would determine whether a "1" or "0" is written into the left end of the shift register during a given flash of light. On the three units shown in this figure, the state of charge represents the string "010". Periodic pulses of light would both provide the power and serve as the synchronizing clock signals. Electrons would collect at an electrode at the right end of the chain.

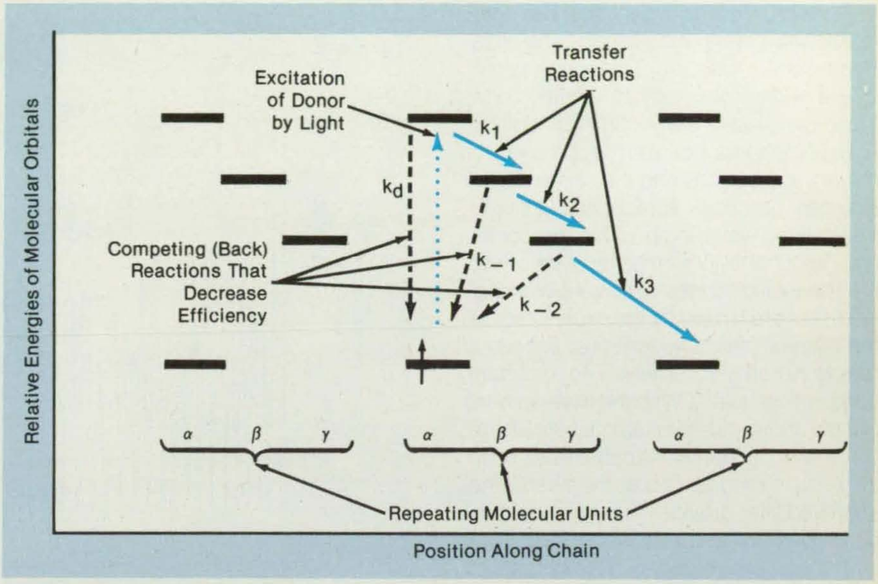

Figure 1. The **Shift of an Electron** is initiated by the excitation of the donor (α) molecular subunit. The presence of an electron (representing a "1") in the second unit is represented by the small upward-pointing arrow.

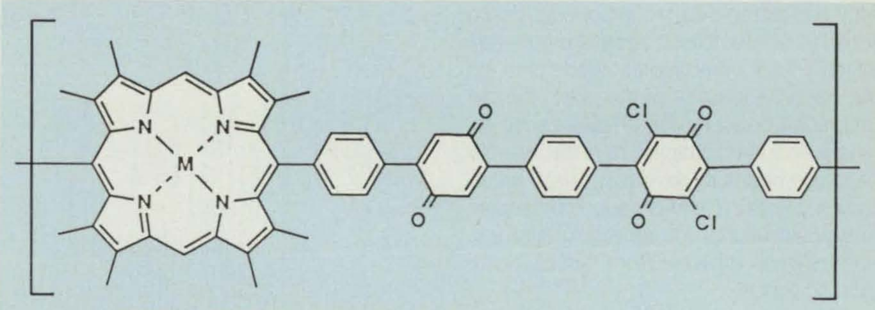

Figure 2. This **Repeating Unit of a Polymer** has energy levels distributed according to the scheme shown qualitatively in one of the repeating units in Figure 1. This polymer would be put into the active state (000...0) by electrochemical oxidation of all porphyrin species; a "1" would be written on the left side of the molecule by reducing the ring. The porphyrin could be built from functionalized segments.

The generic requirements for the proper function of systems like the one in Figure 1 include the following: (1) the forward transfer from the excited donor must be much faster than the corresponding radiative plus nonradiative decay to the donor ground state ($k_1 \gg k_d$); (2) all forward transfers must be faster than reverse transfers ($k_2 \gg k_{-1}$ and $k_3 \gg k_{-2}$); and (3) the transfer of electrons from the excited donor (k_1) must be much faster than the recombination rate (k_{-2}) to avoid a "bottleneck" at the connection between repeating units.

The intermediate state serves the vital function of allowing a first extremely fast transfer of charge to compete with unproductive decay of the donor excited state. The residence of the electron at the intermediate prevents the confusion of the electronic "bits" in adjacent cells. This intermediate also provides a large distance between the acceptor and donor states within a single repeating unit. Because these electron-transfer reactions decay approximately exponentially with distance, intermediates are essential for efficient transfer of charge over long distances. The molecule is chosen to have an intermediate electronic state from which a thermodynamically allowed reverse transfer of an electron is forbidden.

The clock-cycle time must be much longer than the time required to transfer an electron from donor to donor. Also, the duration of the pulse of light must be short enough to suppress the shift of charge along more than one repeating unit at a time. Multiple excitation cycles per clock cycle can be used to optimize the yield (because the probability of charge transfer during each cycle could be less than 1). Writing one bit every other clock cycle avoids the "bottleneck" problem but halves the density of information.

Figure 2 illustrates a repeating molecular unit of the type that might be used to implement the scheme of Figure 2. This unit contains a porphyrin, quinone(1), quinone (2) chain. The rate could be tuned by alteration of the linking units; for example, by addition of a rigid saturated spacer bicyclo[2,2,2]octane unit. M could be Zn or Pd, for example. Both give stable porphyrins in the two oxidation states. By altering the metal, the lifetime of the excited donor state could be tuned to optimize the quantum yield for the transfer of electrons.

This work was done by David N. Beratan of Caltech for **NASA's Jet Propulsion Laboratory** *and by Jose N. Onuchic of the Instituto de Fisica e Quimica de Sao Carlos, Brazil. For further information, Circle 8 on the TSP Request Card.*

This invention is owned by NASA, and a patent application has been filed. Inquiries concerning nonexclusive or exclusive license for its commercial development should be addressed to the Patent Counsel, NASA's Resident Office-JPL [see page 16]. Refer to NPO-17606

Improved Design for Birefringent Filter

Highly selective laser tuning is achieved without thin plates of questionable optical quality.

Langley Research Center, Hampton, Virginia

An improved birefringent filter has been developed for use with a broad-band-emission laser; for example, Ti:sapphire, which offers wide frequency tunability. Such broad-band lasers are becoming popular in scientific laboratories and may be useful in military applications and the separation of isotopes. For many applications, a single, well-defined wavelength within the continuous spectral output range must be selected. The tuning ranges of current birefringent filters are limited by the thicknesses of the thinnest plates, which must exceed a few hundred micrometers to maintain good optical quality. With the development of new, more-widely-tunable lasers, these filters are frequently inadequate to span the entire tuning ranges of the lasers. The improved filter provides improved narrow-band operation and wavelength selectivity.

The typical birefringent filter consists of several plates fabricated from optical material that exhibits double refraction or birefringence. Polarized light incident on one surface of a single plate is split into ordinary and extraordinary components, which travel at different velocities in the material. When these components recombine on the opposite surface of the plate, the net difference between the phases of the ordinary and extraordinary rays causes the resultant beam to have a different polarization. Because losses depend on angles and polarizations, the emerging light has an amplitude different from that of the incoming light.

Wavelength selectivity is possible because the outgoing beam of light is identical to the incoming beam at some values of the net phase difference. A series of plates of different thicknesses gives the necessary flexibility to achieve high losses at all but a few wavelengths. These highly transmitted wavelengths are tunable by variation of the angle of the incoming beam with respect to the optical axis of the material.

The new filter design improves the traditional design by providing a method of increasing the wavelength separation between the highly transmitted peaks. The usual method of increasing this separation is to fabricate thinner plates. The thicknesses of the thicker plates are integral multiples of the thickness of the thinnest plate.

The problem is that optical qualities of very thin plates are questionable. The solution provided by the improved design is to fabricate plates with thicknesses that are not integral multiples of that of the thinnest plate, but are rather integral multiples of the difference between the thicknesses of the two thinnest plates. To a large extent, the resultant wavelength selectivity of the improved device is equivalent to that which would be achieved in a similar device that has a thin plate of thickness equal to this difference between thicknesses.

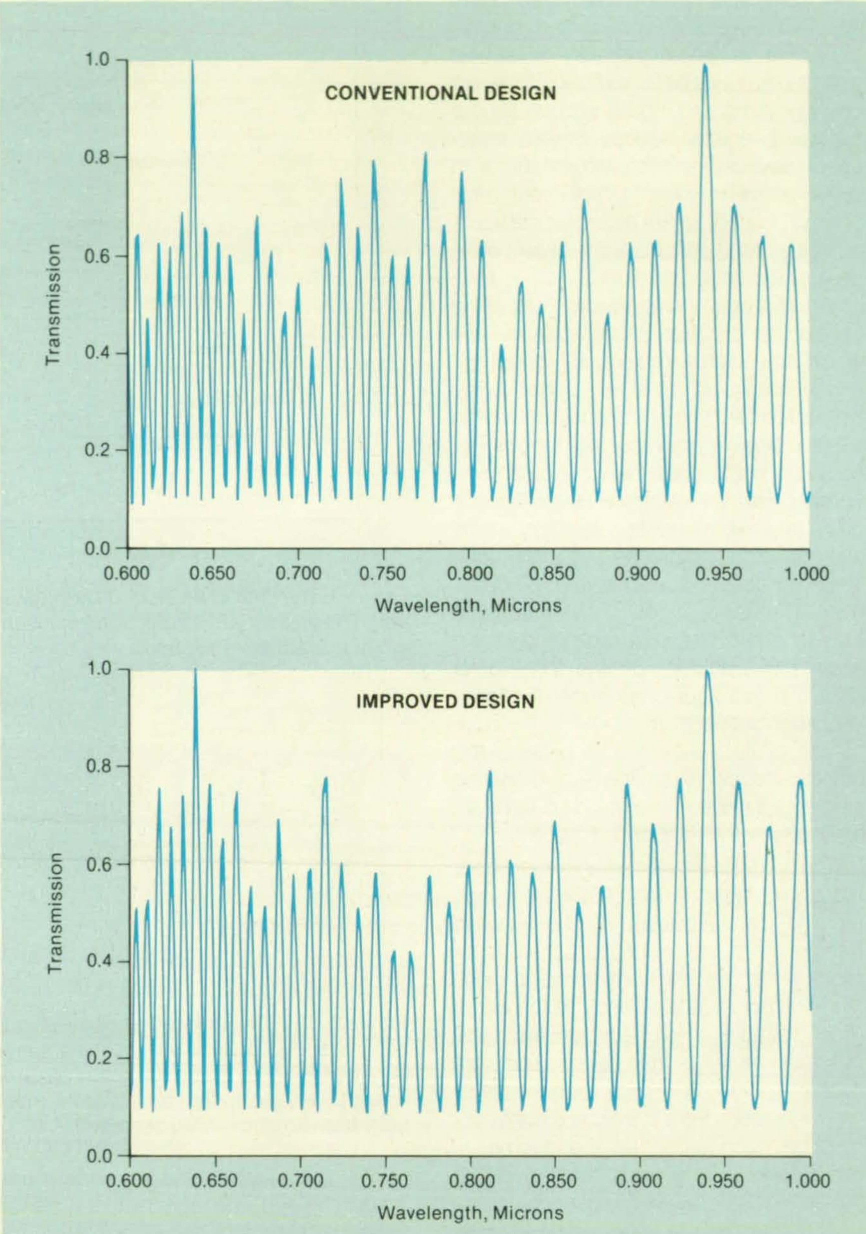

The **p-Polarized Components of Light Transmitted Through Filters** are compared. The upper curve is for an improved filter that consists of plates with thickness of 0.5, 0.75, 1.5, and 4.5 mm. The lower curve is for a traditional filter made of plates 0.25, 0.50, 1.5, and 4.5 mm thick. The comparison shows that nearly identical selectivity is achieved with the improved filter design, without the necessity of fabricating the 0.25-mm plate.

This work was done by Clayton H. Bair of **Langley Research Center**. *For further information, Circle 151 on the TSP Request Card.*

Inquiries concerning rights for the commercial use of this invention should be addressed to the Patent Counsel, Langley Research Center [see page 16]. Refer to LAR-13887

Books and Reports

These reports, studies, handbooks are available from NASA as Technical Support Packages (TSP's) when a Request Card number is cited; otherwise they are available from the National Technical Information Service.

Response of Ceramic Insulation to Aerothermodynamic Heating

A simplified theoretical model predicts the thermal behavior of composite materials.

The thermal conductivities determined from an engineering model can be used to predict accurately the thermal responses of multicomponent insulation on spacecraft, a study has found. The types of insulation studied include such composite parts as an alumina-enhanced thermal barrier backed by low-density fibrous refractory material. Multicomponent insulation could be used in future spacecraft and will be exposed during reentry and aerobraking maneuvers in the outer atmosphere to environments even harsher than that of the Space Shuttle.

The study showed that the internal responses of various types of multicomponent insulation to aerothermodynamic heating can be calculated with the help of a computer program that implements an engineering model for thermal conductivity. The transfer of heat by internal radiation plays a major role in the responses of fibrous materials at high temperatures and is incorporated into the model and program.

A high-energy airstream was directed at specimens by passing air through a constricted-arc heater and expanding it through a conical nozzle. Temperatures on the surfaces of the specimens were as high as 1,800 K. Hypersonic flow through the test chamber was attained by maintaining a constant airmass flow rate and the appropriate pressure ratio between the arc heater and heat exchanger located at the outlet of the chamber.

The specimens consisted of tapered insulation rings surrounding disks, the flat faces of which were exposed to the airstreams. Each disk was made of two different insulating materials bonded together with a layer of glass adhesive. The outer surface of the model was coated with a reaction-cured glass. Six thermocouples were installed in each disk: one just under and in contact with the glass coating, one in contact with the glass bond, and four others at various depths in the disk.

The thermal-conductivity model represents the material in terms of interlocking walls of fibers that define uniform cubic pores. Anisotropy is represented by placing fewer fibers in the walls oriented along the weak direction. One-dimensional flow of heat with additive contributions of conduction in the solid, conduction in the gas, and radiation are assumed.

The thermal-conductivity model and program were combined with a thermal-response program that executes an implicit finite-difference procedure for the calculation of the transient transport of thermal energy through a one-dimensional isotropic material. The combination program predicted the dependence of the temperature upon time and depth in the specimens during exposure to the arc jet. The input data for the computation included the composition of each material in the composite, physical properties from the engineering model, and average values of an emittance-adjustment parameter and a bonding efficiency parameter.

This work was done by David A. Stewart and Daniel B. Leiser of **Ames Research Center**. *To obtain a copy of the report, "Thermal Response of Integral Multicomponent Composites to a High-Energy Aerothermodynamic Heating Environment with Surface Temperature to 1800° K," Circle 147 on the TSP Request Card.*
ARC-12156

Materials

Ethynyl-Terminated Imidothioethers and Derived Resins

Novel materials and resin blends prepared from them show excellent processability and mechanical properties.

Langley Research Center, Hampton, Virginia

Structural resins with favorable combinations of such properties as long-term environmental durability over moderate temperature ranges, tolerance to damage, and resistance to solvents are required for use in hot areas on advanced and commercial aircraft. The new toughened epoxies exhibit excellent properties, but the tempertures at which they can be used are limited.

Bismaleimide resins are some of the base materials being formulated to develop materials that can be used at moderate temperatures. Accordingly, work has been conducted on the use of the acetylenic (ethynyl) group to cross-link and extend the chains of oligomers and polymers to obtain materials that can perform at higher temperatures. This work has been extended to ethynyl-terminated imidothioethers (ETI's).

Novel ETI's were prepared from the reaction of N-(3-ethynylphenyl)maleimide and aromatic dimercaptans. Blends of ETI's and ethynyl-terminated arylene ether (ETAE) oligomers of various molecular weights were also prepared (see figure). The physical and mechanical properties of the cured blends followed a trend depending upon the crosslink density. In general, the blends exhibited excellent processability and showed good fracture toughness, resistance to solvents, and adhesive and composite properties.

The ETI's constitute new compositions of matter. The properties of cured ETI's are similar to those of cured bismaleimides of similar structure. The ETI's are formed as mixtures of stereoisomers (d, l, and meso forms) and, as such, have a lower and broader range of melting temperatures than do bismaleimides of similar structure. These factors make ETI's more amenable than comparable bismaleimides are to processing into adhesive tapes and prepregs via melt techniques. The ETI's exhibit lower melt temperatures, higher fracture toughnesses, and better adhesive properties than comparable bismaleimides.

As an example, an ETI was blended with an equal weight of an ETAE oligomer with a number average molecular weight of 8,000 g/mole (see figure). The resulting blend was processed into moldings and adhesive specimens by heating to 250 °C under a pressure of 100 to 200 psi (0.7 to 1.4 MPa) and held for 0.5 h. The fracture toughness (K_{IC}, critical stress intensity factor) of the neat resin was approximately 1,500 psi•in.$^{1/2}$ (1.6 N•m$^{-3/2}$). Titanium-to-titanium tensile shear specimens of the cured blend provided average tensile shear strengths of 4,500 psi (31.0 MPa) at a temperature of 25 °C, 2,700 psi (18.6 MPa) at 150 °C, 2,200 psi (15.2 MPa) at 177 °C, and 2,550 psi (17.6 MPa) at 177 °C after 1,000 h at 200 °C. The failed specimens exhibited predominately cohesive failures. The flash from one of the specimens exhibited a glass-transition temperature of 245 °C.

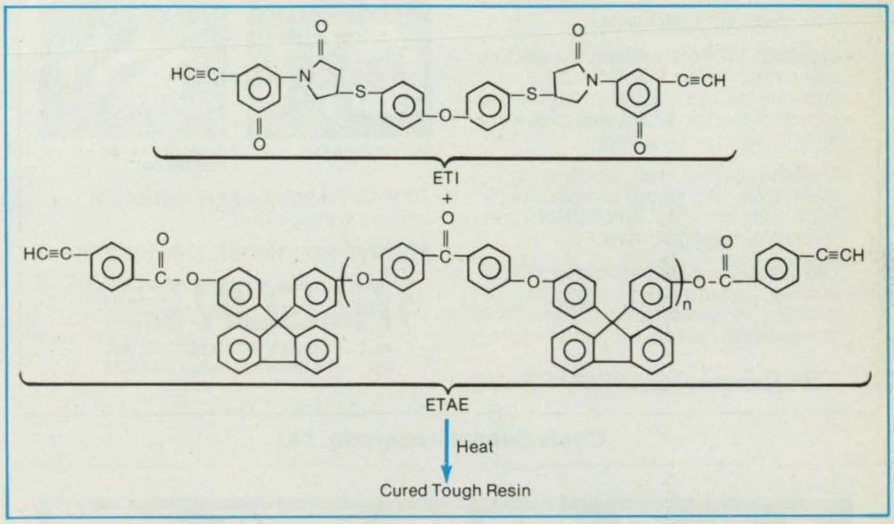

This **Blend Derived From ETI and ETAE Oligomers** exhibits an attractive combination of mechanical properties, including high toughness.

Unsized carbon/graphite fiber (AS-4) was solution-coated with a 1,4-dioxane solution (40 percent solids content) of 1:1 ETI/ETAE (8000) on a drum winding machine. The prepreg was dried (volatile content less than 1 percent), stacked unidirectionally in a stainless steel mold, and consolidated by heating to 190 °C and holding at 190 and 250 °C each for 0.5 h under 200 psi (1.4 MPa). The panel (calculated resin content approximately 38 percent) was free of voids, as evidenced by ultrasonic scanning. The composite specimens exhibited flexural strength, flexural modulus, and short-beam shear strength of 246.0 kpsi (1.70 GPa), 16.8 mpsi (116 GPa), and 10.8 kpsi (75 MPa) at 25 °C and 109.8 kpsi (757 MPa), 9.2 mpsi (63 GPa), and 4.2 kpsi (29 MPa) at 150 °C, respectively. The flexural strength and modulus after aging 1,000 h at 200 °C in circulating air were 221.9 kpsi (1.530 GPa) and 13.5 mpsi (93 GPa) at 25 °C and 190.1 kpsi (1.311 GPa) and 13.9 mpsi (96 GPa) at 150 °C, respectively.

The new materials were tested primarily as adhesives and composite matrices and were found to have useful properties in terms of processing, resistance to high temperature, fracture toughness, and resistance to solvents. They also have desirable mechanical properties. These materials are potentially useful for aerospace and nonaerospace applications.

This work was done by Paul M. Hergenrother and John W. Connell of **Langley Research Center** *and R. G. Bass of Virginia Commonwealth University. For further information, Circle 73 on the TSP Request Card.*
LAR-13910

Books and Reports

These reports, studies, handbooks are available from NASA as Technical Support Packages (TSP's) when a Request Card number is cited; otherwise they are available from the National Technical Information Service.

Flammabilities of Graphite-Reinforced Composites

Composites made with epoxy and other matrices are compared with each other.

A report describes tests and comparisons of the flammabilities, thermal properties, and selected mechanical properties of composite materials made of epoxy and other matrices reinforced by graphite fibers. These composites are also compared with a baseline epoxy/fiberglass composite. The report considers such properties as the limiting oxygen index (a measure of the minimum concentration of oxygen that supports combustion of the material in question), smoke evolution, products of thermal degradation, total heat release, heat-release rate, loss of mass, spread of flames, resistance to ignition, and thermal stability.

A panel made of the epoxy-matrix composite had the greatest total heat release and heat-release rate, smoke evolution, loss of mass, and carbon monoxide evolution. It also had the lowest limiting oxygen index — that is, the greatest propensity to burn.

On the other hand, a composite panel with a matrix blended from vinylpolystyrylpyridine and bismaleimide had the lowest heat release and heat-release rate and the highest limiting oxygen index — valuable properties in passenger aircraft structures. This composite also exhibited much greater flexural strength and tensile strength than did the baseline epoxy/glass composite.

A panel made of a different composite also based on the vinylpolystyrylpyridine-bismaleimide matrix had the lowest flame-spreading index. A panel made of composite based on a polystyrylpyridine matrix generated the least smoke. All graphite-reinforced composites were self-extinguishing.

This work was done by Demetrius A. Kourtides of **Ames Research Center**. *Further information may be found in NASA TM-100049 [N88-16825], "Review of Thermal Properties of Graphite Composite Materials."*

Copies may be purchased [prepayment required] from the National Technical Information Service, Springfield, Virginia 22161, Telephone No. (703) 487-4650. Rush orders may be placed for an extra fee by calling (800) 336-4700.
ARC-12165

Pyrolysis Products of Dimethyldichlorosilane

Silicon carbide appears to be formed along two different reaction paths.

A report describes an experimental study of the chemical reactions and the chemical products of the chemical-vapor deposition of silicon carbide from dimethyldichlorosilane. This topic is important because it relates to the current interest in lightweight refractory materials for use in advanced aircraft and spacecraft. Of particular interest here are the conditions that help or hinder the deposition of strong, fully dense, pure silicon carbide — typically in the pores of substrates to form composites.

Experiments focused on the gaseous byproducts were conducted in a mullite reactor tube in a resistance-heated furnace. Dimethyldichlorosilane was vaporized and carried into the reactor tube, sometimes with hydrogen and/or other gases, in a carrier gas of nearly pure argon. The distribution of temperature in the reactor was measured with a thermocouple. A small sample of the gases entering and leaving the reactor was sent to a chromatograph for analysis.

Experiments focused on the solid product were conducted in a quartz reaction tube. The heated reaction zone was followed by an air condenser and a glass-wool filter. The reactor was weighed before and after to determine the weight of the product. A sample of the solid product was subjected to elemental analysis. In some cases, the condenser product was subjected to infrared analysis; it was also pyrolized, and the resulting pyrolysis gases were analyzed in the chromatograph.

The analyses showed that at a temperature of 700 to 1,100 °C and a contact time of about 1 minute, SiC may form by two chemical-reaction paths. One appears to involve the formation, at about 800 °C, of a solid mixture of silicon carbide, silalkanes, cyclics, and carbosilanes. This mixture contains large quantities of hydrogen and chlorine and reacts slowly to form silicon carbide. The other path involves reactions among the pyrolysis gases formed in the decomposition of the dimethyldichlorosilane. At about 1,000 °C, these gases may be reduced by hydrogen to form silicon and carbon, which could then react to form silicon carbide.

All of the solid material formed could be trapped in the pores of a substrate; but unless the reaction conditions are chosen appropriately, the solid material would not be pure silicon carbide. A major portion could be a mixture containing carbon, hydrogen, and chlorine. This solid could react slowly to form silicon carbide at high temperature or could hydrolyze when exposed to the atmosphere.

During these processes, the solid can shrink, forming defects or voids or becoming contaminated. The proportion of impurities remaining may be greater when a lower reaction temperature is used in order to prevent the deterioration of silicon carbide fibers at high temperatures in silicon carbide/silicon carbide composites by the attack of HCl, a product of the pyrolysis. One remedy might be to develop a postcuring procedure to form pure silicon carbide or at least a protective coat of silicon dioxide and silicon carbide.

This work was done by D. E. Cagliostro and S. R. Riccitiello of **Ames Research Center** *and M. G. Carswell of San Jose State University. To obtain a copy of the report, "An Analysis of the Pyrolysis Products of Dimethyldichlorosilane in the Chemical Vapor Deposition of Silicon Carbide," Circle 148 on the TSP Request Card.*

Inquiries concerning rights for the commercial use of this invention should be addressed to the Patent Counsel, Ames Research Center [see page 16]. Refer to ARC-12169

Computer Programs

COSMIC: Transferring NASA Software

COSMIC, NASA's Computer Software Management and Information Center, distributes software developed with NASA funding to industry, other government agencies and academia.

COSMIC's inventory is updated regularly; new programs are reported in *Tech Briefs*. For additional information on any of the programs described here, circle the appropriate TSP number.

If you don't find a program in this issue that meets your needs, call COSMIC directly for a free review of programs in your area of interest. You can also purchase the annual *COSMIC Software Catalog*, containing descriptions and ordering information for available software.

COSMIC is part of NASA's Technology Utilization Network

COSMIC® — *John A. Gibson, Director,*
(404) 542-3265
The University of Georgia, 382 East Broad Street, Athens, Georgia 30602

Computer Programs

These programs may be obtained at a very reasonable cost from COSMIC, a facility sponsored by NASA to make computer programs available to the public. For information on program price, size, and availability, circle the reference number on the TSP and COSMIC Request Card in this issue.

Electronic Systems

Program for Engineering Electrical Connections

Harmony of system and cabling engineering designs is assured.

DFACS is an interactive multiuser computer-aided-engineering software tool for system-level electrical integration and cabling engineering. The purpose of the program is to provide the engineering community with a centralized data base for putting in and gaining access to data on the functional definition of a system, details of end-circuit pinouts in systems and subsystems, and data on wiring harnesses. The primary objective is to provide an instantaneous single point of interchange of information, thus avoiding error-prone, time-consuming, and costly shuttling of data along multiple paths.

The DFACS program, which is centered around a single data base, has built-in menus that provide easy input of, and access to, data for all involved system, subsystem, and cabling personnel. The DFACS program enables parallel design of circuit data sheets and harness drawings. It also recombines raw information to generate automatically various project documents and drawings, including the Circuit Data Sheet Index, the Electrical Interface Circuits List, Assembly and Equipment Lists, Electrical Ground Tree, Connector List, Cable Tree, Cabling Electrical Interface and Harness Drawings, Circuit Data Sheets, and ECR List of Affected Interfaces/Assemblies. Real-time automatic production of harness drawings and circuit data sheets from the same reservoir of data ensures instant harmony of system and cabling engineering designs. DFACS also contains automatic wire-routing procedures and extensive error-checking routines designed to minimize the possibility of engineering error.

The DFACS program was developed in 1987. It is designed to operate on a DEC VAX mini or micro computer using Version 5.0/03 of INGRES, a relational data-base system. INGRES is available through Relational Technology, Inc.

This program was written by Joseph W. Billitti of Caltech for **NASA's Jet Propulsion Laboratory**. *For further information, Circle 49 on the TSP Request Card.*
NPO-17619

Fabrication Technology

Simulating a Factory via Software

This software system generates a simulation program from the user's responses to questions.

The AMPS/PC system is a simulation software tool designed to aid the user in defining the specifications of a manufacturing environment and then automatically writing code for the target simulation language, GPSS/PC. The domain of problems that AMPS/PC can simulate is that of manufacturing assembly lines with subassembly lines and manufacturing cells.

The user defines the problem domain by responding to the questions from the interface program. On the basis of the responses, the interface program creates an internal problem-specification file. This file includes the manufacturing-process network flow and the attributes for all stations, cells, and stock points. AMPS then uses the problem-specification files as input for the automatic code-generator program to produce a simulation program in the GPSS target language. The output of the generator program is the source code of the corresponding GPSS/PC simulation program.

The system runs entirely on an IBM PC running PC DOS Version 2.0 or higher and is written in Turbo Pascal Version 4, requiring 640K of memory and one 360K disk drive. To execute the GPSS program, the PC must have resident the GPSS/PC System Version 2.0 from Minuteman Software. The AMPS/PC program was developed in 1988.

This program was written by Bernard J. Schroer, Shou X. Zhang, and Fan T. Tseng of the University of Alabama, Huntsville, for **Marshall Space Flight Center**. *For further information, Circle 1 on the TSP Request Card.*
MFS-28398

Software for Numerically Controlled Machining

The APT code is enhanced.

The APT computer code is one of the most widely used software tools for complex numerically controlled (N/C) machining. "APT" is an acronym for Automatically Programmed Tools and is used to denote both a computer language and the software that processes that language. Development of the APT language and software system was begun over 20 years ago as a U. S. government-sponsored industry and university research effort. APT is a "problem-oriented" language that was developed for the explicit purpose of aiding N/C machine tools.

Machine-tool instructions and geometry definitions are written in the APT language to constitute a "part program." The APT part program is processed by the APT software to produce a cutter-location (CL) file. This file can then be processed by postprocessors supplied by the the user to convert the CL data into a form suitable for a particular N/C machine tool. The present offering of the APT system represents an adaptation, with enhancements, of the public-domain version of APT IV/SSX8 to the DEC VAX-11/780 computer for use by the Engineering Services Division of the NASA Goddard Space Flight Center. Enhancements include the super pocket feature, which allows concave polygon pockets.

Recent modifications to APT include the expansion of the sizes of arrays and buffers to accommodate larger part programs, the insertion of a few user-friendly error messages, and the correction of programming errors that affect the POCKET command and some of the sculptured-surface commands (notably SSURF and SCURV).

The APT system software on the DEC VAX-11/780 computer is organized into two separate programs: the load complex and the APT processor. The load complex handles the table-initiation phase and is usually run only when changes to the APT processor capabilities are made. This phase initializes character-recognition and syntax tables for the APT processor by creating FORTRAN block data programs.

The APT processor consists of four components: the translator, the execution complex, the subroutine library, and the CL editor. The translator examines each APT statement in the part program for recognizable structure and generates a new statement, or series of statements, in an intermediate language. The execution complex processes all of the definition, motion, and related statements to generate cutter-location coordinates.

The subroutine library contains routines that define the algorithms required to process the sequenced list of intermediate-language commands generated by the translator. The CL editor reprocesses the cutter-location coordinates according to commands supplied by the user to generate a final CL file. A sample postprocessor included in the program translates a CL file into a form for use with a Wales Strippit Fabramatic Model 30/30 sheet-metal punch. The user should be able to readily develop postprocessors for other N/C machine tools.

The APT language is statement-oriented, sequence-dependent language. With the exception of such programming techniques as looping and macros, statements in an APT program are executed in a strict first-to-last sequence. To provide programming capability for the broadest possible range of parts and of machine tools, and the curved-super-pocket feature that allows arcs and straight lines to bound the pocket, APT input (and output) is generalized, as represented by three-dimensional geometry and tools, and arbitrarily uniform, as represented by the moving-tool concept and output data in absolute coordinates.

The APT system software is written in FORTRAN 77 for batch and interactive execution and has been implemented on a DEC VAX series computer under VMS 4.4. The enhancements for this version of APT were last updated in 1988.

The enhancements of this program were written by D. A. Premo, computer consultant, under contract to **Goddard Space Flight Center**. *For further information, Circle 100 on the TSP Request Card.* *GSC-13214*

Mechanics

Inspecting the Full Circumferences of Tubes

An optical tool would surround a tube for fast, thorough inspection.

Marshall Space Flight Center, Alabama

A proposed tool for the inspection of external welds on a tube would give a view of a full circumferential strip of the outer surface. The tool would be similar to the borescopes used to inspect the interiors of tubes. Instead of fitting inside a tube, however, the new tool would encircle it.

When a conventional borescope is used to inspect the outer surface of a tube, it must be scanned manually over the tube and continually reoriented so that its view remains perpendicular to the surface. With the new encircling tool, inspection would be more reliable and less time consuming.

The tool would contain a sheath of optical fibers to carry the image of the surface from a lower lens to an upper lens (see figure). The lower lens, in the shape of an annulus, would turn rays of light from the surface, directing them into the optical fibers. The upper lens, also an annulus, would magnify the image from the fibers for observation by the user. A light source would surround the sheath to illuminate the tube.

This work was done by John P. Geddes of Rockwell International Corp. for **Marshall Space Flight Center**. *No further documentation is available.*
MFS-29221

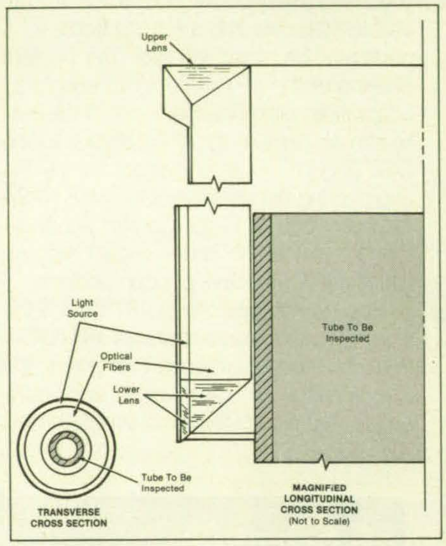

The **Inspection Tool** would be essentially a borescope that has been turned inside out so that it looks at a tube from the outside instead of the inside.

Borescope With Large Depth of Focus

Clear, focused images are easier to obtain.

Marshall Space Flight Center, Alabama

The modification of a commercial borescope yields clear, glare-free images of defects on the inside of a tube. The instrument offers a large depth of focus and therefore can be used in tubes of varying inside diameter (see figure).

A borescope with fused optical fibers (Diaguide 3AD50A-0202 or equivalent) was selected because the fusion eliminates the uneven honeycomb lighting effect seen through unfused-fiber borescopes. When uneven lighting is thus eliminated, subtle defects become visible.

The focal length of the borescope can be adjusted continuously from 0.13 in. (0.32 cm) to infinity. The borescope can easily furnish a sharply focused image of the wall of the tube, which, in the original application, ranges in diameter from 0.19 to 1 in. (0.48 to 2.5 cm). In contrast, borescopes with unfused fibers are restricted to focal lengths of about 0.25 in. (0.64 cm).

The outside diameter of the borescope is 0.08 in. (2 mm), and its working length is 39 in. (99 cm). Because its 3,000 quartz op-

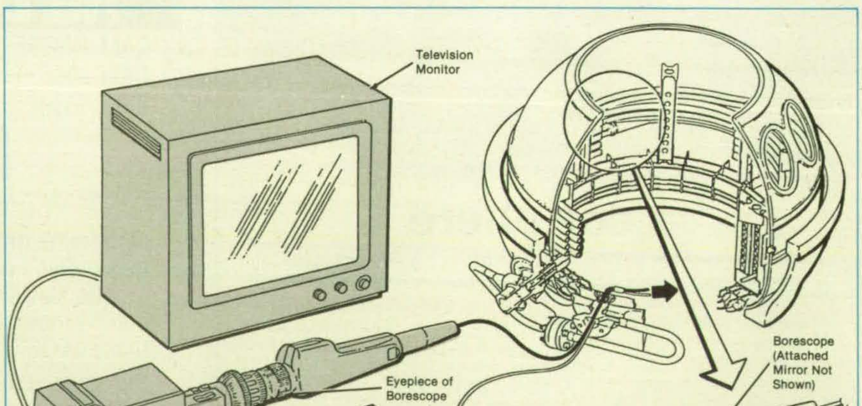

The **Borescope Is Used To Examine** the diverging wall of a tube. The wall is illuminated by light from a fiber distinct from the fused-fiber cable used for viewing. The viewing cable holds a right-angle mirror at its tip (not shown) so that it can look sideways. The image appears, magnified, on a monitor.

tical fibers are fused together, they are rigid. Thus, the fused-fiber borescope cannot be bent to aim it, unlike the unfused-fiber version. However, the greater clarity of the image more than makes up for the inflexibility.

As purchased, the borescope gives a straight-through view. A right-angle mirror is attached to the end of the borescope to direct the line of sight laterally to the wall of the tube. Instead of the integral light source that is part of the borescope as supplied, a separate light source is added — one that can be manipulated to eliminate glare and accentuate shadows. The new source is a single strand of plastic fiber, 0.02 in. (0.5 mm) in diameter, illuminated at one end by a standard 150-W lamp. (Care must be taken not to overheat the plastic fiber. A glass fiber or bundle of glass fibers might be preferable.) While the borescope is held stationary, the illuminating fiber can be moved inward and outward and can scan the wall to reduce scattering of light by a defect (such as a ripple on a weld joint) and increase contrast.

A video camera with a 50-mm lens is attached to the eyepiece of the borescope by a snap-on connector. The camera transmits a clear, magnified image to a television monitor.

This work was done by Kamal S. Guirguis of Rockwell International Corp. for **Marshall Space Flight Center**. *No further documentation is available.*
MFS-29461

Multiple-Inlet/Single-Outlet Orifice Plate

Susceptibility to blockage is reduced.

Marshall Space Flight Center, Alabama

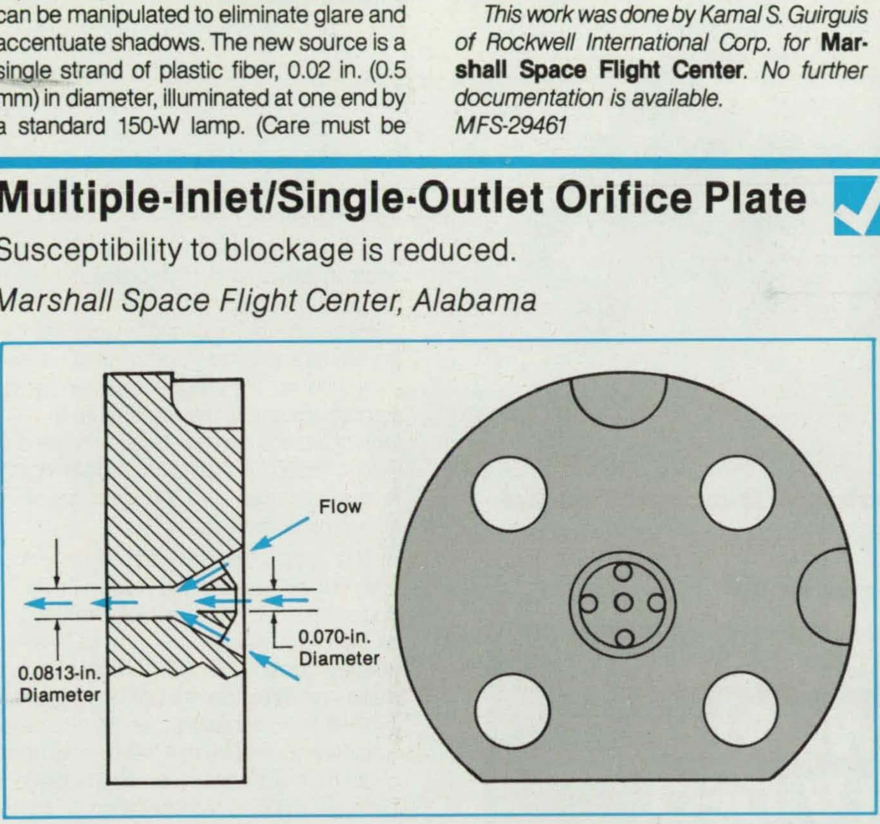

Figure 1. The **Multiple-Inlet/Single-Outlet Orifice** is machined in a plate in place of a single perpendicular hole of 0.0813-in. (2.07-mm) diameter.

An orifice plate for the control of flow has multiple slanted inlets leading to a single outlet. The multiple-inlet/single-outlet orifice is less susceptible to blockage than is a single hole drilled through the plate perpendicular to its surface. The multiple-inlet/single-outlet orifice plate is easily calibrated for various flow rates and fits in place of the simple orifice plate with no other modifications.

As shown in Figure 1, the multiple inlet holes converge into the controlling outlet hole, which is slightly wider. Because the outer ends of the slanted holes are in a slanted, recessed surface, they are unlikely to be blocked by a flat object placed on the orifice plate. Even if one becomes blocked by a particle of contaminant, the others are likely to remain clear. The flow characteristics of the multiple-inlet/single-outlet orifice are similar to those of a single hole (see Figure 2).

This work was done by Robert L. Godown of Rockwell International Corp. for **Marshall Space Flight Center**. *For further information, Circle 16 on the TSP Request Card.*
MFS-29407

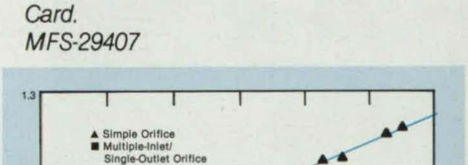

Figure 2. The **Rate of Flow as a Function of Pressure** was measured in a single orifice of 0.0813-in. (2.07-mm) diameter and in the multiple inlet/single-outlet version shown in Figure 1.

Thermal-Transient Testing of Turbine Blades

A thin surface layer is heated rapidly.

Marshall Space Flight Center, Alabama

A testing apparatus applies pulses of heat to a turbine blade to determine its resistance to thermal fatigue. The unit uses nonintrusive inductive heating and records the distribution of temperature on the blade with an infrared video camera. It allows precise control of heating and cooling.

The unit is designed for testing blades used in advanced high-pressure, high-temperature turbines. Such blades are damaged by thermal fatigue from thermal transients and large differences of temperature. During the thermal transient at the start of operation, the material at the surface of a blade can be stressed beyond its yield stress, causing it to undergo low cycle fatigue damage and incipient cracking after a number of starts.

The apparatus (see figure) generates heat in a thin layer on the blade, simulating approximately the effect of the start of operation of the turbine. It uses high-frequency currents to induce heat; the unit makes no direct contact with the blade. A cyclical flow of coolant can be alternated with the pulses of heat. A thin layer of nickel could be electrodeposited on the blade to enhance the induction heating.

This work was done by William R. Wagner and Louis H. Pidcoke of Rockwell International Corp. for **Marshall Space Flight Center**. *No further documentation is available.*
MFS-29416

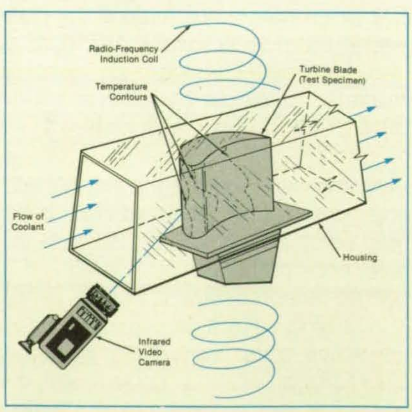

An **Infrared Camera Views a Turbine Blade,** to make a map of the temperature on its surface. The blade is alternately heated by induction current, then cooled by flow through the housing.

Improved Hub Fairings for Helicopters

Drag is reduced by a cambered hub fairing.

Ames Research Center, Moffett Field, California

Preliminary wind-tunnel experiments have shown that a new generic configuration for a fairing for a helicopter rotor hub can reduce the contribution of the hub to overall aerodynamic drag. Investigations continue with a view toward developing specific fairing configurations that would reduce hub drag by 50 to 80 percent. This has considerable importance for the conservation of fuel and efforts to increase operating range because, on a typical modern helicopter, the rotor hub causes 30 to 50 percent of the total drag.

A conventional hub fairing is symmetrical above and below the plane of the rotor. During forward flight, the flow of air converges, then diverges in the gap between the hub fairing and the fuselage. This condition gives rise to considerable interference drag, as does the converging/diverging flow between two side-by-side symmetrical airfoils (see Figure 1).

The new generic fairing has a flat bottom, which eliminates the converging/diverging boundary by straightening the surfaces that face each other. This arrangement reduces the interference drag, similarly to the reduction of interference drag by the flattening of the facing surfaces of two side-by-side airfoils (see Figure 2).

The new fairing is larger than its symmetrical predecessor. Because of its camber, it adds some lift. Disadvantageously, it also adds some skin friction, induced drag, and pressure drag. However, the placement of the cambered fairing adjacent to the fuselage and/or pylon can produce a net benefit by favorably modifying the flow around the whole helicopter. A large portion of the reduction in overall drag attributed to the cambered fairing is due to the elimination of the separated flow between the fairing and the pylon (or fuselage) and elimination of the eddy shed from the upper corners of the pylon.

This work was done by Robert H. Stroub, Larry A. Young, David R. Graham, and Alexander W. Louie of **Ames Research Center**. *For further information, Circle 150 on the TSP Request Card.*
ARC-12288

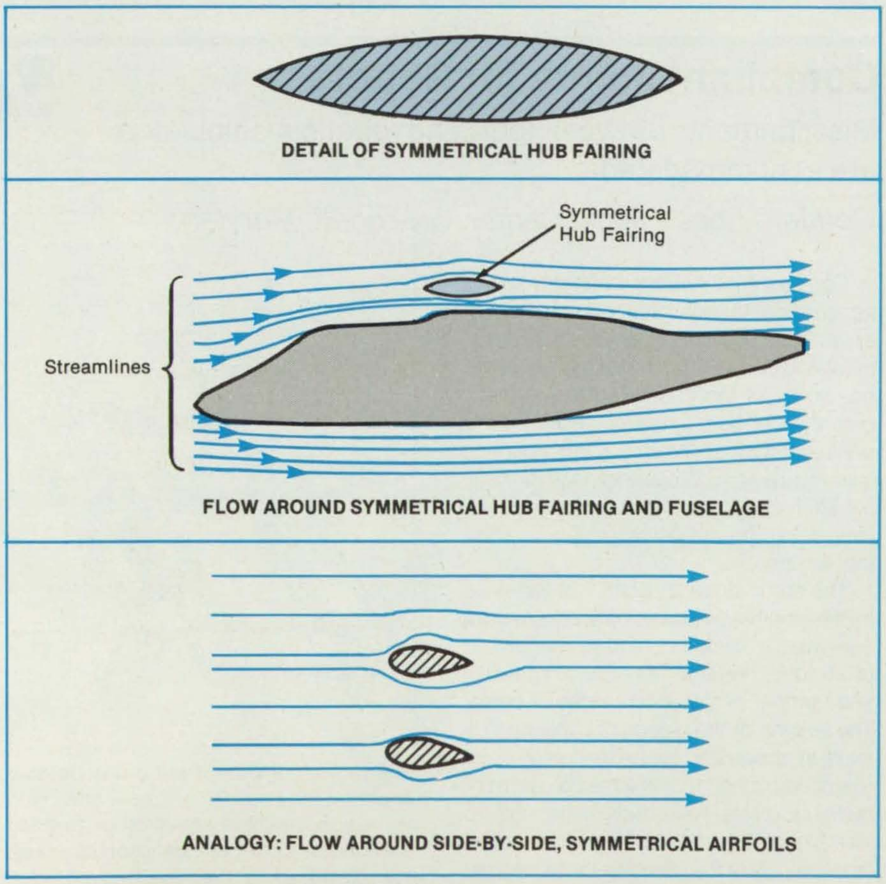

Figure 1. The **Converging-and-Diverging Flow** between the symmetrical hub and the fuselage, like the converging-and-diverging flow between symmetrical airfoils, causes interference drag.

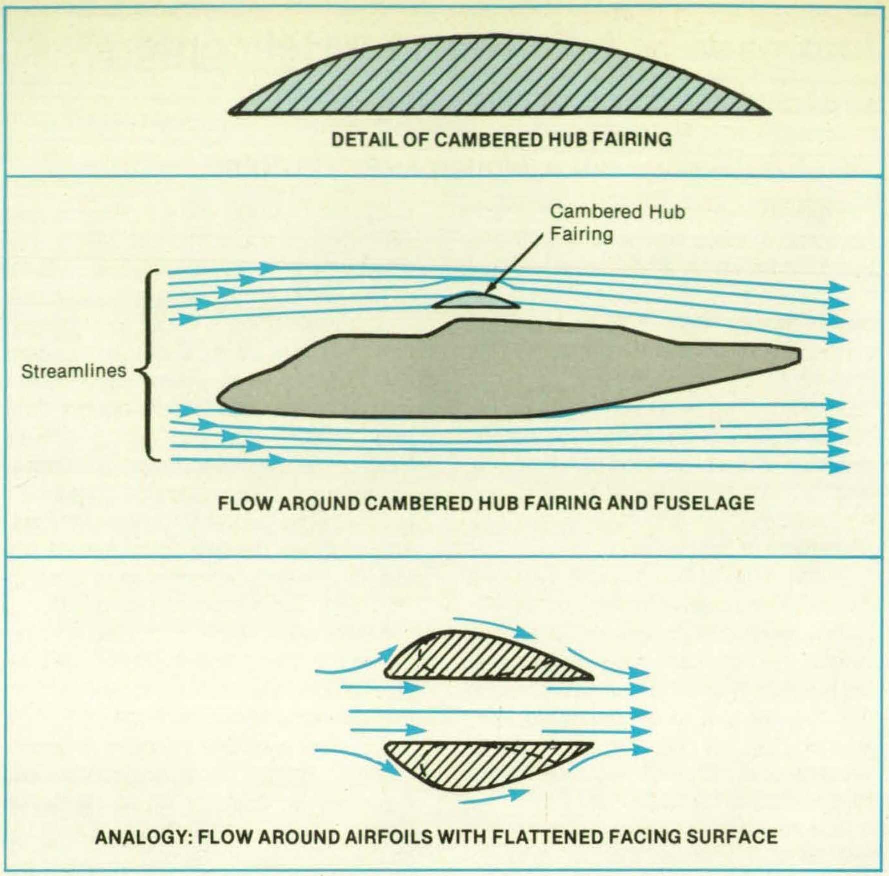

Figure 2. With the **New Cambered Hub Fairing**, streamlines over the hub are deflected downward toward the fuselage, as though the hub fairing were an integral part of the fuselage.

Compliant Joints for Robots

Misalignments between tools and robotic manipulators are accommodated.

Goddard Space Flight Center, Greenbelt, Maryland

Compliant joints have been devised to accommodate misalignments of tools and/or workpieces with respect to robotic manipulators. A typical joint of the new type has some of the characteristics and appearance of both a universal-joint and a cable-spring-type flexible shaft coupling (see Figure 1). As in cable-spring-type flexible shaft couplings, the compliance is derived from the elastic properties of short pieces of cable.

The compliance of a joint is determined by the lengths, distances between, relative orientations, thickness of strands, number of strands, material, amount of pretwist, and number of the short pieces of cable. The lengths of the pieces of cable can be fixed at assembly, either manually or by use of adjusting mechanisms like worm or hydraulic drives. A worm-drive mechanism (see Figure 2) could also be used to adjust lengths to vary the compliance as needed during operation.

The six degrees of freedom (translation along, and rotation about, each of the three principal axes shown in Figure 1) of the joint are referred to its geometric center.

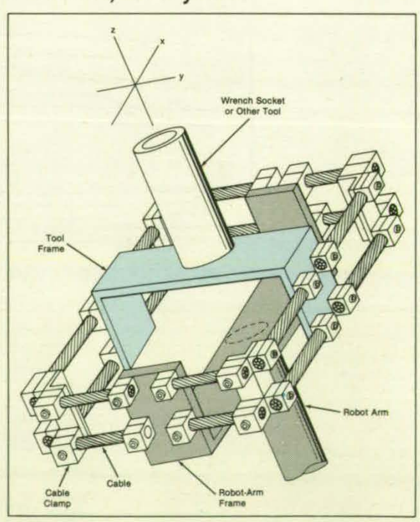

Figure 1. This **Compliant Joint Holds a Tool** that may have to be misaligned with respect to the robot arm in order to grasp theworkpiece.The complianceof the pieces of cable allows for the misalignment.

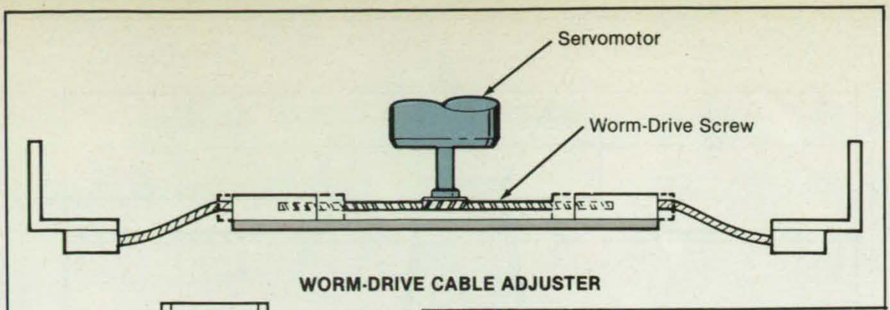

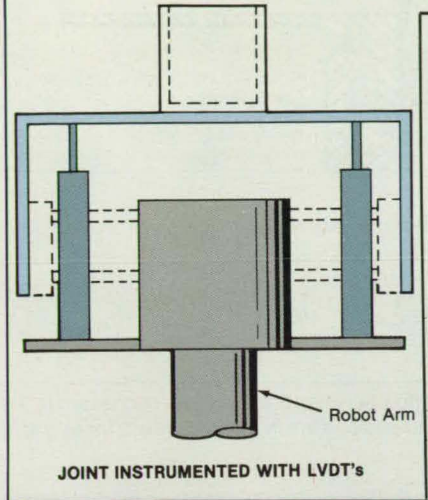

Figure 2. The **Worm-Drive Mechanism** (above) lengthens or shortens the small pieces of cable on a side of the joint to increase or decrease the compliance. Linear variable-differential transformers (below) can be installed on the joint to measure flexure.

As a result, translation and rotation are decoupled from each other; that is, translation along an axis does not produce rotation about the same or another axis, and rotation about an axis does not produce translation. This simplifies the design of the control system needed to achieve the desired translational and rotational motions.

The joint can be instrumented with linear variable-differential transformers (LVDT's) (also shown in Figure 2) to measure deflections. The outputs of the LVDT's can be processed into signals that indicate the misalignment of the tool with respect to the robot hand. These signals can be combined, through suitable processing, with signals indicative of the position and orientation of the robot hand to obtain an indication of the position and orientation of the tool in the frame of reference of the workspace. The outputs of the LVDT's could also be used as feedback control signals for the orientation of the tool.

This work was done by James J. Kerley, Jr., of **Goddard Space Flight Center**. *For further information, Circle 119 on the TSP Request Card.*

This invention is owned by NASA, and a patent application has been filed. Inquiries concerning nonexclusive or exclusive license for its commercial development should be addressed to the Patent Counsel, Goddard Space Flight Center [see page 16]. Refer to GSC-13127

Fixed-Position Isolation Valve

A lightweight, compact device blocks or allows flow.

NASA's Jet Propulsion Laboratory, Pasadena, California

A connection box and mating plugs constitute a device to allow or block the flow of fluid. The device acts as an isolation valve in the sense that it can be set in the open or closed configuration. However, it is not strictly a valve in the sense that the con-

Circle Reader Action No. 323

figuration cannot be changed during operation without spilling the fluid. The device is intended for use where changes between the open and closed configurations are meant to be infrequent. The principle virtues of the device are its light weight and compactness.

When assembled, the device includes a body, an outer cap, an inner cap, and either a long or a short plug. Two O-rings seal the caps and one O-ring seals the plug to the body, so that the seals are triply redundant for extra protection against leaks.

The long plug is screwed into the body when it is desired to block the flow. The combination of a polytetrafluoroethylene coat and the wedge action of its conical surface provide a tight seal when this plug is seated and tightened. The short plug is, in effect, a third, innermost cap and is used when the flow is not to be blocked.

This work was done by Frank S. McKulla, Louis V. Leonardi, and Siu Chun of RCA Corp. for **NASA's Jet Propulsion Laboratory**. *For further information, Circle 39 on the TSP Request Card.*
NPO-17707

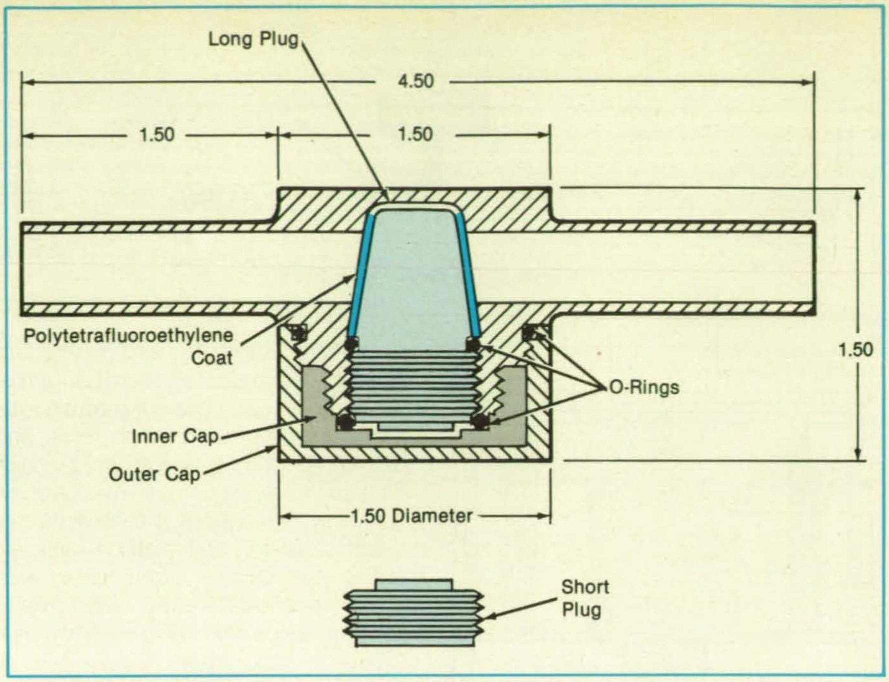

The **Long or Short Plug** is used to block or allow flow between the two pipes connected to the body. Three O-rings provide redundant seals. Dimensions are in inches and are for example only.

Books and Reports

These reports, studies, handbooks are available from NASA as Technical Support Packages (TSP's) when a Request Card number is cited; otherwise they are available from the National Technical Information Service.

Characteristic-Wave Approach Complements Modal Analysis

Aspects of estimation of unmodeled dynamics are discussed.

A report discusses the solution of the nonhomogeneous governing matrix equation for the dynamics of short vibrational pulses propagating as characteristic waves in a large structure. These characteristic waves are used to estimate that portion of the vibrational response that is not represented by a finite-element mathematical model of the structure. It is necessary to take this approach because such a finite-dimensional approximation of a distributed-parameter system like a large structure can fail to describe the contribution of high frequencies to dynamic responses in cases of impulsive or concentrated loads.

The structure is considered to be excited by the application of repeated stress pulses to specified joints. The general solution to the resulting nonhomogeneous equation is a closed-form matrix•vector equation for the stress propagating through a given joint at a given time step as a function of the applied pulses and of a matrix defined by the coefficients of transmission and reflection at the joints. Fourier series are chosen to represent the repeated stress pulses. It is shown how to use Z transforms to solve the wave equation for the responses at discrete times.

This type of analysis is applied to analyze the response, to repeated pulses, of a beam clamped at one end and free at the other. In particular, it is shown that under appropriate conditions, the steady-state response can exceed the excitation. This condition is associated with resonance. In general, this analysis shows all the qualitative characteristics that occur under arbitrary periodic excitations of the beam. It also shows those of quasi-periodic excitations, inasmuch as such excitations can be obtained by linear superpositions of periodic excitations.

This work was done by Michail Zak of Caltech for **NASA's Jet Propulsion Laboratory**. *To obtain a copy of the report, "Characteristic Wave Approach as a Complement to Modal Analysis," Circle 91 on the TSP Request Card.*
NPO-17741

Upwind Algorithm for Parabolized Navier-Stokes Equations

Supersonic flow about a cone is calculated accurately.

A report presents the theoretical basis of a computer code that solves the parabolized Navier-Stokes equations of supersonic and hypersonic flow. For increased accuracy in resolution of the details of strong aerodynamic shocks, the code incorporates an implicit, finite-volume, upwind numerical-integration scheme. The code has performed well in numerical simulations of flows around simple bodies.

The Navier-Stokes equations are said to be "parabolized" when they are simplified by assuming that the flow is steady and that the viscous derivatives in the streamwise direction are negligible in comparison with those in the crossflow direction. The system of equations is closed by the ideal-gas law, nondimensionalized, and transformed to general curvilinear coordinates. The equations are then put in the form of a tensor integral conservation law: this assures the numerical conservation of fluxes of mass, momentum, and energy, while facilitating the development of a finite-volume numerical-integration scheme that has reduced sensitivity to singularities of the computational grid.

The parabolized Navier-Stokes equations are solved relatively efficiently by marching in space rather than in time. The region of interest is divided into small, finite hexahedral slabs that are added successively as the numerical integration proceeds. The spatial propagation of information about the flow field is represented locally by a steady-state version of Roe's scheme, in which numerical fluxes are defined according to solutions of Riemann problems. The algorithm incorporates upwind dissipation terms in the crossflow directions to capture strong shock waves without requiring the user to specify smoothing coefficients. It is accurate to second order in the crossflow direction.

The code was used to calculate laminar flow of mach 7.95 about a circular cone of 10° half angle at angles of attack of 12°, 20°, and 24°. The computed position of the outer shock and pressure coefficients agreed closely with the corresponding measurements in an experiment by a previous author. The code was also applied to a mach 7.4 flow about a pointed body composed of elliptical cones joined at the bases, at angles of attack of 0° and 10°. Although experimental data are not yet available for comparison, the results are promising in that the computed flow includes such features as an oblique shock wave and an expansion fan that emanates from the "breakpoint" of the body.

This work was done by Scott L. Lawrence and Denny S. Chaussee of **Ames Research Center** *and John C. Tannehill of Iowa State University. Further information may be found in AIAA paper A87-42061, "Application of an Upwind Algorithm to the Three-Dimensional Parabolized Navier-Stokes Equations."*

Copies may be purchased [prepayment required] from AIAA Technical Information Services Library, 555 West 57th Street, New York, New York 10019, Telephone No. (212) 247-6500.
ARC-12146

Machinery

Hardware, Techniques, and Processes

Books and Reports

Stabilizing Wheels for Rover Vehicle

Extra wheels would prevent tipping, aid in climbing banks, and help in righting after overturning.

NASA's Jet Propulsion Laboratory, Pasadena, California

A proposed articulated, normally-four-wheeled vehicle would hold an extra pair of wheels in reserve. The extra wheels could be deployed to lengthen the wheelbase on slopes, thereby making the vehicle more stable. The extra wheels could also be deployed to aid the vehicle in negotiating a ledge or to right the vehicle if it has turned upside down. The concept promises to make remotely controlled vehicles more stable and maneuverable in such applications as firefighting, handling hazardous materials, and carrying out operations in dangerous locations.

The extra wheels would be drive wheels mounted on arms so that they can pivot on the axis of the forward drive wheels. Both the extra wheels and the arms could be driven by chains, hydraulic motors, or electric motors.

During ordinary travel, the extra wheels would be kept out of the way and idle. During a dangerous turn on a steep slope, however, the extra wheels would be deployed like outriggers to make contact with the ground (see Figure 1). The deployed wheels would increase the horizontal distance between the center of gravity and the point of contact farthest downhill, thereby enhancing stability.

The extra wheels could also be deployed when the forward main wheels have encountered a steep bank and are stalled (see Figure 2). The arms of the extra wheels would be rotated upward and forward to bring the extra wheels to the top of the bank. As soon as the extra wheels would make contact with the terrace, they would start driving, along with the main wheels, lifting the front of the vehicle to the terrace. The arms of the extra wheels would rotate rearward until the extra wheels make contact with the ledge behind the front wheels. They would start driving again to help the rear wheels boost the entire vehicle to the terrace. When the vehicle has fully mounted the bank, the extra wheels would be returned to their original position. The main wheels would once again drive the vehicle forward.

When the vehicle has overturned, the arms would be rotated to bring the extra wheels to the front of the vehicle. At the same time, the forward main wheels would be rotated on their arms toward the rear. The extra wheels would drive so as to raise the front of the vehicle and continue to drive and rotate on their arms until they make contact with the rear main wheels. At that point, the extra wheels would lock and the rear main wheels would drive, climbing the extra wheels. The rear wheels would rotate forward on their arms until they would climb on the forward main wheels, turning the vehicle over. The extra arms and wheels would brace the vehicle during this maneuver. Finally, the arms of the main wheels would return the main wheels to their normal position, and the extra arms and wheels would return to their original position.

This work was done by Earl R. Collins, Jr., of Caltech for **NASA's Jet Propulsion Laboratory**. *For further information, Circle 75 on the TSP Request Card.*

This invention is owned by NASA, and a patent application has been filed. Inquiries concerning nonexclusive or exclusive license for its commercial development should be addressed to the Patent Counsel, NASA Resident Office-JPL [see page 16]. Refer to NPO-17495

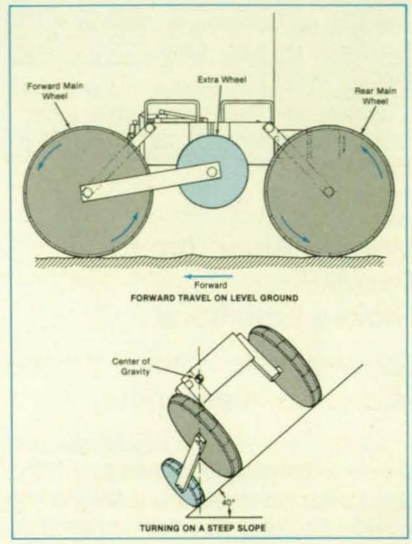

Figure 1. **When the Vehicle Travels** on a relatively-flat, level surface, the extra wheels are nested out of the way. On a steep slope, arms move the extra wheels downward so that they prevent the vehicle from tipping over. In the configuration shown here, the extra wheels provide support on slopes up to 40°.

Figure 2. In this **Ledge-Climbing Sequence** (above), the extra wheels move forward, pull up the front main wheels, and rotate to help the rear main wheels climb. To right the upside-down vehicle (below), the extra wheels move forward, raise the front of the vehicle, and lock, allowing the rear wheels to climb forward. The rear main wheels continue their movement until they restore the vehicle to its upright orientation and the extra wheels have been stowed in their out-of-service position.

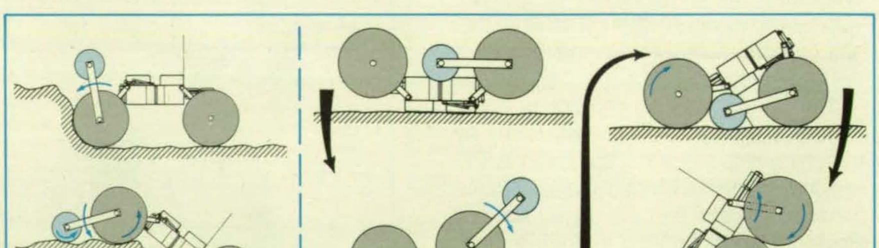

Modification of Gear Teeth To Reduce Vibrations

Computer simulations yield data useful in designing for low noise.

Lewis Research Center, Cleveland, Ohio

The effects of modifications in the shape of gear teeth upon the static transmission error and dynamic loading of the gears are now analyzed systematically with the help of computer simulations. Design curves are generated by conducting numerical simulations of dynamic effects at successive incremental modifications of gear systems operated at various applied loads. The modifications that result in minimum dynamic effect can then be determined from the design curves.

The new analytical procedure was demonstrated by applying it to a simple power-transmission system containing two identical spur gears (see Figure 1). The tips of the teeth have been relieved along various lengths and in various amounts (see Figure 2). The dynamic equations of the system involve the moments of inertia of the motor, load, gears, and shafts; the torsional stiffnesses of the shafts and gears; transmission errors; pitch errors; errors in the locations of teeth; friction; and input and output torques. The analysis of meshing to determine the static transmission error and sharing of load among teeth requires the solution of four simultaneous equations that involve the loads, point(s) of contact, compliances of the teeth, and errors in position.

The equations of motion were linearized and solved in an iterative procedure. A constant input torque was assumed, and the output torque was assumed to fluctuate as a result of the variations with time of the stiffness, friction, and damping in the gear mesh. The initial angular displacements were obtained by preloading the input shaft with the nominal input torque. The initial angular speeds were the nominal operating speeds. The calculated angular displacements and the speeds calculated during each increment of time were compared with the assumed initial values. Unless the differences between them were smaller than preset tolerances, the calculation was repeated, using the averages of the initial and calculated values as the new initial values.

The data generated in these calculations include static transmission errors, loads on teeth, and transmission errors, all as functions of roll angle. Other outputs include error amplitudes at various tooth-mesh harmonics and dynamic factors (ratios of dynamic to static loads) versus speed for modified and unmodified tooth profiles. An "effective error" is calculated from the frequency components of the static transmission error. The effective error was found to be a sensitive indicator useful for optimizing gear-tooth-profile modifications. Additional calculations produced such design curves as error amplitudes and maximum dynamic factors as functions of the length of profile modification for various harmonics. An overview of the data leads to the following conclusions:

- The modifications of the teeth significantly affect the dynamic characteristics of the system;
- The dynamic factor can be simulated analytically by the effective error calculated from the frequency components of the static transmission error of a pair of gears;
- The effective error is a good indicator for selection of the length and amount of modification to reduce the dynamic load;
- The length of the zone of modification should be increased or decreased if the gears are to be operated at greater or less, respectively, than the design load;
- An increase in the applied load or a decrease in the total amount of tip relief reduces the sensitivity of the gears to changes in the length of the zone of modification; and

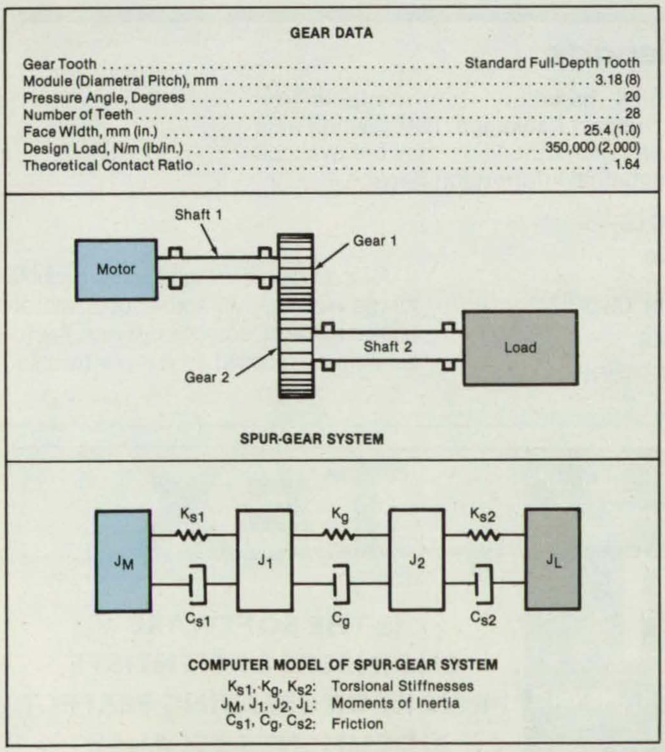

Figure 1. This **Simple Power-Transmission System** containing two identical spur gears was analyzed by a computer simulation of its dynamics to determine the effects of modifications of the gear teeth.

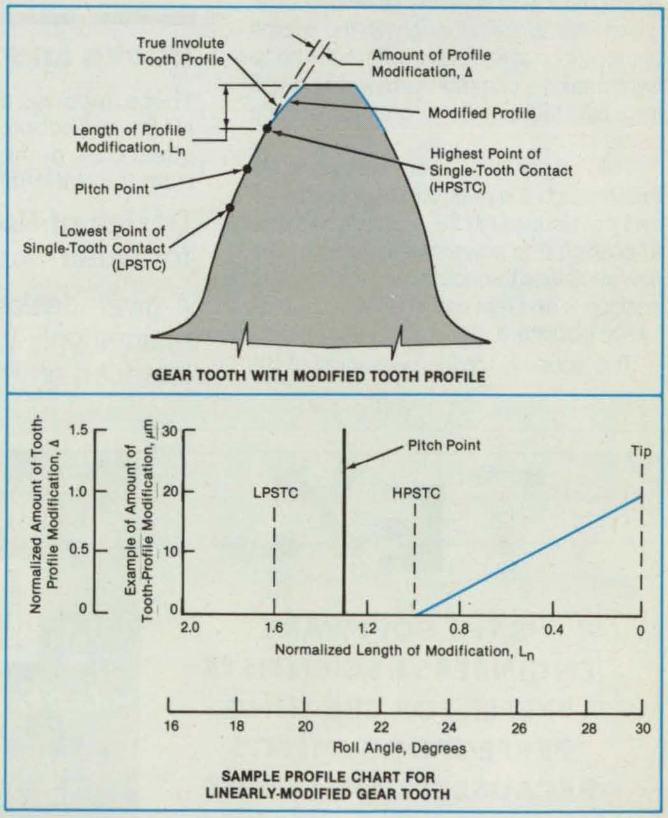

Figure 2. **Each Gear Tooth** in the system of Figure 1 was modified by the removal of some material at the tip. While this modification has little effect on the static performance of a set of gears, it exerts considerable influence over the dynamic performance of realistic gears.

• The dynamic loads on the teeth of gears that must operate in a range of loads can be minimized by an optimum modification of the teeth.

This work was done by Dennis P. Townsend and Fred B. Oswald of **Lewis Research Center** *and Hsiang Hsi Lin of Memphis State University. Further information may be found in NASA TM-89901 [N87-28918], "Profile Modification To Minimize Spur Gear Dynamic Loading."*

Copies may be purchased [prepayment required] from the National Technical Information Service, Springfield, Virginia 22161, Telephone No. (703) 487-4650. Rush orders may be placed for an extra fee by calling (800) 336-4700.
LEW-14738

Back-to-Back, Counterrotating Turbopumps

Two pumps in one package deliver high pressures.

Marshall Space Flight Center, Alabama

A pair of counterrotating turbopumps is mounted back to back in a novel one-piece volute housing. The housing serves as a spool piece into which the two pumps are inserted, one from each end. The pump package was designed to provide fuel and oxidizer to a rocket engine at high pressures; modified versions might be useful in providing other two-fluid high-pressure flows or redundant high-pressure flow of a single fluid.

In other turbopump/engine designs, the two turbopumps are driven by individual turbines and/or flows from common gas generators and packaged as individual units. Typically, the flow of driving gas is ducted from one pump to the other. This requires a duct or ducts for the hot gas and adds turbine stages and airfoils to each pump.

In the new pump package (see figure), the housing includes the turbine inlet and outlet volutes. Each pump is independent of the other and contains its own turbine, which shares the housing with the turbine of the other pump. Thus, in effect, the housing contains a common turbine that is split into two independent, counterrotating parts.

The hot gas that powers the turbine enters through the inlet volute at position 1 and travels through the first turbine stage at position 2 to power the fuel pump. The flow continues through the second stage at position 3 and leaves through the exit volute at position 4.

This scheme for the packaging of the turbopumps enables easy replacement of each pump/turbine assembly. The two turbines, when installed together in the spool piece, are sealed with piston rings.

This work was done by Alfred M. Palgon, Bruce R. Branstrom, and Frank N. Burgy of United Technologies Corp. for **Marshall Space Flight Center**. *No further documentation is available.*

Inquiries concerning rights for the commercial use of this invention should be addressed to the Patent Counsel, Marshall Space Flight Center *[see page 16]**. Refer to MFS-28349*

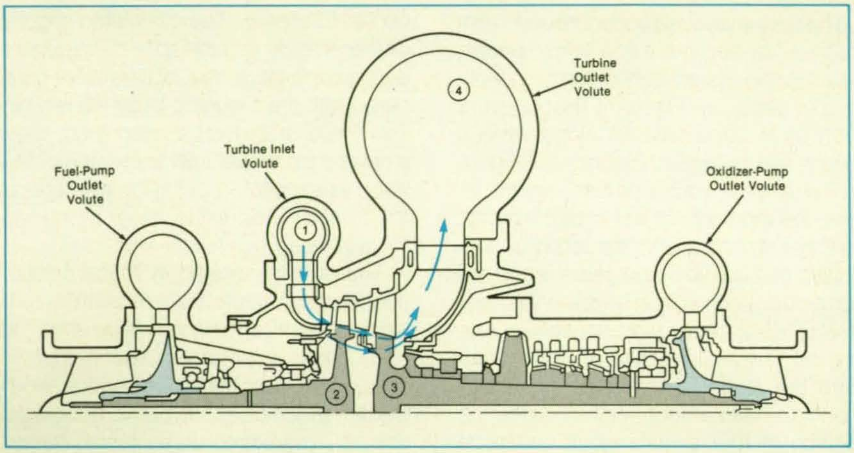

The **Back-to-Back Turbines** of the two turbopumps share the single turbine housing, which contains the turbine inlet and outlet volutes.

Books and Reports

These reports, studies, handbooks are available from NASA as Technical Support Packages (TSP's) when a Request Card number is cited; otherwise they are available from the National Technical Information Service.

Design of Robots for Outer Space

A given design is usually optimal only in its intended environment.

A report discusses the design of robots for use in zero gravity and vacuum, with attention to the differences between the requirements imposed on designs by outer space and by terrestrial applications. Terrestrial robots are typically designed for multiple purposes and for minimal cost. Outer-space robots are typically designed specialized to one task where cost has a relatively low priority. Thus, a design that is optimal in one environment is unlikely to be optimal in another.

The design of a robot for outer space must satisfy a number of criteria, some of which conflict or compete with each other. With variations from case to case, these criteria include some or all of the following:

- Low arm mass to reduce energy required for launching and for moving the robot,
- High ratio of payload mass to arm mass,
- Rigid arm for simplicity of control and accuracy of positioning,
- Long reach,
- High velocity of the robot hand,
- Reliability, and
- Low power consumption.

Mathematically, the design-optimization problem is stated generally as the minimization of a function $F(\mathbf{x})$, where $\mathbf{x}$ is an n-dimensional vector that represents the design variables (e.g., the lengths of the links) of the robot arm. The constraints on the design (e.g., reach, forbidden zones, maximum loads, maximum power consumption, or minimum speeds) are expressed in various linear and nonlinear equations.

For example, it is desired to increase the reach; this requires an increase in power, but minimal power consumption is also desired. The designer might let F be the ratio of power consumed to maximum reach and attempt to minimize F subject to the constraint that the power consumed lie between a specified minimum and maximum. The torque and power factors in F are obtained from the applicable equations of statics and dynamics that describe the loads, positions, and joint torques of the robot arm. A numerical optimization routine is used to find the $\mathbf{x}$ that minimizes F.

To test the general approach, the author applied it to the reach/torque problem for a terrestrial robot kinematically similar to one used in industry. Some of the results indicate that the kinematic design is not efficient with respect to power consumption and that in a gravitational field, the axes of motors in those joints that produce large motions with large links should be vertical rather than horizontal. Other results indicate that the motor-torque constants should be higher than those used in standard industrial robots. This might be accomplished by the use of motors with rare-earth magnets.

This work was done by Gerald P. Roston of Caltech for **NASA's Jet Propulsion Laboratory**. *To obtain a copy of the report, "A Technique To Aid in the Design of Robots for Use in Space Applications," Circle 77 on the TSP Request Card.*
NPO-17113

Fabrication Technology

Hardware, Techniques, and Processes

Computer Programs

Positioning X-Ray Film With String and Magnets

End markers contain magnets and lead for radiographic identification and positioning.

Marshall Space Flight Center, Alabama

Yet another of several related techniques has been devised to position x-ray film in normally inaccessible places for the inspection of welded joints. In this case, the film is to be placed behind a weld joint in a tubelike structure.

To the ends of a strip of x-ray film are attached markers made partly of lead and partly of magnets. String is attached to holes in the markers and used to pull the film through the structure to the approximate position of the joint to be inspected (see figure). Magnets on the outside of the structure are then used to pull the film into the precise position.

The lead in the markers is easy to identify in the radiographic images. In case the correct position of the film cannot be determined from the outside, the position can be determined from the locations of the markers in radiographic images and adjusted iteratively during a short sequence of x-ray shots. Thus, fewer shots are required than in a random trial-and-error sequence, and the resulting images are more accurate.

This work was done by William D. LaRosa and Jeffrey E. Anders of Rockwell International Corp. for **Marshall Space Flight Center**. *No further documentation is available. MFS-29448*

Lead/Magnet Markers and String are attached to the ends of strips of x-ray film to facilitate positioning.

Squeezing Salvages Oversize Seals

Thermal and mechanical properties of the seal material are used to advantage.

Marshall Space Flight Center, Alabama

A simple sizing tool compresses a polychlorotrifluoroethylene seal to a smaller diameter. In the particular manufacturing situation for which the tool was made, seals that had been machined to excessive inside diameters had to be scrapped. By use of the new tool, a seal that might have been scrapped can be squeezed to slightly smaller inside and outside diameters, then remachined to the correct inside diameter. (In this application, the outside diameter is less critical and need not be remachined.)

The tool includes three aluminum rings, the inner surfaces of which have diameters slightly larger than those of the three outer diameters of the seal. The rings and seal are drawn down a conical hole in a fixture until the taper squeezes the rings tightly onto the seal (see figure).

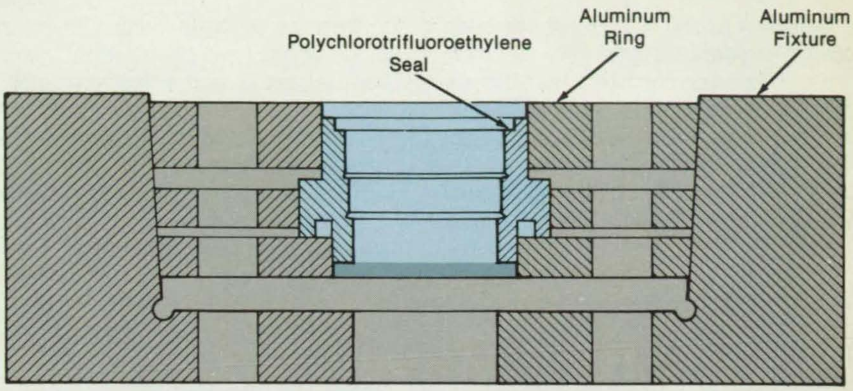

A **Polymer Seal Is Held** by aluminum rings, then compressed by differential thermal expansion between the seal and the rings. The inner diameter of the seal is thus reduced by a small amount that is sufficient to enable remachining to the specified size.

The tool works by taking advantage of the cold flow, thermal expansion, and creep of the seal material. The assembly of ring, seals, and fixture is heated to a temperature of 225 to 250 °F (107 to 121 °C) for 2 to 12 hours, the exact time to be determined by experiment. If unrestrained, the seal material would expand by 0.006 (fractional change in linear dimensions), while the aluminum rings would expand by 0.0012.

Because the greater expansion of the seal is restrained by the lesser expansion of the rings, the seal is placed under a compressive stress initially upon heating. While the assembly is maintained at the high temperature, the stress is relieved. The seal material can creep from 0 to 14 percent, depending on the time at the high temperature. After the assembly is cooled to room temperature, the pilot holes and inside diameters of the seal are machined as specified.

This work was done by Gerald M. Stewart of Rockwell International Corp. for **Marshall Space Flight Center**. *For further information, Circle 28 on the TSP Request Card.*
MFS-29527

Electrodeposited Nickel Reinforces Outlet Neck

Selective plating reinforces the affected part.

Marshall Space Flight Center, Alabama

Selective plating with nickel has been used to reinforce the outlet-neck assembly of the combustion chamber of a rocket engine. The plating operation was performed at the final stage of assembly. Other options for reinforcement would require the complete replacement of the outlet-manifold assembly and, consequently, months of delay.

Selective plating for reinforcement and/or repair has been practiced for years in both terrestrial and aerospace applications. In this particular application, the stresses in the assembly were greater than anticipated. Selective plating provided a relatively cheap way of thickening the metal in the affected regions to reduce the stresses to acceptable levels.

In preparation for plating, all of the affected weld joints are polished flush with the adjacent material to provide a smooth plating surface. The areas not to be plated are covered with foam and/or otherwise masked. A plating cell is attached to the outlet assembly (see figure) to provide the required flow of plating solution. The nickel is then deposited on the assembly to a thickness of about 0.285 in. (7.2 mm).

The deposited nickel is ground and polished at its edges to blend smoothly into the base material. The integrity of the bond between the deposited nickel and the base material is tested by fluorescent-penetrant inspection. As a further test of integrity, the deposited nickel is subjected to a pull test.

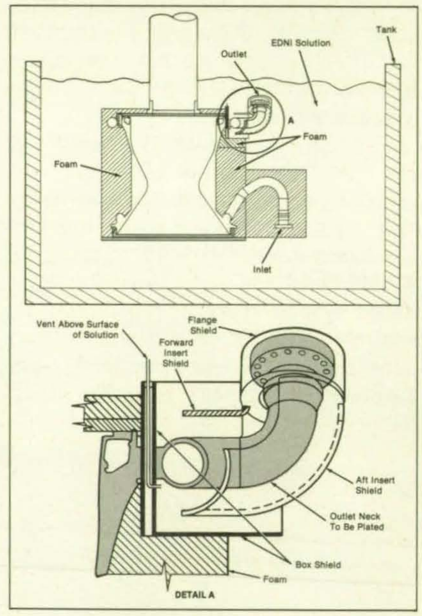

A **Plating Cell Is Built** around the part to be plated to enforce the correct flow of plating solution.

This work was done by Theodore C. Adams and William D. LaRosa of Rockwell International Corp. for **Marshall Space Flight Center**. *For further information, Circle 93 on the TSP Request Card.*
MFS-29447

Weld-Bead Shaver

A tool produces a smooth joint without overcutting.

Marshall Space Flight Center, Alabama

A hand-held power tool shaves excess metal from the inside circumference of a welded duct. The tool removes excess metal deposited by the penetration of a tungsten/inert-gas weld or by spatter from an electron-beam weld. It produces a smooth transition across the joint.

Compressed air drives an air motor in the tool, which in turn drives a carbide cutter at 2,700 revolutions per minute. The cutter shaves the inner weld bead as it is moved around the joint (see figure). The operator adjusts the depth of cut to remove the bead flush with the parent metal.

The tool replaces a rotary ball and side cutter. The new tool is easier to use and is not prone to overshaving, which thins and weakens the wall of the duct. The new tool also cuts faster, removing 35 in. (89 cm) of weld bead per hour. In contrast, the rotary ball and side cutter remove only 7 to 8 in. (18 to 20 cm) of weld bead per hour.

This work was done by Kamal Guirguis and Daniel S. Price of Rockwell International Corp. for **Marshall Space Flight Center**. *No further documentation is available.*

Inquiries concerning rights for the commercial use of this invention should be addressed to the Patent Counsel, Marshall Space Flight Center [see page 16]. Refer to MFS-29593

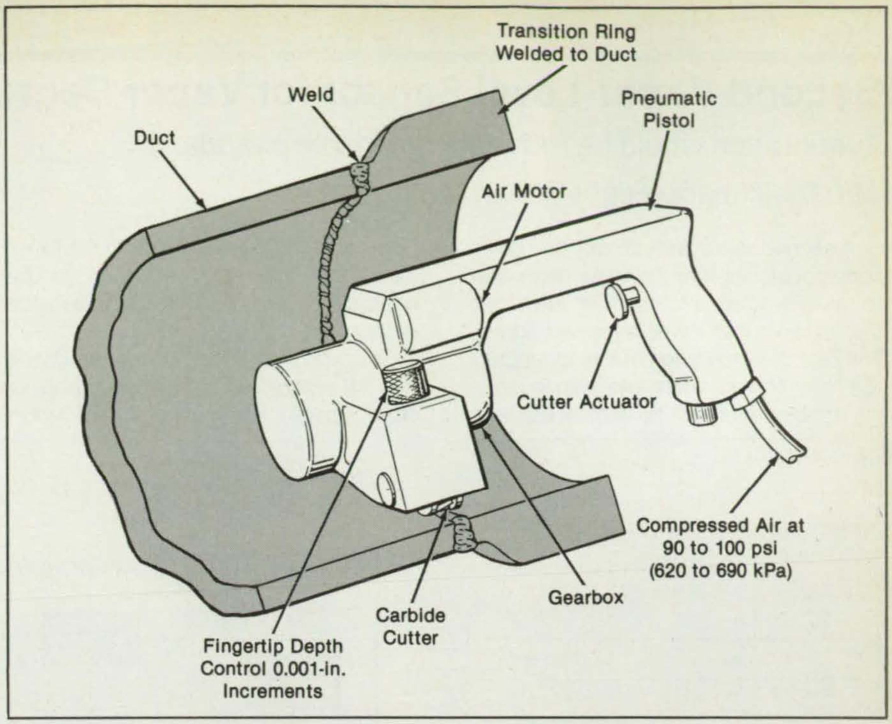

The **Carbide Cutter** shaves material from the weld bead as the user moves it.

Calibration for On-Machine Inspections

Measurements of machined parts are made faster, more convenient, and more reliable.

Marshall Space Flight Center, Alabama

A permanent calibration setup on a numerically-controlled machine tool enables the fast and reliable calibration of automated probes for the inspection of workpieces while they are still mounted on the machine. The setup includes one or more artifacts, the dimensions and locations of which are known precisely and are stored in the memory of the computer that controls the machine. Before the probes are used to inspect a newly machined part, they are used to check the artifacts. The probe measurements are compared with the values in memory to determine whether the probe readings need adjustment.

The artifacts include precise bushings, slotted blocks, and balls. The measurement surfaces on both the bushings and the blocks are internal. They are therefore protected from damage. For example, three bushings are mounted on the worktable or fixture of a five-axis machining center. The bushings serve as calibration points for the workzone and provide a check on the rotary axis. On a three-axis machining center, two bushings are inserted in the table at opposite corners of the workzone to provide datum surfaces and provide a check on dimensional accuracy across the workzone along mutually-perpendicular horizontal axes. The multiple artifacts yield much more information than a single artifact would.

Two slotted blocks are mounted on a vertical turret lathe on opposite sides of the table (see figure). Each block contains a slot 0.5 in. (12.7 mm) wide and 0.25 in. (6.35 mm) deep. The blocks furnish two vertical-axis points and three horizontal-axis points on each side of the table, 48 in. (121.92 cm) apart.

This work was done by Carlton L. Haymaker, Jr., of Rockwell International Corp. for **Marshall Space Flight Center**. *For further information, Circle 40 on the TSP Request Card.*
MFS-29523

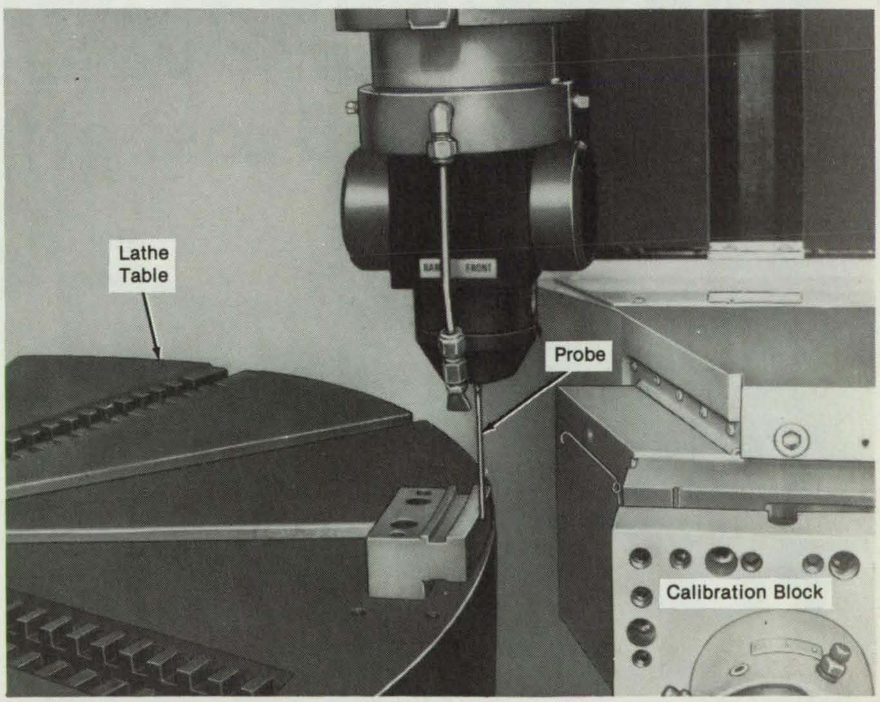

A **Measuring Probe Approaches** a slotted calibration block on a vertical turret lathe. If the probe measurements are within preset limits, the probe is allowed to measure the dimensions of a workpiece on the lathe. After the measurements, the probe is used once more on the block. If the posttest measurements are acceptable, the measurements of the workpiece are considered valid.

Second Vapor-Level Sensor for Vapor Degreaser

Evaporation would be reduced during idle periods.

Marshall Space Flight Center, Alabama

A second vapor-level sensor can be installed at a lower level in a vapor degreaser to make it possible to maintain the top of the vapor at that lower level (see figure). The rate of evaporation of the 1,1,1-trichloroethane solvent decreases with increasing freeboard height (the vertical distance from the top of the degreaser to the top of the vapor). Thus, the lower sensor can be used during idle periods to reduce the evaporation of solvent.

To switch vapor levels in accordance with the schedule of production, a 7-day or other suitable timer controls a solenoid valve, which directs steam to a modulator valve controlled by one of the sensors. A manual switch is also available to override the timer. The modulator valve in use opens to admit steam to the heaters when the top of the vapor goes below its sensor.

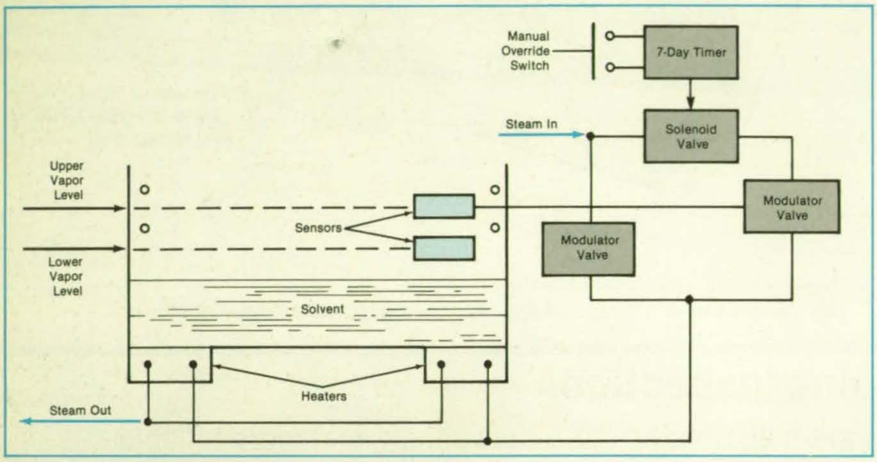

A **Vapor-Level Sensor** is added at a second, lower vapor level. The upper or lower vapor level is selected by a timer or by a manual override switch.

The effect of the lower vapor level has been measured. In a study reported in the fourth edition of the Tool and Manufacturing Engineers Handbook, an increase in the ratio of freeboard height to the width of a degreaser from 0.50 to 0.75 reduced the rate of emission of solvent by 46 percent. Thus, the relatively simple and inexpensive installation of a second sensor provides a substantial benefit, without the major capital cost of building a new vapor degreaser with greater freeboard height.

This work was done by Nance M. Painter and Richard K. Burley of Rockwell International Corp. for **Marshall Space Flight Center**. *No further documentation is available.*

MFS-29493

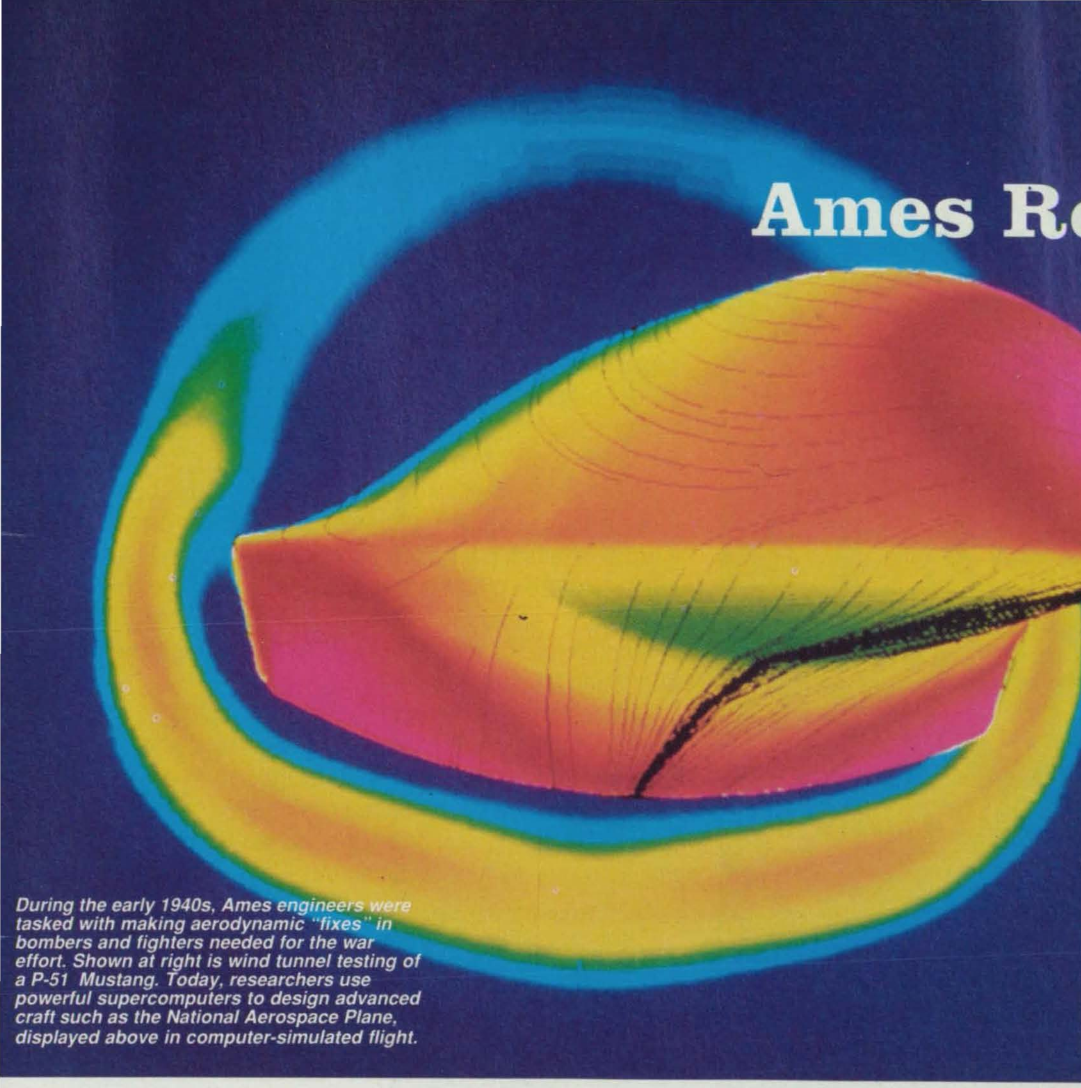

Ames Research Center:

During the early 1940s, Ames engineers were tasked with making aerodynamic "fixes" in bombers and fighters needed for the war effort. Shown at right is wind tunnel testing of a P-51 Mustang. Today, researchers use powerful supercomputers to design advanced craft such as the National Aerospace Plane, displayed above in computer-simulated flight.

A Half-Century Of Excellence

In the current era of rapid technological change, 50 years is a remarkably long period for a research institution to remain viable. But as the Ames Research Center begins its second half-century of service in 1990, the NASA center is still a premier member of the group of federal laboratories that comprise one of the nation's great assets for research and technology development.

Facilities at Ames have grown steadily over the years. With its two sites—Moffett Field and Dryden Flight Research Facility at Edwards Air Force Base, CA—Ames has become a world leader in four important categories of aeronautical facilities: supercomputers, wind tunnels, flight simulators, and flight testing. "In many instances, the research conducted in these facilities could not be pursued elsewhere," said Dr. Dale Compton, director of the Ames Center. "This serves to attract both the most exciting research problems and the best researchers to the center."

Computational Aerodynamics

The discipline of computational fluid dynamics (CFD) has been a mainstay in Ames' research program for over 15 years, and is expected to remain so well into the next century. CFD offers powerful analytical, simulation, and predictive tools to describe the complex physics of aerodynamic flow. Scientists use CFD to numerically simulate the flow fields around realistic computer models of advanced aircraft. By solving sets of partial equations on some of the world's fastest computers, scientists also compute the flow around a variety of aerospace configurations on the latest graphic support equipment.

Ames' Numerical Aerodynamic Simulation (NAS) supercomputer facility provides hardware and software support for CFD and related research conducted by more than 1000 government, industry, and university scientists nationwide. With the integration of increasingly powerful supercomputers, NAS eventually will allow aircraft designs, formerly requiring years of evolution using wind tunnels and high-risk flight testing, to be accomplished in hours or days with numerical simulations. Experts predict that the NAS central processor will reach a speed of one trillion computations per second by the year 2000.

To date, researchers have generated solutions for steady and unsteady; inviscid and viscous; and subsonic, transonic, and supersonic flows for a variety of flight vehicles. With the advent of the National Aerospace Plane (NASP) program, hypersonic flows have become a major thrust of CFD research and development. One of the key elements of this program is the recognition that a signifi-

cant portion of the design of such a vehicle will have to be accomplished by CFD since ground test facilities do not exist for the high speeds and energy levels inherent in flight at Mach numbers of up to 25, and there is no data base of technology and experience as is available for more conventional aircraft.

Artificial intelligence (AI) techniques promise to accelerate the development and application of CFD. Expert systems are already being explored to help the CFD scientist divide a complex flow region into several zones, each of which can then be discretized using relatively simple grids. At the other end of the numerical simulation process, visualizing the computed results, AI will be used to analyze the resulting flow patterns and identify those deemed to be of most interest. Such tools will give the aerodynamicist a means to quickly identify problem areas, speed the solution process, and possibly even suggest alternative configurations.

As CFD technology improves, the role of the wind tunnel will change. For the next several decades, however, wind tunnel testing and CFD will be complementary in the design and analysis of aircraft.

Wind Tunnel Testing

Ames boasts one of the world's finest collections of wind tunnels. Its National Full-Scale Aerodynamics Complex (NFAC)—featuring the 40- by 80-Foot Wind Tunnel, the 80- by 120-Foot Wind Tunnel, and the Outdoor Aerodynamic Research Facility—provides the U.S. with the capability to perform ground-based aerodynamic and acoustic experiments at speeds from static to nearly 350 mph on large- and full-scale aerospace vehicles and components.

The 40- by 80-Foot Wind Tunnel is a closed-circuit tunnel originally built during World War II to evaluate the takeoff and landing characteristics of full-scale aircraft. It has been used to test fighter planes, lifting-body configurations, large-scale supersonic transport and space shuttle models, vertical and short takeoff and landing (V/STOL) aircraft, and jet engine noise-suppression systems. Currently, it is being used to test rotorcraft and powered-lift aircraft. The facility supports a number of national and international vehicle programs: the Army's family of light helicopters, the V-22 Osprey tilt-rotor aircraft, the National Rotorcraft Noise Reduction Program, and the U.S./U.K. Advanced Short Takeoff and Vertical Landing (ASTOVL) Aircraft Program.

A major modification project has resulted in repowering the wind tunnel and adding an open-circuit leg with an 80'x120' test section. Because of its size, the appendage makes it possible, for the first time, to safely investigate full-scale rotor systems and V/STOL aircraft at very low forward flight speeds in a ground-based facility with minimum wind tunnel wall effects. It permits the evaluation of models or actual aircraft as large as the Boeing 737. Both tunnel test sections are lined with sound absorption material to allow researchers to gather acoustic data on test articles.

The third NFAC facility, the Outdoor Aerodynamic Research Facility (OARF), is used to obtain ground-based hover and acoustic data on full- or small-scale rotorcraft and V/STOL aircraft and propulsion systems. The OARF is an open-air facility with a mounting area capable of handling models and aircraft sized for installation in the 40- by 80-foot and 80- by 120-foot wind tunnels. The control room and most of the model support systems are located underground to provide minimum interference during testing. The OARF data acquisition system and model interfaces are identical to those of the NFAC wind tunnels to facilitate direct comparison between static and "wind-on" data and checkout of models prior to tunnel entry.

Flight Simulators

Ground-based flight simulation, another important tool in the development of new aircraft and spacecraft, began at Ames in the late 1950s. The first simulations studied the stability and control characteristics of aircraft at a limited up-and-away flight condition using very simple hardware: analog computers, a chair with a control stick, and a voltmeter display. Increasingly sophisticated motion-based simulation capabilities were developed over the years, starting with the pitch/roll chair and evolving to the current six-degree-of-freedom Vertical Motion Simulator with its interchangeable cabs. Today, computer graphics image-generation systems provide highly realistic out-the-window scenes, with the flexibility of displaying terrain from anywhere in the world (or space). Problems currently addressed with simulators range from space shuttle steering and braking system design to full mission human factors investigations and multi-aircraft air-to-air combat. They are used for accident investigations, competitive "flyoffs," and for flight control software development and validation.

Ames' simulator research led to the establishment of a strong aeronautical human factors staff and the Man-Vehicle Systems Research Facility (MVSRF), a unique national laboratory designed to study human factors in aviation safety. The MVSRF enables scientists to assess the effects of automation, advanced instrumentation, crew interaction, and fatigue on human performance in aircraft.

The facility includes two commercial transport cockpit simulators and an air traffic control (ATC) simulator. A Boeing 727-200 simulator, operational since 1984, provides a current-technology cockpit environment mounted on a six-degree-of-freedom motion base. The Advanced Concepts Flight Simulator features programmable color graphics displays in place of the usual complement of electromechanical displays and provides simplified, context-sensitive modes for accepting flight crew command and control inputs. Both flight simulators are capable of full mission simulation. The ATC system simulator offers a realistic ATC environment for the study of air/ground communications as they affect crew performance.

Flight Research

Ames conducts extensive flight research to validate analytic or ground-based experimental results; to explore basic fluid and flight mechanics phenomena; and to investigate advanced design concepts. Research vehicles include rotorcraft and powered-lift aircraft, high-performance aircraft, and unique experimental vehicles.

R-CAB simulator cockpit and visual display of the Vertical Motion Simulator

Since 1946, the Dryden facility has played a pivotal role in U.S. flight research, testing a variety of radical craft from lifting bodies to rocket planes. Ames-Dryden's current projects include the X-29 advanced technology demonstrator built by Grumman Aerospace Corporation for a program sponsored by the Defense Advanced Research Projects Agency (DARPA). The X-29 features a forward-swept wing made of composite materials that offers an up to 20 percent weight reduction in comparison with conventional aft-swept wings. Other innovations include a digital flight control system; flaperons that combine the functions of flaps and ailerons in a single airfoil; and forward canard wings whose angles relative to the airflow are adjusted 40 times a second as a means of improving flight efficiency and aircraft agility. The X-29 program is intended to demonstrate that this combination of technologies makes it possible to build smaller, lighter, and more efficient aircraft without sacrificing performance.

Another ongoing research project at Dryden uses a modified F-18 Hornet to study airflow interactions during high angle-of-attack flight. Currently, the extremely complex flows encountered on fighter planes at high angles-of-attack cannot be modeled adequately during the design process. As a result, the aircraft's high-alpha characteristics remain an estimate until it enters development and flight operations. The F-18 research program is expected to generate a data base and develop methods that will permit more efficient design of high-performance aircraft, thereby minimizing costly post-production design fixes.

The first phase of the NASA study involved more than 100 flights at up to 55 degrees angle-of-attack. Separate visual studies of the airflow were made with smoke, cloth tufts attached to the plane's exterior surface, and an oil-based dye released from small orifices at the nose of the craft. Flow patterns recorded on film, videotape, and on the aircraft's surface were compared with computer and wind tunnel predictions.

For the project's second phase, scheduled to begin this summer, thrust vectoring vanes will be installed around the F-18's exhaust nozzles. The movable vanes will change the direction of the engines' exhaust thrust and help to control the aircraft when its rudders, ailerons, and elevators become less effective during flights at angles-of-attack up to and beyond 70 degrees.

A History Of Innovation

One of the first research laboratories established by the National Advisory Committee for Aeronautics, the Ames Center has a long tradition of award-winning technological advances. In addition to its work on U.S. aircraft projects, Ames made major contributions to the Mercury, Gemini, and Apollo programs, to planetary exploration, and to the space shuttle program. The following is a chronological look at significant Ames events and achievements over the last half-century.

1939 Ames ground breaking December 20, 1939.

1941 The first two tunnels at Ames, the 280 mph 7- by 10-foot wind tunnels, begin operation.

Deicing research program begins with Lockheed 12A test craft and later Curtiss C-46. Results used on B-17 and B-24 bombers.

1942 Completion of 680 mph 16-Foot Wind Tunnel, then fastest in existence

1944 40- by 80-Foot Wind Tunnel completed June 1944, large enough to test full-scale aircraft with engines running.

1945 R.T. Jones develops swept-wing theory at NACA-Langley. Moves to Ames August 1946, further develops theory and applications.

1947 First sweptback wing flies on North American F-86 fighter.

1949 Flight of first aircraft, the Grumman F-6F, to do variable stability flight research (making one plane fly like another for test research).

1950-1960 Hypervelocity wind tunnel work gets underway at Ames with shock tubes, arc-jets, light gas guns, and counter flow devices.

1952 Harvey Allen develops blunt body theory for space vehicles, solves problem of intense aerodynamic heating during atmosphere reentry.

1955 Supersonic rule area developed by R.T. Jones. Minimizes drag of supersonic craft by limiting parts of vehicle cut by Mach cones.

1958 Ames invents the lifting body, wingless craft able to fly back into the atmosphere from space, survive entry heating, and land. Idea evolves into the space shuttle.

1961 X-15 rocket plane makes first hypersonic flight at Dryden, eventually reaches 4500 mph and 350,000 feet.

1965-1968 Pioneer Project series 6-9 spacecraft launched into solar orbit to study solar wind and cosmic rays.

1966-1969 Biosatellites 1, 2, and 3 fly plants, insects, fertilized eggs, and primates into orbit and return them to Earth. Scientists find a variety of effects of weightlessness on living systems.

1970 Computational fluid dynamics begins with creation of the CFD branch and the arrival in 1971 of Illiac, then world's fastest supercomputer.

1971 Ames acquires high-altitude U-2 aircraft for astronomy, atmospheric, and earth resource studies, including some of the first measurements of background radiation left over from the big bang.

1972 Pioneer 10 launched to Jupiter, makes first trip through Asteroid belt.

Ames begins tilt-rotor program; by 1981 has developed a practical new aircraft, the XV-15, which can take off vertically and then fly 500 miles at speeds up to 300 mph.

1974 Ames begins development of exterior tiles and other materials eventually used to protect space shuttle during intense heating of atmosphere entry.

1975 Dedication of Kuiper Airborne Observatory, May 21, 1975. The Kuiper, a converted C-141 transport with a 36-inch infrared telescope, discovered Uranus' rings, Venus' cloud composition, star formation, and supernova mechanisms.

1976 First flight of the AD-1 oblique wing aircraft. Rigid, straight wing of this scissor-like craft can rotate horizontally to 60 degree angle to fuselage for swept-wing efficiency. Has potential for practical, quiet Mach 2 supersonic transport.

1979 Pioneer 11 completes first trip to Saturn in September 1979 after flight across solar system.

HiMAT super-maneuverable, remote-piloted test vehicle flies at Dryden. HiMAT wing is the first designed by a computer.

1981 Construction begins on the Galileo Probe spacecraft, designed to make the first entry—and then fly 500 miles deep—into the atmosphere of Jupiter.

1983 SETI (Search for Extraterrestrial Intelligence) program begins at Ames, uses existing telescopes to listen for radio signals from other intelligent species in our galaxy and beyond.

IRAS spacecraft launched with Ames-developed telescope; in two years, IRAS makes the first whole-sky survey in the infrared.


For the tough jobs they call Motorola.
Like transmitting photo data from Neptune after 12 years in space. Or baseband processors for Advanced Communications Technology Satellites. Or transmitting scientific and photo data during Magellan's Venus Radar Mapping Mission.
TOUGH JOBS WE CAN DO FOR YOU.
Space Comm. Systems
Frequency Sources
TT&C Subsystems
NB/WB Microwave Comm.
NB/WB Secure Comm.
Power Converters
SGLS User Transponders
Deep-Space Transponders
TDRSS User Transponders
SDLS User Transponders
Near-Earth Transponders
GPS User Receivers
High-Data-Rate Modems
Baseband Processors
Spaceborne Radars
Space Station Comms.
Ground Support Equipment
Call the pioneers in space communications 602/732-3015 or write to Box 2606, Scottsdale, AZ 85252.
Circle Reader Action No. 655
MOTOROLA INC.

1984 Ames selects instruments, investigators, and establishes science team for SIRTF, a large, orbiting infrared telescope 1000 times more sensitive than IRAS.

1986 First version of the AX-5 hard space suit, proposed for space station Freedom, completed August 1986.

The X-29 forward-swept-wing aircraft begins flight testing at Ames-Dryden.

1987 Ames formalizes research for Space Station with contributions in human factors, expert systems, space robots, astronaut suits, materials research, microgravity studies, environment systems, astrometric telescopes. First measurements implicating man-made chemicals in stratospheric ozone destruction made over Antarctica. Ames provides project management, science and aircraft support for international expedition.

1988 Cray Y-MP 832 supercomputer installed in NAS facility; at one billion computations per second, ups NAS system speed four times. NAS system provides first three-dimensional simulations of full aircraft flight, viscous flow.

1989 Aerobraking techniques developed for low-orbit maneuvers (in-space orbit-plane changes for National Aerospace Plane) and high-orbit maneuvers (to cut down velocity of spacecraft on return from Mars or moon).

1990 The first self-repairing flight control system is demonstrated on NASA's F-15 Highly Integrated Digital Electronic Control research aircraft based at Ames-Dryden. It detects in-flight failures and automatically reconfigures an aircraft's ailerons, rudders, and elevators, allowing pilots to continue their mission or land safely.

NAS facility receives world's first Cray Y-MP 8128 supercomputer. With 128 million words of mainframe memory and 256 million words of high-performance secondary memory, it offers four times the memory of the Y-MP 832.

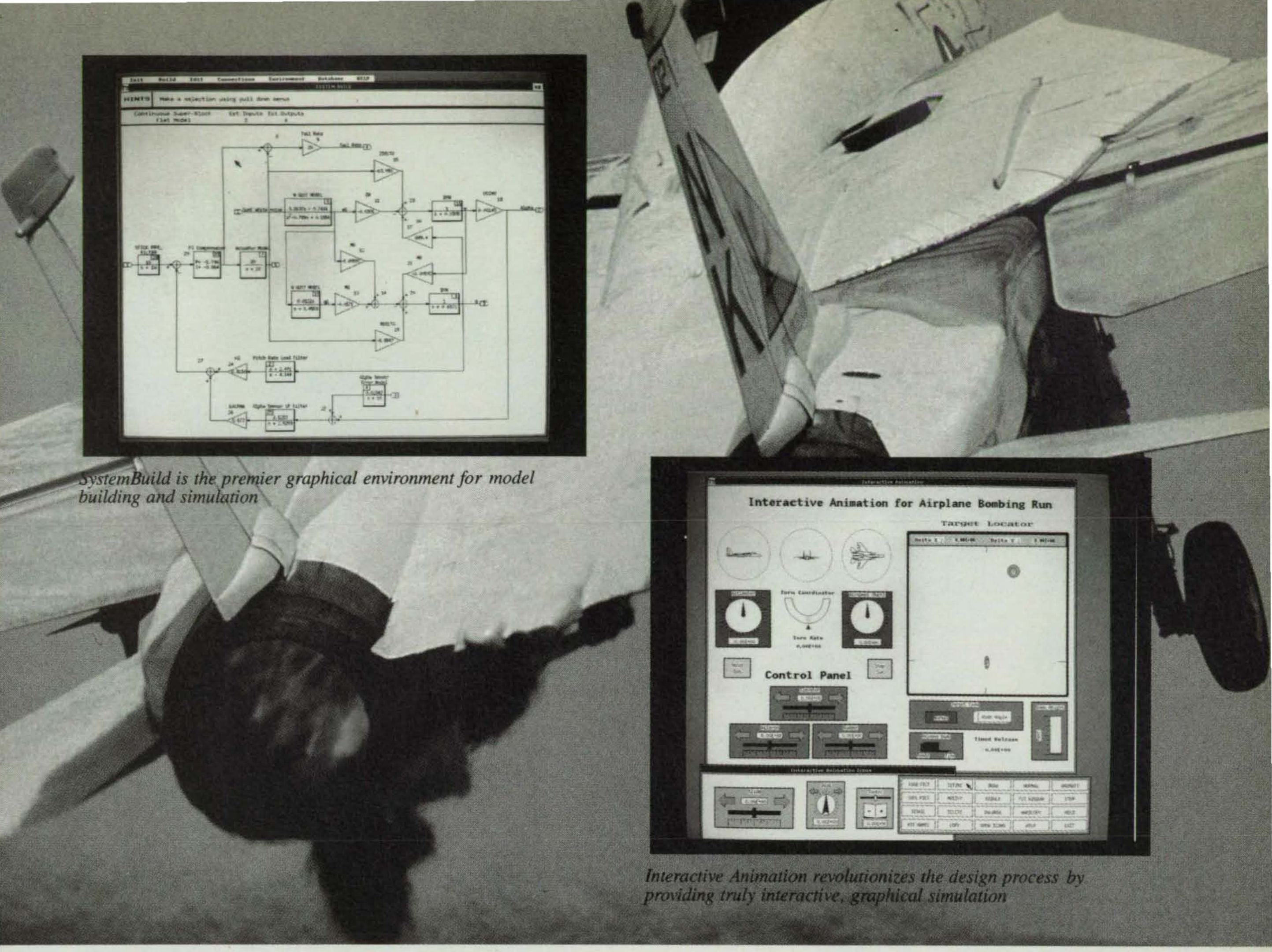

SystemBuild is the premier graphical environment for model building and simulation

Interactive Animation revolutionizes the design process by providing truly interactive, graphical simulation

TAKE CONTROL WITH MATRIXx.

Only one family of products offers a streamlined software environment for each phase of control system development — the ISI Product Family. For aerospace, automotive, computer peripherals, industrial control, and material processing.

Build a complex graphical system model. Analyze the system and design a controller. Run real-time animated simulations. Plot the results. Refine the design. Generate real-time Fortran, C, or Ada code. Download it into a target processor. Run it in real-time. All with one family of software products.

- Solve arithmetic and engineering problems without programming in Fortran or C.
- Design multivariable engine controllers faster.
- Optimize controllers for nonlinear robotics applications.
- Model and simulate complicated nonlinear braking systems for antilock brake control.
- Create innovative satellite attitude controllers using the latest robust design techniques.
- Simulate aircraft and missile guidance systems before expensive hardware testing.
- Prototype systems in hours — not months.

Analysis and Design
MATRIX$_X$®:
- Engineering and mathematical analysis
- Programming
- Comprehensive 2- and 3-D graphics

Expansion Modules:
- Control Design
- Robust Control
- Optimization
- Digital Signal Processing
- System Identification

Modeling and Simulation
System Build™:
- Mouse-driven graphical modeling
- Nonlinear, hybrid, multi-rate, and event-driven simulation
- 75+ engineering blocks
- 6 integration algorithms

Expansion Modules:
- Interactive Animation
- Remote Simulation
- Simulation Accelerator
- Automatic Documentation
- Project Database

Real-Time Code Generation
AutoCode™:
- Automatic Code Generation in Ada, C, or Fortran

Implementation and Testing
AC-100™:
- Real-time multi-processor system
- "Hardware-in-the-loop" control

MATRIXx is the least expensive engineering analysis product available today.

Engineering professionals worldwide continue to rely on ISI's products to streamline control system design. Now it's your turn. **Call 408-980-1500** for information, a complete set of Data Sheets, or the phone number of your nearest sales representative.

integrated systems inc.

2500 Mission College Blvd.
Santa Clara, California 95054
Tel: (408) 980-1500
Fax: #408-980-0400

DESIGN • SIMULATION • CODE GENERATION • IMPLEMENTATION

Circle Reader Action No. 557

Pyramidal Image-Processing Code for Hexagonal Grid

Some properties resemble those of the primate visual cortex.

Ames Research Center, Moffett Field, California

An algorithm is based on the processing of information on the intensities of picture elements arranged in a regular hexagonal grid. The algorithm is called an "image pyramid" because the image information at each processing level is arranged in a hexagonal grid that has one-seventh the number of picture elements of the next lower processing level, each picture element being derived from a hexagonal set of seven nearest-neighbor picture elements in the next lower level. At the lowest level are the fine-resolution elements of the original image.

The algorithm was designed to have some of the properties of the image-coding scheme of the primate visual cortex. The hexagonal lattice was chosen because the image-sampling lattice in primate vision is approximately hexagonal. The other properties include a subband structure, relatively narrow band tuning in both spatial frequency and orientation, relatively high spatial localization, both odd and even (quadrature) kernels, and self-similarity.

At each level, the image is encoded by a shift-invariant linear transformation in which each new coefficient is a linear combination of image samples defined by a kernel of weights (in effect, a filtering function). A weight is assigned to the central element and to its six nearest neighbor elements (see figure). There are seven mutually orthogonal kernels: one low-pass and six high-pass. The low-pass kernel has equal values at all taps. Two high-pass kernels have an axis of symmetry running through the central element and between outer elements at an angle of 30°. Of these two kernels, one is even about the axis of symmetry, the other is odd. The remaining four high-pass kernels are obtained by rotating the odd and even kernels by 60° and 120°, respectively. Each kernel has a norm (square root of sum of squares of taps) of one. The figure illustrates these properties for two of the kernels.

One solution of the equations in the figure yields the following values for the weights:

$$a = \sqrt{2/7}$$
$$b = d = (1-1/\sqrt{7})/3\sqrt{2}$$
$$c = -(2+1/\sqrt{7})/3\sqrt{2}$$
$$e = g = \sqrt{2/3}$$
$$f = 1/3\sqrt{2}$$
$$h = \text{low-pass-filter weight} = 1/\sqrt{7}$$

This sampling scheme can be modified for images in nonregular hexagonal and in orthogonal and skewed rectangular coordinates. It can be applied to an image of any shape that is one period of a hexagonally periodic sequence, provided that the number of picture elements equals a power of 7.

One likely role of the primate visual cortex is to encode the retinal image in components that are less correlated than are the picture elements. The image pyramid provides a model for how this might be done. In this context, the picture elements at the lowest level correspond to the receptive field centers of retinal ganglion-cell inputs. Each hexagon defines the receptive field of a single cortical unit. The coefficients of each basis function describe the weights with which each ganglion cell contributes to the response of the cortical cell. The basis functions defined on the smallest hexagons correspond to the cells tuned to the highest spatial frequencies. Each subsequent level of the pyramid corresponds to cells tuned to lower frequencies. The low-pass basis functions at each level correspond to unoriented pooling units, which in turn are used to create the high-pass units at the next level. These pooling units may correspond to actual cells or may simply define which ganglion cells contribute inputs to the high-pass units at each level.

This work was done by Andrew B. Watson and Albert J. Ahumada, Jr., of **Ames Research Center**. *Further information may be found in NASA TM-100054 [N88-14630], "An Orthogonal Oriented Quadrature Hexagonal Image Pyramid."*

Copies may be purchased [prepayment required] from the National Technical Information Service, Springfield, Virginia 22161, Telephone No. (703) 487-4650. Rush orders may be placed for an extra fee by calling (800) 336-4700. ARC-12178

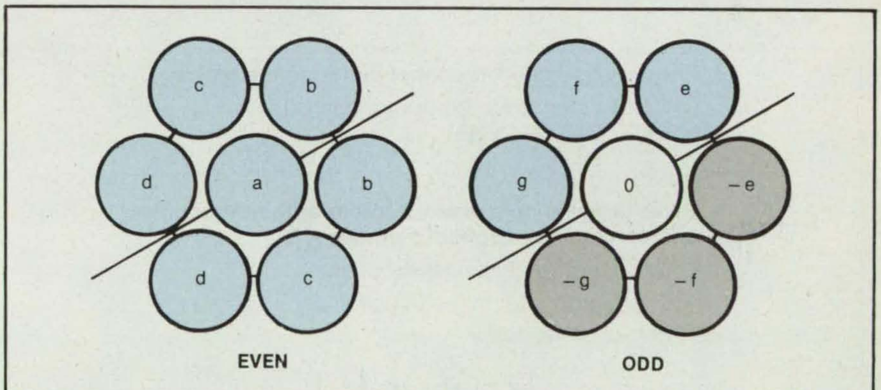

$a^2+2b^2+2c^2+2d^2 = 1$	(Unit Norm)
$2e^2+2f^2+2g^2 = 1$	(Unit Norm)
$a+2b+2c+2d = 0$	(High-Pass ⊥ to Low Pass)
$a^2+b^2+d^2+2bc+2cd = 0$	(⊥ to Self Under Rotation)
$a^2+2bc+2bd+2cd = 0$	(⊥ to Self Under Rotation)
$e^2+g^2-2ef-2fg = 0$	(⊥ to Self Under Rotation)
$2eg-2ef-2fg = 0$	(⊥ to Self Under Rotation)

These **High-Pass Kernels** have an axis of symmetry at 30° from the horizontal. The equations describe the fundamental constraints upon the high-pass kernels. A low-pass kernel (not shown) is simply a constant *h* at each sampling point.

Stochastic Feedforward Control Technique

A class of commanded trajectories is modeled as a stochastic process.

Langley Research Center, Hampton, Virginia

The Advanced Transport Operating Systems (ATOPS) research and development program conducted by NASA Langley Research Center is aimed at developing capabilities for increases in the capacities of airports, safe and accurate flight in adverse weather conditions including shear winds, the avoidance of wake vortexes, and reduced consumption of fuel. Advances in techniques for the design of modern controls and increased capabilities of digital flight computers coupled with accurate guidance information from the Microwave Landing System (MLS) make the achievement of some of these goals feasible. The stochastic feedforward control technique was developed within the context of the ATOPS program.

The main objective of a control law is to enable a dynamic system to track a desired or commanded trajectory selected from a given class of trajectories as closely as possible in the presence of random and deterministic disturbances and despite uncertainties about the system. The feedforward controller tries to track the desired or commanded trajectory, whereas the feedback controller tries to maintain the state of the plant near the desired trajectory. Modern control theory has concentrated more attention on the important feedback control problem, while the feedforward control problem has received less attention.

The feedforward control problem is formulated as a stochastic optimization problem and is embedded into a stochastic output feedback problem in which the plant contains unstable and uncontrollable modes. As the standard output feedback algorithm requires an initial gain that stabilizes the plant, a new algorithm was developed to obtain the feedforward control gains.

The formulation of the feedforward problem in a stochastic, rather than the standard deterministic, setting is significant in two ways. First, the class of desired trajectories from which the actually commanded path is selected can be effectively described as a random process generated by a dynamical system driven by a white-noise process. The second, and more important, implication of a stochastic optimization formulation is the tacit understanding that "perfect tracking" is often not possible for various reasons, including (a) uncertainties about, or variations in, the parameters of the plant (b) the nonlinearities in the plant, and (c) unmatched initial conditions. The necessary conditions have been shown to result in coupled linear matrix equations that imply that when a solution exists, it is indeed the globally-optimal control gain.

The feedforward control law has been used to develop a methodology to design combined feedforward/feedback control laws. This method has been applied to the design of a digital automated landing system for the ATOPS research vehicle, a Boeing 737-100 aircraft.

This work was done by Nesim Halyo of Information and Control Systems, Inc., for **Langley Research Center**. *Further information may be found in NASA CR-4078 [N87-25806], "A Combined Stochastic Feedforward and Feedback Control Design Methodology with Application to Autoland Design."*

Copies may be purchased [prepayment required] from the National Technical Information Service, Springfield, Virginia 22161, Telephone No. (703) 487-4650. Rush orders may be placed for an extra fee by calling (800) 336-4700.

LAR-13796

Circle Reader Action No. 442

Pipeline Time- and Transform-Domain Reed-Solomon Decoders

A modified algorithm simplifies the designs.

NASA's Jet Propulsion Laboratory, Pasadena, California

The modification of previous decoding algorithms leads to simplified conceptual designs for time- and transform-domain Reed-Solomon (RS) decoders suitable for implementation as very-large-scale integrated (VLSI) circuits. The new conceptual decoders determine simultaneously the errata-locator and errata-evaluator polynomials as part of a simplified scheme for the corrections of errors and erasures in RS codes.

The previous algorithm for time-domain decoding, based on a modification of the Berlekamp-Forney method, corrects both errors and erasures by the use of the method of continued fractions or its equivalent, Euclid's algorithm. In this algorithm, the continued-fraction subalgorithm is used to find the error-locator polynomial from the remainder of the formal power series for the Forney syndrome. The disadvantage of this algorithm is that two polynomial multiplications must then be performed to compute the errata-locator polynomial and the errata-evaluator polynomial from the known error-locator polynomial.

In the new algorithm for time-domain decoding, the Euclidean algorithm is used to solve the Berlekamp-Forney key equation for the errata-locator polynomial and the errata-evaluator polynomial directly and simultaneously. The advantage of this approach is that separate computations of the errata-locator polynomial and the errata-evaluator polynomial are not necessary. The new decoding algorithm is highly suitable for implementation in both VLSI circuitry and in software on a general-purpose computer.

The previous algorithm for transform-domain decoding, based on the algorithm invented by Forney, also corrects errors and erasures. By use of the Euclidean algorithm, the transform-domain decoding algorithm can also be simplified. By the same procedure as that used in the time-domain decoder, one can obtain the errata-locator polynomial.

The figure shows block diagrams of (255,223) RS time-domain and transform-domain decoders. Each block diagram can be separated into two parts. The first parts, labeled as "I," have similar VLSI architectures. The architecture of the transform-domain decoder is simpler than that of the time-domain decoder because the transform-domain decoder needs only two regular function blocks in part II, while the time-domain decoder requires three function blocks in part II.

The inverse-transform unit in the transform-domain design contains 255 similar cells in the (255,223) RS decoder. It is estimated that these 255 cells occupy only a moderate amount of area and that their geometric arrangement can be regular and simple. However, this advantage of the transform-domain decoder is valid only for moderately-short RS codes. If long RS codes are used to enhance the performance of the system, the transform-domain decoder needs a large inverse-transform block. The number of cells needed in an inverse-transform block increases exponentially with the integer m [where $N = 2^m - 1$ is the length of an (N, I) RS code]. However, the number of transistors needed in the time-domain decoder goes up only linearly as m increases. Therefore, for long codes, the time-domain decoder is more appealing.

This work was done by In-Shek Hsu, Trieu-Kie Truong, L. J. Deutsch, and E. H. Satorius of Caltech and I. S. Reed of USC for **NASA's Jet Propulsion Laboratory**. *For further information, Circle 50 on the TSP Request Card.* NPO-17510

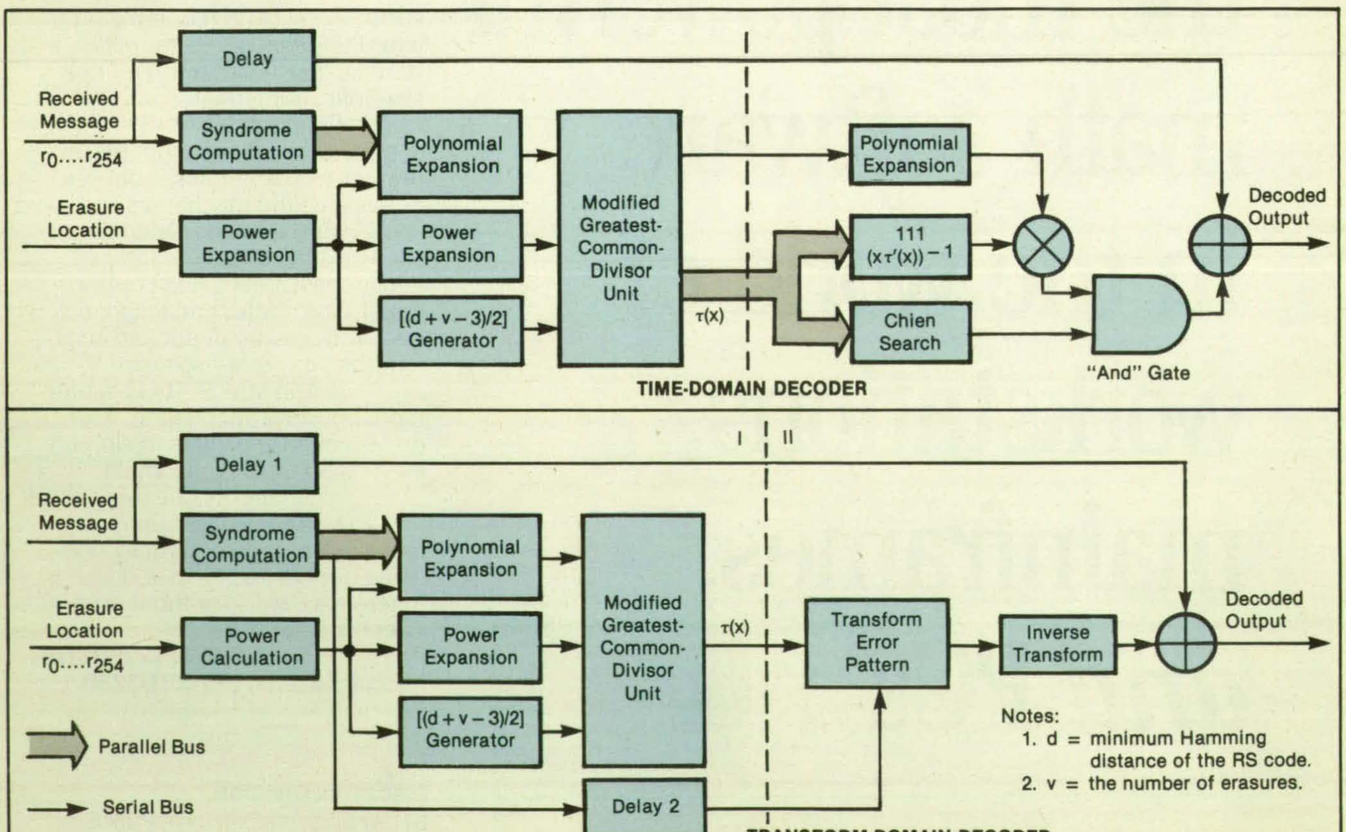

These **Time- and Transform-Domain RS Decoders** have modular, regular architectures that are simpler than those of earlier versions and are suitable for implementation in VLSI circuitry.

Sensor Detects Overheating of Perishable Material

An enzyme reaction gives a visual indication of temperature abuse.

NASA's Jet Propulsion Laboratory, Pasadena, California

An experimental temperature sensor changes color rapidly and irreversibly when its temperature rises above a predetermined level. Similar devices could be used to detect temperature abuse — that is, whether foods or medicines that should be refrigerated have been exposed to excessive temperatures during shipment and storage. Even brief exposures can cause hidden spoilage or deterioration. By viewing a sensor of this type, a receiving clerk could tell immediately whether a product has been maintained at safe temperatures and is therefore acceptable.

The sensor is based on reactions of enzymes in paraffins. The paraffins (such as hexadecane, pentadecane, and tetradecane) are blended so that the mixture melts at a temperature considered the maximum safe value — say −4 °C for frozen foods. In the solid paraffin blend, the reactions take place at an insignificant rate because the reactants diffuse slowly. As soon as the paraffin blend melts, however, the reactants diffuse more rapidly through the liquid. The reaction rate increases more than a million times, and the enzymes change color within a few minutes. If the temperature drops and the paraffins resolidify, the new color remains.

In a demonstration of the principle, glass beads coated with the enzyme horseradish peroxidase were added to molten hexadecane containing p-anisidine in a culture dish and placed in a refrigerator. When the mixture was hard, more molten hexadecane containing p-anisidine and hydrogen peroxide in an aqueous phosphate buffer was poured on it and solidified in the refrigerator. No color developed in the dish, even after 21 days of refrigeration.

When the dish was removed from the refrigerator for an hour, the paraffin melted and the contents of the dish turned a distinctive reddish brown. The contents retained the color after being returned to the refrigerator and resolidified.

This work was done by Jonathan S. Dordick and Alexander Klibanov of the Massachusetts Institute of Technology for **NASA's Jet Propulsion Laboratory**. *For further information, Circle 72 on the TSP Request Card.*

In accordance with Public Law 96-517, the contractor has elected to retain title to this invention. Inquiries concerning rights for its commercial use should be addressed to

Technology Licensing Office
Mail Code E32-300
Massachusetts Institute of Technology
Cambridge Massachusetts 02139

Refer to NPO-17585, volume and number of this NASA Tech Briefs *issue, and the page number.*

New on the Market

The ELF-50D Field Monitor from Walker Scientific Inc., Worcester, MA, **measures extra-low-frequency electromagnetic radiation** from powerlines, TVs, VDTs, office equipment, industrial machinery, and home appliances. The handheld unit features two switch-selectable measurement ranges: from 1 milligauss to 2 gauss and a high up to 20 gauss. Radiation levels are displayed on a 3 1/2 digit LCD.
Circle Reader Action Number 798.

RGB Spectrum's **High-Resolution Video Mixer (HRVM)** generates complex images in real time by combining video output from two genlocked workstations or graphics systems displaying up to 1280 x 1024 pixels. The HRVM uses one workstation to calculate the foreground image while the other calculates the background image and then combines them via a chroma key. Overlays as thin as one pixel are easily handled by high-speed circuitry.
Circle Reader Action Number 800.

"Save the Planet," **environmental awareness software** program from Save the Planet Shareware, Pitkin, CO, demonstrates the complex and severe climatic changes caused by atmospheric pollution. The IBM-compatible program explores the interrelated topics of fossil fuel combustion, population increases, forest destruction, and the atmospheric chemistry associated with ozone-destroying CFCs and greenhouse gases, such as CO_2 and methane. It includes an animated sequence showing the size increase of the Antarctic ozone hole since 1985.
Circle Reader Action Number 794.

The SMZ-U **zoom stereo microscope** from Nikon Inc., Garden City, NY, offers a 10:1 zoom ratio, and constant focus for magnifications from 3.75x to 450x. The microscope features strategically-located operator controls for ease of use and modular components for customization. A two-position beam splitter module contains two ports for the simultaneous use of closed-circuit television and photomicrographic equipment.
Circle Reader Action Number 796.

The FrameThrower™ high-definition **videographics processor** from Symbolics Inc., Burlington, MA, provides high-performance real-time color graphics and video capabilities for VME-based workstations. The processor displays images across the entire spectrum of video resolutions, including all popular broadcast, computer, and proposed HDTV formats, with a single board. Applications include medical imaging, photo reconnaissance, simulation, and scientific visualization.
Circle Reader Action Number 792.

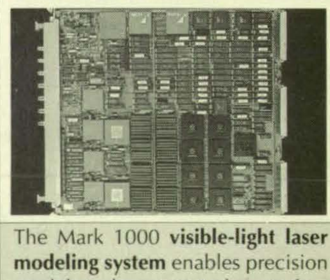

The Mark 1000 **visible-light laser modeling system** enables precision models to be generated up to four times faster than with ultraviolet-light laser systems, according to the manufacturer, Quadrax Corp., Portsmouth, RI. The Mark 1000 can rapidly produce complex 3D models within hours after completion of a design on a CAD system, dramatically shortening the overall part design and tooling cycle. Potential application areas include the automotive, aerospace, medical, packaging and electrical/electronic industries.
Circle Reader Action Number 790.

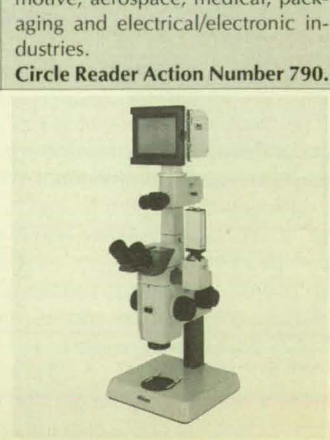

New on the Market

Dolphin Scientific's **Desktop Signal Processor**™ offers 25 to 450 million floating point operations per second, when configured with one to eighteen DSP32C processors, and handles data rates up to 1600 Mbytes/sec. Interfaces include up to 40 analog channels, four 32-bit digital ports, serial ports, and RS232 ports. The Desktop Signal Processor can be connected to IBM PC/AT and Macintosh II hosts or can run without a host system for real-time applications involving control and monitoring functions.
Circle Reader Action Number 780.

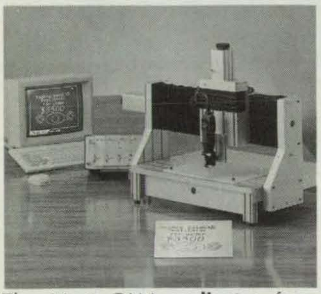

The MasterCAM **replicator** from Techno, New Hyde Park, NY, produces instant 3D prototypes from machinable wax, wood, plastics, and non-ferrous metals. The desktop system consists of a choice of seven sizes of computer-controlled, three-axes milling tables; a multi-axes motion controller; cables; hardware/software instruction manuals; and the MasterCAM software. MasterCAM features true 3D geometry construction plus IGES and CADL converters.
Circle Reader Action Number 786.

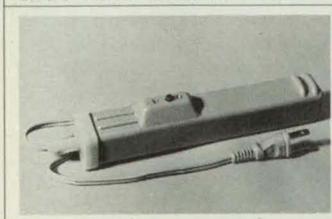

A handheld **demagnetizer** from Techni-Tool Inc., Plymouth Meeting, PA, degausses video screens, computer monitors, measuring tools, dies, tool bits, and many other objects. The one-pound unit's continuous service hour is 2.5 minutes; the correlative magnetic flux generation is 6.3v.
Circle Reader Action Number 788.

The Convolvotron high-speed digital signal processing system from Crystal River Engineering, Groveland, CA, allows users, for the first time, to experience and employ **three-dimensional sound reproduction.** The product consists of a two-card set of IBM PC compatible processors and enables listeners, wearing standard headphones, to locate in space up to four independent simultaneous sound sources. The system's 128 parallel multiply/accumulate/shift processors make it 20 times faster than conventional DSP systems. The Convolvotron is currently used for research and advanced development in hearing research, architectural acoustics, flight simulators, and virtual reality.
Circle Reader Action Number 778.

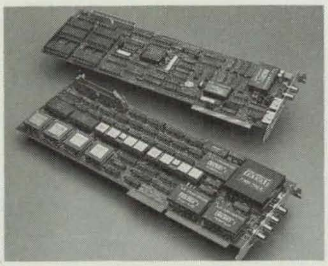

The ultra-compact CX-101 **monochrome CCTV camera** from Chinon America Inc., Mountainside, NJ, uses a MOS-type imaging chip to deliver 80,000 pixel resolution. Its F/1.8 lens and advanced chip enable light sensitivity as low as 2 lux. The 1-13/16" x 2-3/4" x 1" camera weighs just 6.3 ounces and is easy to position in a number of locations, making it useful for robotic vision and inspection applications in quality control, manufacturing, and production.
Circle Reader Action Number 782.

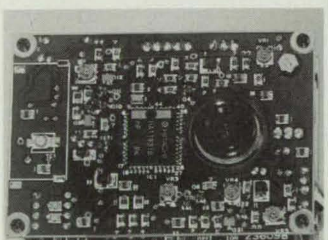

"Nondestructive Inspection of Composite Materials," 15-hour **video course** from Industrial Quality Inc., Gaithersburg, MD, illustrates the life cycle of composite materials, with emphasis on nondestructive inspection methods and equipment. The course provides an overview of ultrasonic and radiographic principles and systems; holographic, optical, and infrared techniques; composite structures, and repair; and composite performance.
Circle Reader Action Number 784.

New on the Market

The XS-420 **thermal imaging camera** from Xedar Corp., Boulder, CO, generates flicker-free images at a resolution of 270 x 270 elements and provides approximately 0.2°C thermal resolution. Based on the pyroelectric non-cooled sensor, the XS-420 is the first camera to offer performance characteristics similar to cooled scanning systems, but is much easier and less costly to operate than a cooled system. The complete camera including 50mm f/.7 Germanium optic and 1.5 inch viewfinder weighs only 8.5 lbs.

Circle Reader Action Number 776.

The Turbomixer from Turbomixer Corp., Washington, DC, uses a rotating stainless steel coil to mix, disperse, and grind virtually any fluid with viscosities up to 2 million CPS. Operating as a nonpulsating open-chambered pump, it is the only **mixing impeller** designed to efficiently draw material into its zone of effectiveness from above and below. When rotated by a handheld drill or bench mixer, Turbomixer's unique action includes coil impingement, impacting vortices, rapid acceleration, and container impingement. Lab and commercial models are designed as accessories to a standard 3/8 inch variable speed drill. They can also be used in bench-scale drill press-type mixers and retrofitted to clamp-on type mixers equipped with a chuck.

Circle Reader Action Number 768.

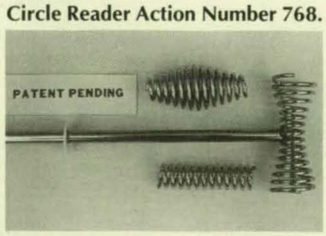

The Roadrunner II™ **bus extender** from ICS Electronics Corp., San Jose, CA, provides a 300K bytes/sec. data transfer rate with a built-in protocol for error-free data transmission. Link distance is up to 5000 meters using fiber optic cable. It features full IEEE 488/GPIB/HP-IB/CS-80 compatibility. Priced at $2500, the Roadrunner II comes with coaxial or fiber optic cable drivers and a user's manual.

Circle Reader Action Number 770.

PSS, Santa Monica, CA, has introduced AdaRAID, a **symbolic debugger** for simplified Ada software development and maintenance. AdaRAID supports multiple CPUs running concurrently, Ada data types, and Ada, JOVIAL, and 1750A assembler programs. Other features include break points, watchpoints, timing, tracing, stepping, walkbacks, and histories of last n executions. All features are available on assembly instructions or Ada (and JOVIAL) source statements.

Circle Reader Action Number 772.

ROBOTWORLD™, a high-speed intelligent **robotic assembly system** from Motoman Inc., Troy, OH, consists of individual placement, manipulation, and vision modules — each capable of independent action. It offers .002" accuracy and .005" repeatability and can be programmed in the Iconic High Level, RAIL, or MPW "C" languages. Applications include assembly, inspection, processing, gauging and packaging of electronic and medical components.

Circle Reader Action Number 774.

A new **structural adhesive** from American Cyanamid Co., Wayne, NJ, withstands temperatures up to 371° C and successfully bonds composite laminates and high-temperature metallic substrates, including stainless steel and titanium. The FM® 680 is an aluminum-filled, condensation polyimide supported on a fiber glass cloth and is available as a film adhesive, with a primer, and in foam and paste forms.

Circle Reader Action Number 766.

New Literature

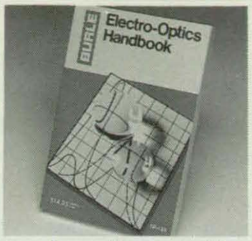

Designed as a reference tool for technicians, engineers, and scientists, BURLE INDUSTRIES' **Electro-Optics Handbook** features sections covering symbols and terminology, environmental physics data, and natural sources of radiation and atmospheric transmittance. The handbook describes state-of-the-art electro optic devices and provides performance and applications data.

Circle Reader Action Number 710.

Advanced Materials in Aerospace Applications, a comprehensive study of the development, design, and use of engineered materials by the international aerospace industry, is available from ASM International, Materials Park, OH. The study details the commerical activity of more than 500 international aerospace organizations, supplier companies, universities, and institutes during 1989. It features tabular displays of and materials applications related to specific aerospace vehicles, components, and process application areas, and is indexed for easy access to more than 750 technical articles.

Circle Reader Action Number 708.

A 10-page **cryopump brochure** offering design feature, performance specification, and applications data is available free of charge from Varian Associates Inc., Palo Alto, CA. The cryopumps offer a 10^{-3} to 10^{-11} Torr range and incorporate a closed-loop high-power refrigeration system that uses gaseous helium as the working medium. Applications include semiconductor processing, including film sputtering, evaporation, and ion implantation; device processing, including tube processing and component out-gassing; and industrial uses such as space simulation.

Circle Reader Action Number 706.

A free **fiber optic installation handbook** from Integrated Communications Inc., Mt. Arlington, NJ, discusses basic skills, equipment, and methods for effective fiber optic cable installation, connectorization, and testing. The handbook features sections on fiber and cable construction, installation procedures, cable and fiber preparation, connector attachment and finishing, optical fiber splicing, and testing. Technical charts and a glossary are included.

Circle Reader Action Number 704.

The Programmable Logic Device (PLD) Handbook from TAB Books Inc., Blue Ridge Summit, PA, is a comprehensive survey of PLD theory, data, design guidelines, and programming tools. The handbook describes PLD architectural characteristics, technology tradeoffs, logic synthesis and software tools, development systems, programming hardware, and current and future trends in PLD technology. It includes application examples, a logic tutorial, a list of product sources, and package drawings.

Circle Reader Action Number 712.

A 16-page catalog from Tusk Direct Inc., Bethel, CT, features the company's full line of **linear motion components.** The catalog provides diagrams, photos, specification tables, and pricing information for a variety of ball and crossed roller slides, crossed roller positioning slides and tables, and component accessories such as socket screw heads, extension springs, and shafts. The units comprise a broad range of sizes, load capacities, and travel for precision linear motion and positioning.

Circle Reader Action Number 702.

A new report published by Strategic Analysis Inc., Reading, PA, details near- and long-term business opportunities in **superconductors** through the year 2005. Based on field interviews with more than 350 raw material suppliers, fabricators, end-use customers and equipment manufacturers, the two-volume, 900-page study includes detailed global market forecasts and cost/benefit analyses for each known and emerging superconductor application.

Circle Reader Action Number 714.

New Literature

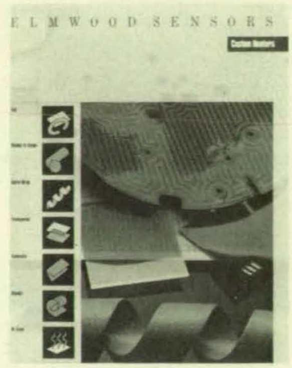

A free catalog from Elmwood Sensors Inc., Pawtucket, RI, helps design engineers specify custom heaters based on individual power requirements, single or multilayer element parameters, material selection, and thermal control requirements. The catalog features **flat, molded-to-shape, spiral wrap, transparent, composite, blanket, and high-temperature heaters** and provides an overview of heater applications and materials.
Circle Reader Action Number 726.

A new catalog from the Barksdale Controls Division of Imo Industries, Los Angeles, CA, features **electromechanical temperature switches** designed to sense and actuate at temperatures between -54° and +316°C. The 20-page catalog contains operating data and specifications for single and dual setting switches in local, mount, remote bulb, and capillary configurations. A variety of Nema-rated enclosures, from water-tight to explosion-proof, are illustrated.
Circle Reader Action Number 720.

TREK's **High Voltage Amplification and Static Measurement Guide** describes key features of the company's high-voltage operational amplifiers and power supplies, noncontacting electrostatic voltmeters, and static measurement and control products. Information on TREK's special services, such as OEM applications, custom designs, and private label products is also included.
Circle Reader Action Number 724.

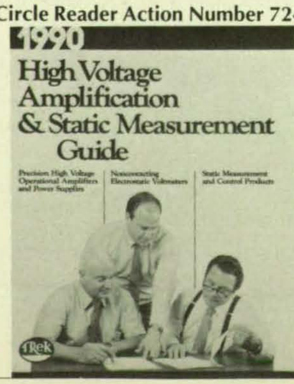

Paracom Inc., Hoffman Estates, IL, is offering a free **parallel programming tutorial.** Using the UNIX-like environment of Helios, the illustrated handbook is designed to acquaint software developers and systems integrators with the potential of transputer-based parallel processing.
Circle Reader Action Number 718.

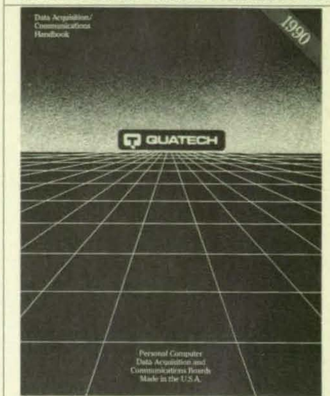

A new handbook from Qua Tech Inc., Akron, OH, features the company's **data acquisition, communication, signal conditioning, and industrial control cards** for IBM PC/AT and PS/2 systems. The 75-page publication contains technical specifications, product descriptions, diagrams, programming examples and applications for 56 products, including the new WSB-100 Waveform Synthesizer and the ES-100/QS-100 Multiport cards.
Circle Reader Action Number 722.

A free 20-page brochure from Burleigh Instruments Inc., Fishers, NY, discusses the theory, operation, and applications of Burleigh's FCL Series of **tunable lasers.** It describes options available for operation in the 1.45 - 1.77 micron or 2.3 - 3.45 micron spectral regions and presents cavity configurations that provide multimode, single frequency or synch-pumped, mode-locked operation in either wavelength region.
Circle Reader Action Number 716.

Subject Index

A

B

C

D

E

F

FOR IBM PC/XT/AT/386/486, PS/2, LAPTOPS

- Add voice recognition to most existing MSDOS programs. TSR program lets you define and activate keyboard macros by voice command. Great for CAD and DTP.
- Record/playback speech and sounds for voice mail, presentations, education, or entertainment. "Desktop audio" sound editing and compression utilities included.

A COMPLETE PRODUCT. Hardware attaches to parallel printer port. **No slots required.** Sturdy vinyl-clad steel enclosure. Includes headset/microphone, printer cable, software and user manual.

MADE IN USA. ONLY $219.95

CALL OR WRITE FOR FREE PRODUCT CATALOG

COVOX INC. 675 Conger St. Eugene, OR 97402
TEL (503) 342-1271 FAX (503) 342-1283 BBS (503) 342-4135

Circle Reader Action No. 380

Pressure, Flow & Temp. Switch

RELIABILITY

Specify Hydra-Electric

If you have special requirements, we can probably save you time and money by satisfying them with one of our standard models. They maintain their accuracy over many thousands of cycles. The "snap-action" disk spring eliminates most problems of aerospace pressure switches. Ask for your copy of the H-E catalog.

Hydra-Electric Co.

3151 Kenwood St., Burbank, CA 91505
(213) 843-6211

89-1

Circle Reader Action No. 427

dc/ac Current Meter

F. W. Bell Model 1776 measures dc and ac currents with interchangeable, non-contact probes. Laboratory-quality instrument operates on 117 Vac or integral rechargeable battery. Introduces virtually no insertion loss on dc readings, and extremely small loss on ac readings.

F.W. Bell, Inc.
6120 Hanging Moss Rd.,
Orlando, FL 32807
Phone: 407-678-6900. Fax: 407-677-5765

Circle Reader Action No. 594

PolyGraf/8™

The hardware and software package offering eight-channel real-time data-acquisition for Mac II computers!

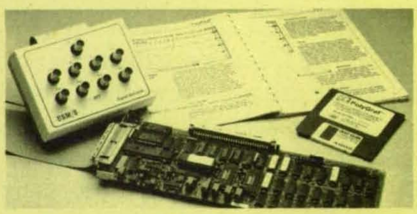

Designed for "plug and play" operation, **PolyGraf/8** gives you the ability to record, display, and playback up to eight channels of continuous data. Additional features permit leaving markers and taking snapshots, examining data trends through log windows and externally triggering multiple recording sessions.

World Precision Instruments, Inc.
375 Quinnipiac Ave • New Haven CT 06513-4445 USA
Telephone: 203-469-8281 • FAX: 203-468-6207

Mac is a registered trademark of Apple Computer, Inc. PolyGraf/8 is a trademark of World Precision Instruments, Inc.

Circle Reader Action No. 585

FREE! 130 Page Catalog

"Optics for Industry"

Free 130 page product catalog from Rolyn, world's largest supplier of "Off-the-Shelf" optics. 24-hour delivery of simple or compound lenses, filters, prisms, mirrors, beamsplitters, reticles, objectives, eyepieces plus thousands of other stock items. Rolyn also supplies custom products and coatings in prototype or production quantities. **ROLYN OPTICS Co.,** 706 Arrowgrand Circle, Covina, CA 91722-2199, (818)915- 5707, FAX (818)915-1379

Circle Reader Action No. 551

IEEE-488

Complete Hardware and Software Solutions

Platforms: EISA, PC/XT/AT, PS/2, 386, RT PC, Macintosh Plus/SE/II, Sun, DEC, Apollo, MASSCOMP, 382, Q-BUS, UNIBUS, VMEbus, MULTIBUS, STD Bus, S-100, and SBX Bus

Operating Systems: DOS, OS/2, XENIX, UNIX, 386/ix, Domain/OS, SunOS, AIX, RT, RSX, RSX, VMS, ULTRIX, VAXELN, PDOS, VERSAdos, RMX-86, Z-DOS, STD-DOS

Support Products: Extenders, Expanders, Converters, Controllers, Buffer, Analyzer

Call for *FREE* Catalog
(800) IEEE-488 • (512) 794-0100

NATIONAL INSTRUMENTS®
The Software is the Instrument™

Circle Reader Action No. 681

Graphics to Video.

- **Video/9U VME Board**, compatible with SGI, SUN, Megatek, and others.
- **Video/300** for the HP9000.
- **CGC** for any workstation.
- **CGC** II with up to 8 inputs.

FRI FOLSOM RESEARCH INC.
Excellence in Imaging™

526 E. Bidwell St., Folsom, CA 95630
(916) 983-1500
TWX: (910) 997-0955 FAX: (916) 983-7236 TELEX: 880-440

Circle Reader Action No. 648

bellows

available off-the-shelf

with costs from as low as $6.05 in 1000 quantity lots, and from $13.61 in 1 - 9 quantities; shipped within 3 days ARO (for quantities of 50 or less).

Our electrodeposited nickel bellows are leak tested (if required) to 1 x 10^{-9} cc/sec., and have no dimensional tolerance greater than ±.005 inch. O.D.'s from 0.250 to 1.000 in., and lengths from 0.185 to 1.230 in. are available.

The close length tolerance of these bellows enables pre-setting, thereby eliminating adjustment or calibration after installation of a bellows assembly.

FREE Sample and Product Guide

The Specialists in Miniature Bellows-Couplings-Contacts

SERVOMETER®
501 Little Falls Road
Cedar Grove, NJ 07009
(201) 785-4630 • Telex: 384233
Fax: (201) 785-0756

Circle Reader Action No. 490

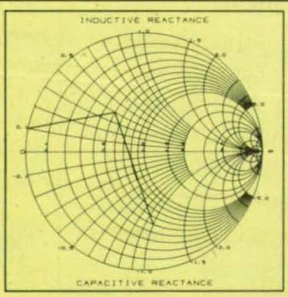

Great Graphics for Scientists and Engineers! FORTRAN, C, QuickBASIC, and Pascal.

Source code. No royalties.

$295.00

INGRAF 2.10 supports video, printers, and plotters

Over 100 routines give you complete control of axes, scaling, windows, and more

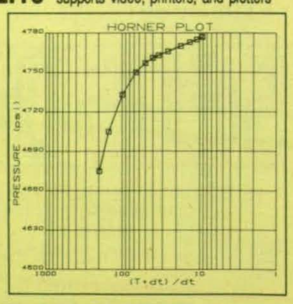

Sutrasoft
10506 Permian Dr.
Sugar Land, TX 77478

Info: (713) 491-2088
Orders: 1-800-888-8460

Circle Reader Action No. 450

Advertiser's Index

***RAC** stands for **Reader Action Card.** For further information on these advertisers, please circle the RAC number on the Reader Action Card elsewhere in this issue. This index has been compiled as a service to our readers and advertisers. Every precaution is taken to ensure its accuracy, but the publisher assumes no liability for errors or omissions.

NASA Tech Briefs, ISSN 0145-319X, USPS 750-070, copyright © 1990 in U.S., is published monthly by Associated Business Publications Co., Ltd. 41 E. 42nd St., New York, NY 10017-5391. The copyrighted information does not include the individual Tech Briefs which are supplied by NASA. Editorial, sales, production and circulation offices at 41 E. 42nd Street, New York, NY 10017-5391. Subscriptions for non-qualified subscribers in the U.S., Panama Canal Zone, and Puerto Rico, $75.00 for 1 year; $125.00 for 2 years; $200 for 3 years. Single copies $10.00. Remit by check, draft, postal or express orders. Other remittances at sender's risk. Address all communications for subscriptions or circulation to NASA Tech Briefs, 41 E. 42nd Street, New York, NY 10017-5391. Second-class postage paid at New York, NY and additional mailing offices.

POSTMASTER: please send address changes to NASA Tech Briefs, 41 E. 42nd Street, Suite 921, New York, NY 10017-5391.

FasMath
Your 386!

Running in our Number Smasher-386/25 AT accelerator, the FasMath delivers 5.5 megawhetstones of numeric throughput.

Unlike the Inboard, which only accelerates 8 MHz ATs, the Number Smasher runs in 6, 8, 10 and 12 MHz 286 motherboards! Standard production is currently available at 20 or 25 MHz, with a list of options that include sockets for up to 8 megabytes of 32 bit RAM, Intel, Cyrix and Weitek Coprocessors, a 64 Kbyte Cache and interface cables for any of the 3 possible 80286 sockets. Running at 25 MHz with the CX83D87, the number Smasher generates 3.7 Megawhetstones, which is a factor of 30 improvement over an 80287 running in an 8 MHz AT.

CYRIX CX83D87 FasMath™ Coprocessor

This new numerics coprocessor from Cyrix Corporation is a high performance CMOS 80387 compatible device. Its features include a 91 bit wide architecture that results in improved speed and accuracy and an idle cutoff that reduces power consumption, making it ideal for laptops. Long running operations such as square root, division, transcendentals, exponents and logs run between 2 and 4 times as fast as identical functions on an 80387. The improved accuracy results in faster convergence when used with error sensitive routines. Driven by NDP Fortran-386, the FasMath delivers 3.72 Megawhetstones at 25 MHz and 5.05 Megawhetstones at 33 MHz.

Number Smasher 386/25™

The new Number Smasher is the fastest PC accelerator brought to market to date. It replaces the 80286 in any AT or compatible with an 80386 running as an asynchronous emulator (see BYTE "PC Accelerators" Nov. 1986 Stephen Fried).

NDP 386 Compilers

MicroWay's NDP Fortran, C and Pascal are available in 386, 386SX and 486 versions. They are all mainframe quality globally optimizing compliers that have been specially optimized for the 386/486 family using intel, Cyrix or Weitek coprocessors. They support the most common dialects, such as UNIX System V or ANSI C with Microsoft extensions, Fortran 77 with VAX VMS extensions, and ISO Pascal. All include the MicroWay GREX graphics library and run under UNIX, XENIX and the popular 386 DOS Extenders.

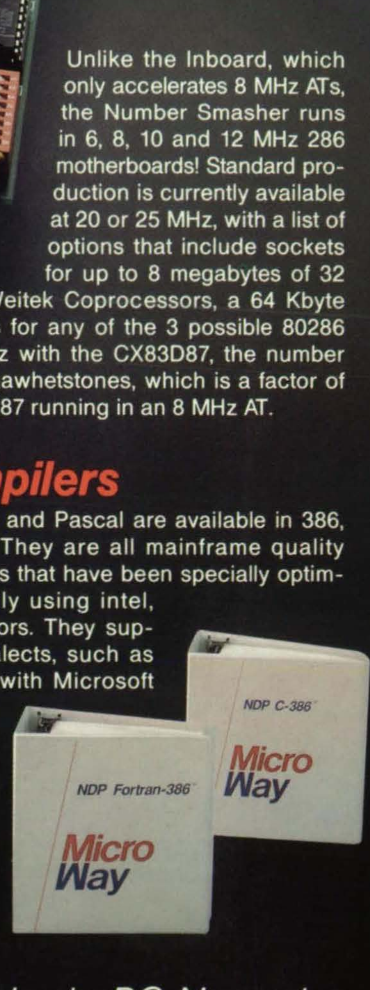

MicroWay

World Leader in PC Numerics

Corporate Headquarters: P.O. Box 79, Kingston, MA 02364 USA (508) 746-7341
32 High St., Kingston-Upon-Thames, UK., 01-541-5466